# Recent Advances on Carbazole-based Oxime Esters as Photoinitiators of Polymerization

Frédéric Dumur

# Recent Advances on Carbazole-based Oxime Esters as Photoinitiators of Polymerization

Frédéric Dumur[a]*

[a] Aix Marseille Univ, CNRS, ICR, UMR 7273, F-13397 Marseille, France

frederic.dumur@univ-amu.fr

**Abstract**

Photopolymerization is currently facing a revolution with the development of new light sources that are light-emitting diodes. Considering the low light intensity of these light sources, new photoinitiators exhibiting a higher reactivity than those used in the past have to be developed. Parallel to this, a great deal of efforts is also devoted to simplify the photocurable resins. With aim at simplifying the composition of the resins, monocomponent systems are actively researched. Indeed, if Type II photoinitiators are efficient structures, these compounds need besides to be combined with additives, complexifying the composition of the resins. In this field, oxime esters that are monocomponent Type I photoinitiators are extensively studied since a few years. In this field, the most impressive developments have been obtained for carbazole-based oxime esters since not less than 100 structures have been proposed during the last three years, demonstrating the intense research activity. In this review, an overview of the recent development concerning carbazole-based oxime esters is presented. Comparisons with reference compounds will also be presented to evidence the interest of these new structures.

**Keywords**

Photoinitiator; carbazole; photopolymerization; LED; low light intensity, oxime esters

## 1. Introduction

Photopolymerization is currently facing a profound revolution as the traditional UV photoinitiators are progressively discarded in favor of visible light photoinitiating systems.[1–19] Interest for developing new photoinitiators is supported by the wide range of applications in which photopolymerization is involved. To illustrate this, photopolymerization is used in research fields such as adhesives, microelectronics, dentistry, coatings, 3D and 4D printing.[20–29] Setting aside the UV technology is supported by the numerous drawbacks of UV light. Notably, dangerousness of UV light can be cited as the primary cause of eviction of UV photopolymerization. Indeed, long-term effects of UV radiation exposure include eye damages (cataracts and eyelid cancers) but also skin cancers.[30–32] Parallel to this, photopolymerization under UV light can result in the release of ozone during polymerization,

constituting another severe drawback.[33] To end, UV photopolymerization can only be done while using expensive and energy-intensive irradiation setups, entailing high running costs. With aim at better controlling the energy usage, new polymerization approaches have to be found. Interest for photopolymerization is also related to the specificities of photo-polymerization compared to the traditional thermal polymerization. Thus, a spatial and a temporal control of the polymerization process can be obtained by photopolymerization (See Figure 1).

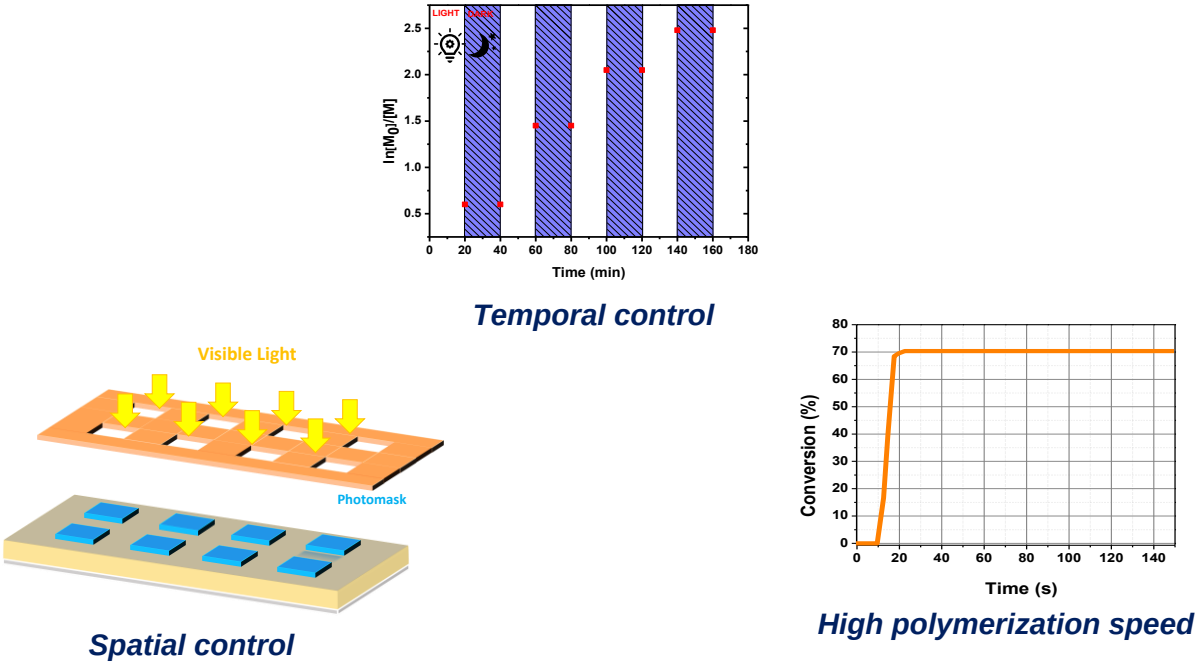


**Figure 1.** The different advantages of photopolymerization compared to the solution-phase polymerization.

Photopolymerization can also be carried out in solvent-free conditions, limiting the release of volatile organic compounds (VOCs).[33] Recently, the development of energy-saving, cheap and compact light sources with long-operating lifetimes have emerged on the market, namely light-emitting diodes.[34] Contrarily to UV light sources that were well-known to release heat during operation, LEDs also enable to polymerize temperature-sensitive monomers. Replacement of UV light by visible light is also related to the higher light penetration which can be achieved in the visible range, as shown in the Figure 2. Indeed, if the light penetration is limited to 600 μm at 350 nm, this latter can achieve several centimetres at 800 nm.[35] Face to these considerations, polymerization of thick samples and even of resins containing fillers can be achieved.

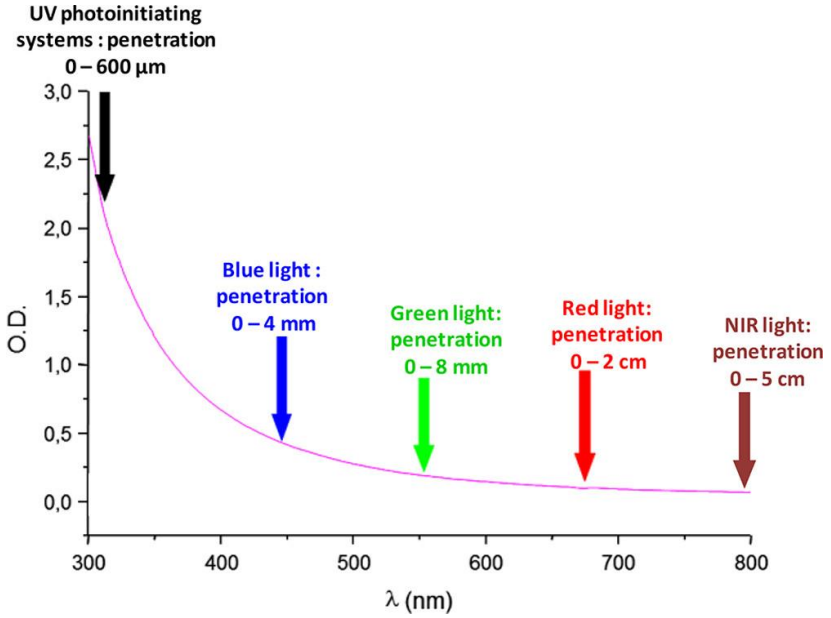


**Figure 2.** Light penetration in a polystyrene latex with an average diameter of 112 nm. Reprinted with permission from Bonardi et al.[35]

Considering that the light penetration is the key parameter for achieving high monomer conversions, a wide range of structures have been examined ranging from truxene derivatives[36] to copper complexes,[37–53] carbazoles,[54–65] chalcones,[28,66–78] zinc complexes,[79] acridones,[80,81] iridium complexes,[82–89] cyanines [90–95] phenazines,[96] push-pull dyes,[97–111] anthracene,[112] porphyrins,[113,114] triphenylamines,[115] thioxanthones,[116–128] dihydro-anthraquinones,[129] metal organic framework (MOFs),[130–132] diketopyrrolopyrroles,[133–135] pyrenes,[136–144] perovskites,[145,146] acridine-1,8-diones.[147–149] perylenes,[150–153] dithienophospholes,[154,155] iodonium salts,[156–163] iron complexes,[97,131,164–169] helicenes,[170,171] pyrrole derivatives,[172] 2,3-diphenylquinoxaline derivatives,[173,174] thiophene derivatives,[175] polyoxometalates,[176–178] camphorquinones,[179,180] phenothiazines,[181] Schiff bases,[182] coumarins,[183–194] naphthalimides,[156,195–211] chromones and flavones,[212–214] curcumin,[215–218] squaraines,[219–222] benzophenones,[223–230] conjugated polymers,[231] and cyclohexanones.[232–235] If these structures could enable to develop highly efficient photoinitiating systems, high monomer conversions could only be obtained by using multicomponent systems, resulting in complex formulations. To illustrate this, several four-component systems were notably reported in the literature, demonstrating the limitations of the photosensitization approach and therefore of the type II photoinitiators.[169,236]

Recently, Type I photoinitiators that are monocomponent photoinitiating systems have been the focus of intense research efforts. Indeed, these unimolecular photoinitiators are capable to undergo a direct photoinduced fragmentation upon absorption of light, generating initiating species. Among Type I photoinitiators that notably include hydroxyacetophenones, benzylketals, benzoin derivatives, $\alpha$-aminoalkylacetophenones, phosphine oxides, *o*-acyl-$\alpha$-oximino ketones, hexaaryl biimidazoles (HABIs), acyloximino esters, $\alpha$-haloacetophenones,

trichloromethyl-*S*-triazine glyoxylates or oxime esters.[237] Among these compounds, the most widely examined structures are undoubtedly oxime esters that are characterized by an easy synthetic access and a relatively good thermal stability.[238,239] The first report mentioning the design of oxime esters has been reported as soon as 1904 by Piguet and coworkers.[240] However, use of oxime esters as photoinitiators of polymerization is more recent since the pioneering works in this field have been carried out by Peeters and coworkers in 1970.[241] From the mechanistic viewpoint, oxime esters are capable to initiate the cleavage of the N-O bond upon photoexcitation, leading to the formation of an iminyl and an acyloxy radical. Subsequent to fragmentation, a decarboxylation reaction can undergo, producing initiating radicals.[239,242–246] Concerning oxime esters and based on the structures commonly used for the design of Type II photoinitiators, carbazole has been identified as a promising scaffold due to its polyaromatic structure exhibiting a good thermal and photochemical stability but also a good solubility in most of the monomers. Carbazole can also be easily chemically modified and carbazole is a cheap starting material enabling to develop low-cost Type I photoinitiators. Numerous carbazole-based oxime esters have been reported during the last three years since not least than 100 structures have been reported during the last three years. In this review, an overview of the recent developments concerning carbazole-based oxime esters is provided. Comparisons with reference systems will also be provided to evidence the interest of these structures.

## 1. Carbazole-based oxime esters

### 1.1. Carbazole-benzophenone hybrid oxime esters

In 2004, the first carbazole-based oxime ester i.e. OXE-02 was reported by Ohwa and coworkers.[247] Interestingly, OXE-02 displayed an outstandingly high sensitivity in resins containing black pigments so that OXE-02 was immediately commercialized by the color filter resist manufacturers.[248–253] From the mechanistic viewpoint, examination of the fragmentation mechanism of OXE-02 by time-resolved electron spin resonance (ESR) and electron spin resonance spin-trapping experiments revealed OXE-02 to undergo a photoinduced cleavage of the N-O bond in first step. Following the photoinduced cleavage, a fast decarboxylation reaction of the acetyloxy radicals can occur, avoiding the regeneration of the starting materials, as classically observed for mononuclear photoinitiators. In the present case and due to the decarboxylation reaction, the recombination of the initially formed radicals can be efficiently avoided (See Figure 3).

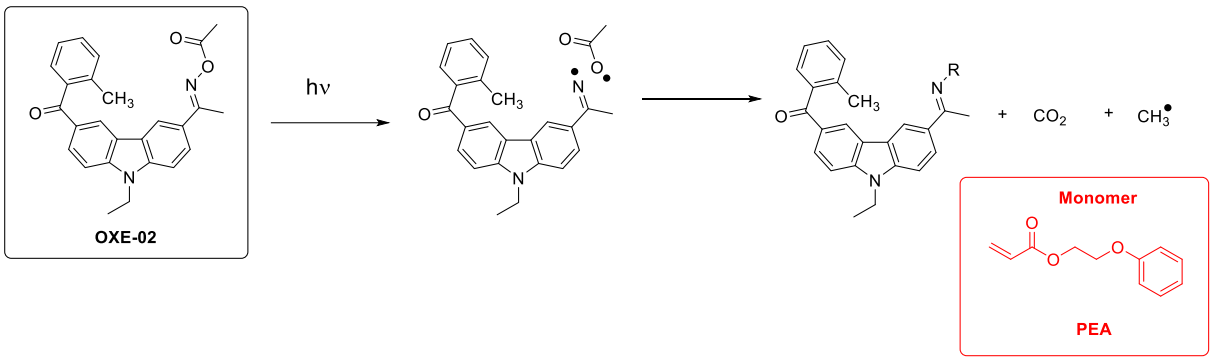


**Figure 3.** Chemical structure of OXE-02, the fragmentation mechanism and the monomer used in this study (R is an undefined group, iminyl radicals being capable to undergo various reactions after photocleavage).

Noticeably, only one initiating and reactive species is formed by photodecomposition of OXE-02. Indeed, iminyl radicals formed in first step cannot undergo a further fragmentation, furnishing radicals unable to add onto acrylic double bonds. Conversely, by decarboxylation of benzoyloxy or acetyloxy radicals, very reactive radicals can be formed, initiating the polymerization process.[254] Examination of the terminal groups obtained during the photopolymerization of 2-phenoxyethyl acrylate (PEA) revealed the initiating methyl radicals to also act as end groups, methyl groups being found at the extremity of the polymer chain. [255] Presence of hydrogen atoms as end groups of polymeric chains and resulting from the recombination and the chain transfer of polymeric chains under growth was also evidenced.

More recently, OXE-02 was revisited by the group of Jun Nie and coworkers with other carbazole derivatives (See Figure 4).[256] In this work, a series of three dyes differing by the solubilizing groups were designed and synthesized. Interestingly, examination of the solubility properties in various solvents and monomers revealed OXE-3 and OXE-5 to exhibit the highest solubility in monomers such as trimethylopropane trimethacylate (TMPTMA), tripropylene glycol diacrylate (TPGDA) and trimethylolpropanetriacrylate (TMPTA) (See Table 1).

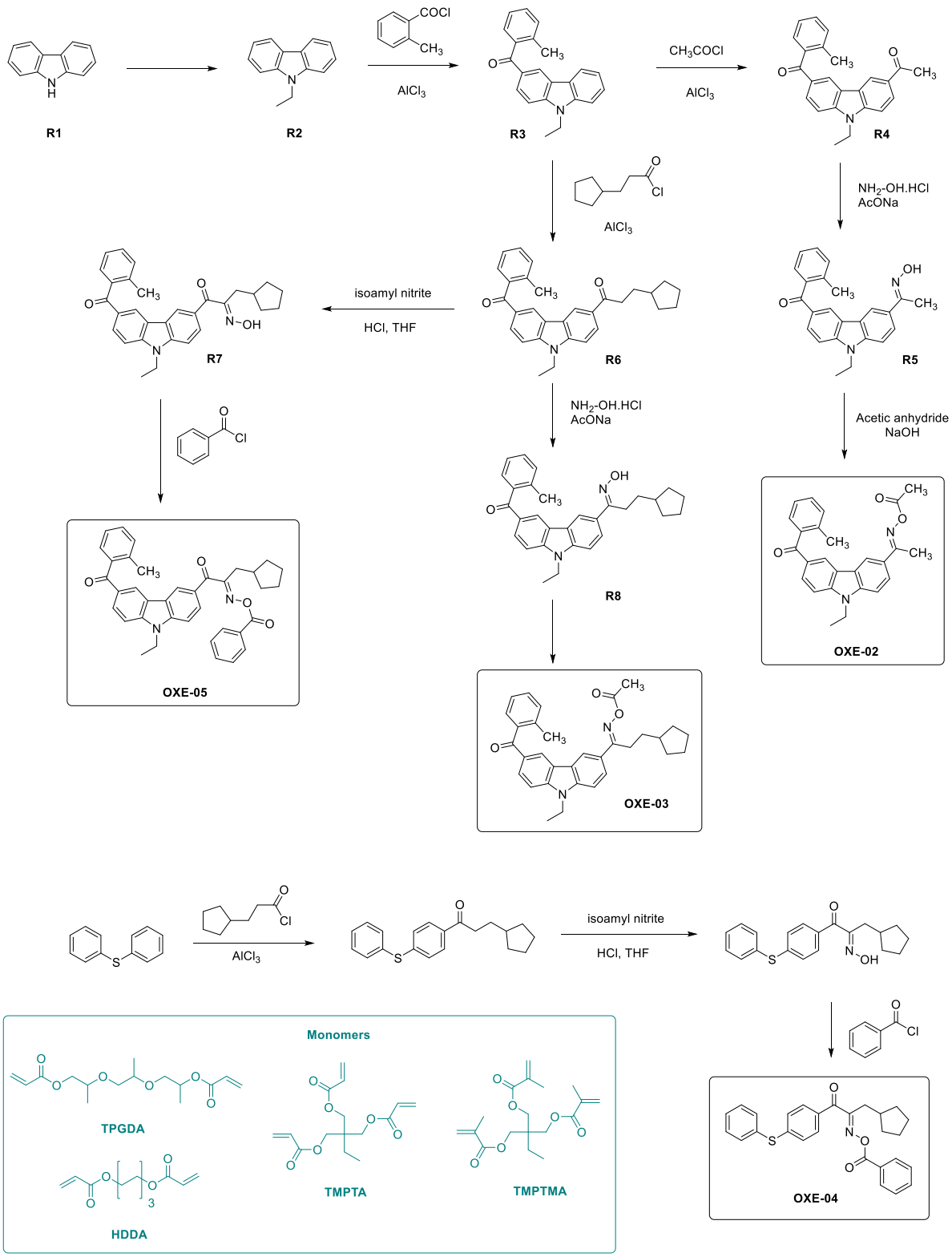


**Figure 4.** Synthetic routes to OXE-02, OXE-03, OXE-05 and OXE-04. Chemical structures of the monomers used in this study.

From the synthetic viewpoint, OXE-02, OXE-03 and OXE-05 could be prepared in 4 steps. Following the functionalization of 2-ethylcarbazole by mean of two consecutive Friedel and Craft reactions, the oxime ester OXE-02 could be obtained by first preparing the ketoxime using hydroxylamine hydrochloride in the presence of sodium acetate, followed by an

esterification with acetyl anhydride in basic conditions. A similar procedure was used for OXE-03. Conversely, a different synthetic approach was used for OXE-05, consisting first to undergo an $\alpha$-oximation of R6 with isoamyl nitrite. Finally, esterification with benzoyl chloride using triethylamine as the base enabled to produce OXE-05. Concerning OXE-04, a similar procedure to that used for OXE-05 was used, except that diphenyl sulfide was employed as the starting material instead of carbazole (See Figure 4).

**Table 1.** Solubility of oxime esters in different monomers and solvents (Solubility was determined by calculating the mass (in gram) of photoinitiator dissolved in 100 g of solvent).

| Solubility | OXE-02 | OXE-03 | OXE-04 | OXE-05 |
|---|---|---|---|---|
| **PGMEA**[a] | 2.6 | 13 | 27.5 | 16 |
| **cyclohexanone** | 16.5 | 26 | 30 | 23 |
| **toluene** | 12.5 | 23 | 28 | 16 |
| **methanol** | 21 | 19 | 5.8 | 1.2 |
| **acetonitrile** | 12 | 15 | 9 | 8 |
| **TPGDA** | 3.6 | 3.2 | 4.5 | 2.9 |
| **TMPTA** | 2.8 | 3.2 | 4.4 | 3.1 |

[a] Propylene glycol monomethyl ether acetate

From the absorption viewpoint, all OXEs showed UV-centered absorption spectra, with absorption maxima located at 336, 337 and 358 nm. Based on their absorption spectra, the different oxime esters were thus adapted for UV photopolymerization experiments. Examination of their photoinitiating abilities using HDDA as the monomer revealed OXE-03 and OXE-05 to furnish monomer conversions as high as 96%. Conversely, a lower monomer conversion (90%) combined with a low polymerization rate was found for OXE-02. Superiority of OXE-03-OXE-05 was assigned to the introduction of the diphenyl sulfide moiety in OXE-04 which extends the $\pi$-conjugated system and can induce a stronger intramolecular electron transfer than in OXE-02. Conversely, higher monomer conversions were obtained with OXE-03 and OXE-05 compared to OXE-02 and can be assigned to a higher solubility of these oxime esters in resins due to the presence of longer solubilizing chains, improving the monomer conversion. Examination of the influence of OXE concentrations on the monomer conversion revealed 0.5 wt% to be the optimum concentration. At higher concentration, presence of an inner filter effect adversely affecting the monomer conversion could be clearly demonstrated. By increasing the light intensity from 10 to 50 mW/cm², the HDDA conversion could be tripled using OXE-03 as the dye at 0.3 wt%. A severe reduction of the induction period was also found, resulting from more radicals produced enabling to overcome oxygen inhibition.[257] Finally, by increasing the light intensity to 80 mW/cm², a clear reduction of the monomer conversion was found, resulting from radicals recombination or chains transfer. Finally, comparison of the polymerization profiles of bifunctional and trifunctional monomers revealed the monomer conversion of bifunctional monomers to be greatly higher than that of the trifunctional ones. Indeed, more than a two-fold reduction of the monomer conversion was observed between HDDA, TPGDA and TMPTMA (See Figure 5).

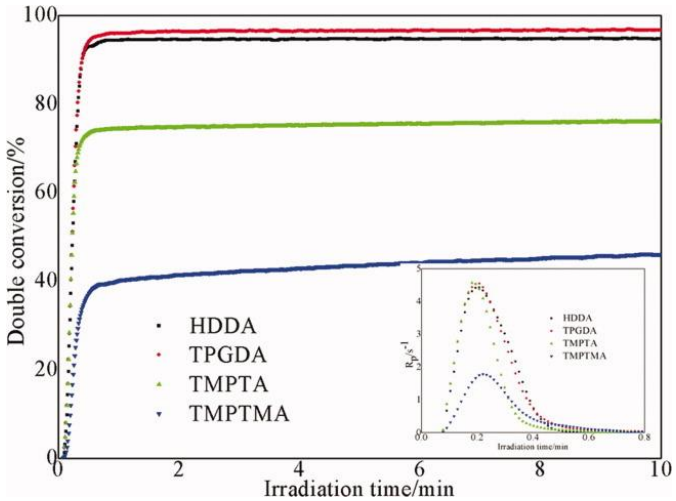


**Figure 5.** Final monomer conversions obtained for different monomers upon irradiation in the UV range while using OXE-05 (0.3 wt%) as the dye. Reproduced with permission of ref. [256].

In 2017, photochemistry and photophysics of OXE-02 were examined in details, this oxime ester being well-known to exhibit excellent performance in pigmented formulations.[258] Indeed, photodecomposition of oxime esters is definitely more complex than that observed for other Type I photoinitiators such as bisacylphosphane oxides, DMPA or benzoin.[259,260] In this work, Barner-Kowollik and coworkers evidenced wavelength-dependent photopolymerization properties of OXE-02 during the polymerization of methyl methacrylate (MMA) upon irradiation between 285 and 435 nm. To determine the different fragments generated upon photoexcitation, photo-CIDNP i.e. photo-chemically induced dynamic nuclear polarization was used. As the main findings, the authors could confirm the fragmentation of OXE-02 via an excited triplet state as mentioned in previous works.[244,245] The excited singlet states $S_1$ and $S_2$ of OXE-02 were determined as being dominated by a mixed $n-\pi^*/\pi-\pi^*$ character. By $^1H$ CIDNP spectroscopy, presence of four compounds resulting from the photocleavage of OXE-02 could be identified in deuterated acetonitrile. As shown in the Figure 6, presence of ethane (compound 2d) resulting from the recombination of methyl radicals, but also of methyl acetate (compound 2e) resulting from the recombination of methyl radical and acetyloxy radicals could be identified. Parallel to this, two imines (Z/E isomers i.e. *Z*-2f and *E*-2f) were also detected. Therefore, the CIDNP results confirmed the photofragmentation of OXE-02 to be based on the cleavage of the N-O bond. Polymerization of methyl methacrylate (MMA) done by pulsed-laser polymerization using a wavelength-tunable laser enabled here again to analyze the polymer end-groups as well as the monomer to polymer conversion at each wavelength. Interestingly, end-groups of the polymer chains remained the same, irrespective of the irradiation wavelength (from 285 to 435 nm). Acetyloxy and methyl groups were clearly determined as end groups of all polymer chains, consistent with the photoproduct obtained in NMR tubes. Examination of the MMA conversion as a function of the irradiation wavelength revealed 405 nm to furnish the highest monomer conversion, at identical number of photons (See Figure 7). These results are counter-intuitive, considering that the monomer conversions significantly mismatch from the absorption properties of OXE-02. To explain this, modification of the light penetration at the different

wavelengths examined was suggested as a possible hypothesis. However, use of the Lambert-Beer law to calculate the amount of absorbed light at the different wavelengths revealed still a mismatch between monomer conversion and light absorption. As other explanation and considering that the MMA conversion was not strictly correlated to the concentration of initiating radical, a lower concentration of radicals favoring the formation of longer polymer chains by reducing the probability of chain termination was also suggested. Finally, formation of radicals via pathways possibly involving conical intersections was also proposed to support the exceptional monomer conversion obtained at 405 nm.[261] Overall, it was determined that the wavelength-reactivity correlations was more complex than anticipated.

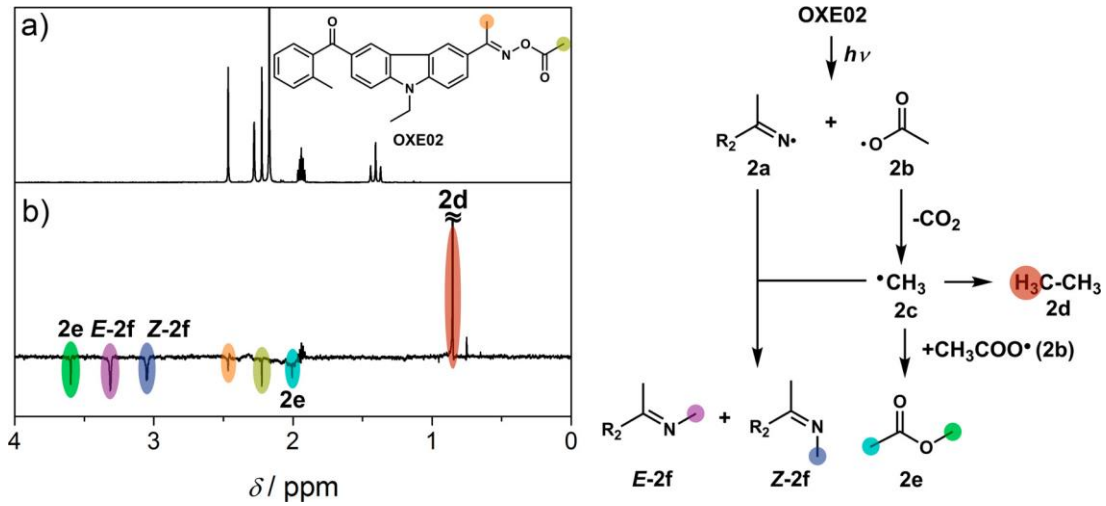


**Figure 6**. (a) $^{1}$H NMR and (b) $^{1}$H CIDNP spectra of OXE-02, recorded in $CD_3CN$ upon excitation at 355 nm with a laser. Reproduced with permission of Ref.[258]

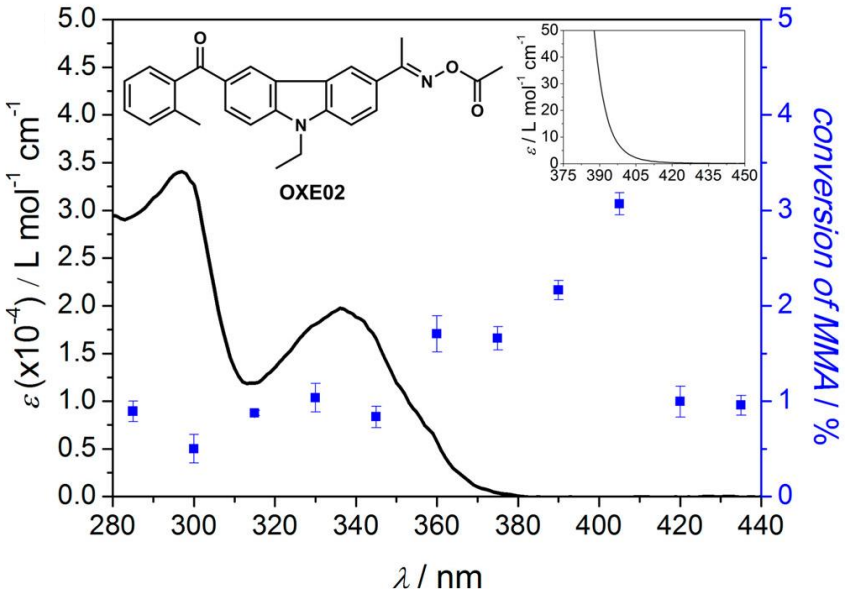


**Figure 7.** Comparison of the UV-visible absorption spectra of OXE-02 and the MMA conversion determined for different irradiation wavelengths at constant photon count (60 μmol) per irradiation wavelength. Reproduced with permission of Ref.[258]

In 2021, a series of five bicarbazole-based oxime esters BC-OXE-1-BC-OXE-5 was designed and synthesized with analogy to the benchmark oxime ester OXE-02 (See Figure

8).[262] Choice of bicarbazole as the chromophore was supported by previous works of the same groups on another family of type I photoinitiators, namely bicarbazole-based oxalates.[263] Noticeably, by using a bicarbazole structure, a slight redshift of the absorption maxima was found for all oxime esters compared to the parent OXE-02 (See Figure 9 and Table 2). Even if only a minor variation of the absorption maxima was found between the different compounds, absorption spectra extending until 400 nm for BC-OXE-1-BC-OXE-3, 450 nm for BC-OXE-4 and BC-OXE-5 could be determined. Especially, introduction of $\alpha$-carbonyl groups in BC-OXE-4 and BC-OXE-5 exerted positive effects on the absorption maxima, shifting the position of the absorption maxima of 5 nm. Interestingly, photoinitiating abilities of BC-OXE-2 and BC-OXE-3 could be compared respectively to that of BC-OXE-4 and BC-OXE-5 bearing $\alpha$-carbonyl groups. Indeed, these two families of dyes differ by the presence or not of of $\alpha$-carbonyl groups.

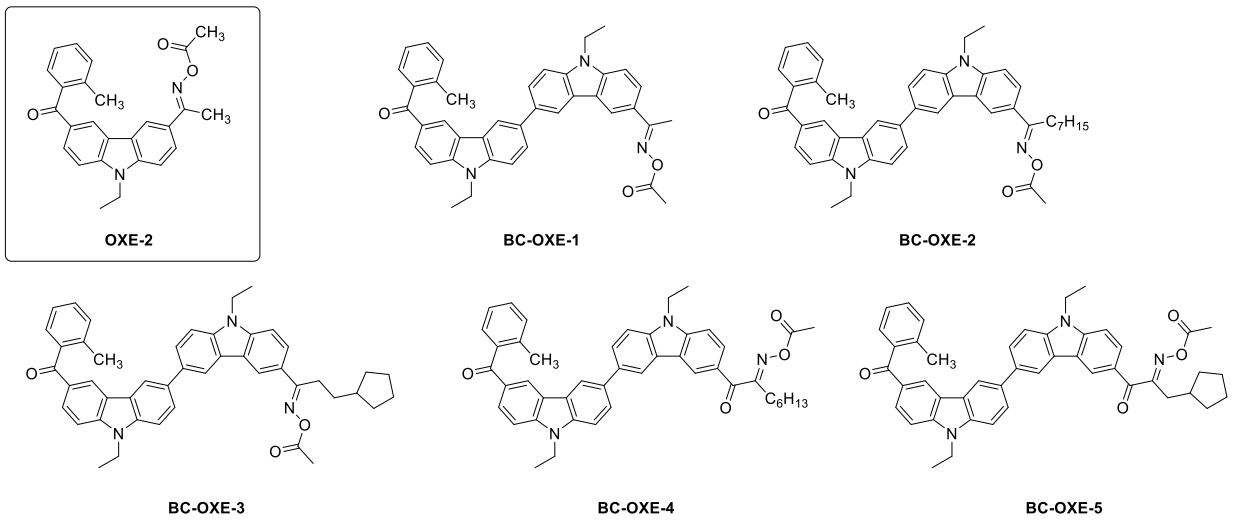


**Figure 8.** Chemical structures of bicarbazole-based oxime esters BC-OXE-1-BC-OXE-5 and monomers.

**Table 2.** Absorption characteristics of bicarbazole-based oxime esters and OXE02 in acetonitrile.

| PIs | $\lambda_{max}$[a] (nm) | $\varepsilon_{max}$[b] | $\varepsilon_{365}$[b] | $\varepsilon_{385}$[b] | $\varepsilon_{405}$[b] | $\varepsilon_{425}$[b] | $\varepsilon_{450}$[b] |
|---|---|---|---|---|---|---|---|
| **OXE 02** | 335 | 18 400 | 2 700 | 100 | 0 | 0 | 0 |
| **BC-OXE-1** | 339 | 24 600 | 12 500 | 2 600 | 400 | 100 | 0 |
| **BC-OXE-2** | 339 | 23 800 | 12 400 | 2 500 | 300 | 100 | 0 |
| **BC-OXE-3** | 339 | 25 800 | 13 400 | 2 700 | 300 | 50 | 0 |
| **BC-OXE-4** | 344 | 26 000 | 21 700 | 11 500 | 3 500 | 700 | 80 |
| **BC-OXE-5** | 344 | 25 900 | 21 600 | 11 600 | 3 800 | 1 100 | 200 |

[a] Maximum absorption wavelength ($\lambda_{max}$) [b] molar extinction coefficient ($\varepsilon$) (L.mol$^{-1}$.cm$^{-1}$).

Interestingly, introduction of alkyl chains of different lengths in BC-OXE-1 - BC-OXE-3 and introduction of $\alpha$-carbonyl groups in BC-OXE-4 and BC-OXE-5 could strongly influence the photolysis properties of oxime esters. In this work, authors also investigated the degradation products formed upon photodecomposition of OXE. In accordance with the well-established photolysis mechanism, cleavage of the N-O bond first produced iminyl and

acetyloxy radicals. Then, by liquid chromatography–mass spectrometry (LC–MS) analyses, different structures resulting from radical recombination could be identified during the photodecomposition of BC-OXE-3 and BC-OXE-5 as shown in the Figure 10.

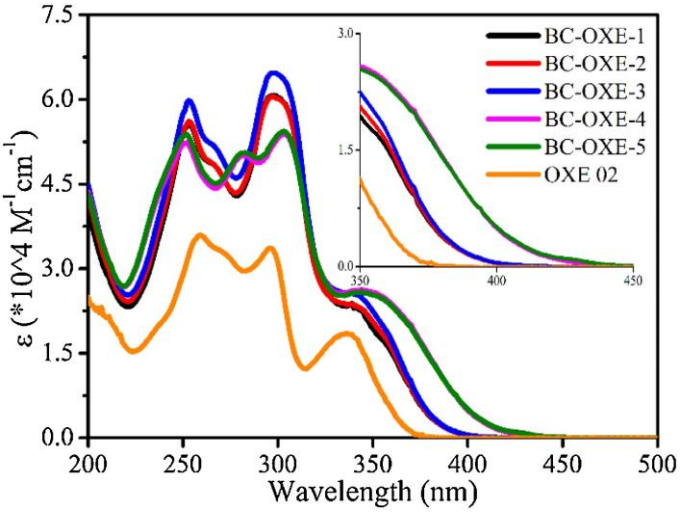


**Figure 9.** UV-visible absorption spectra of bicarbazole-based oxime esters and the reference compound in OXE-02 in acetonitrile. Reproduced with permission of Ref.[262]

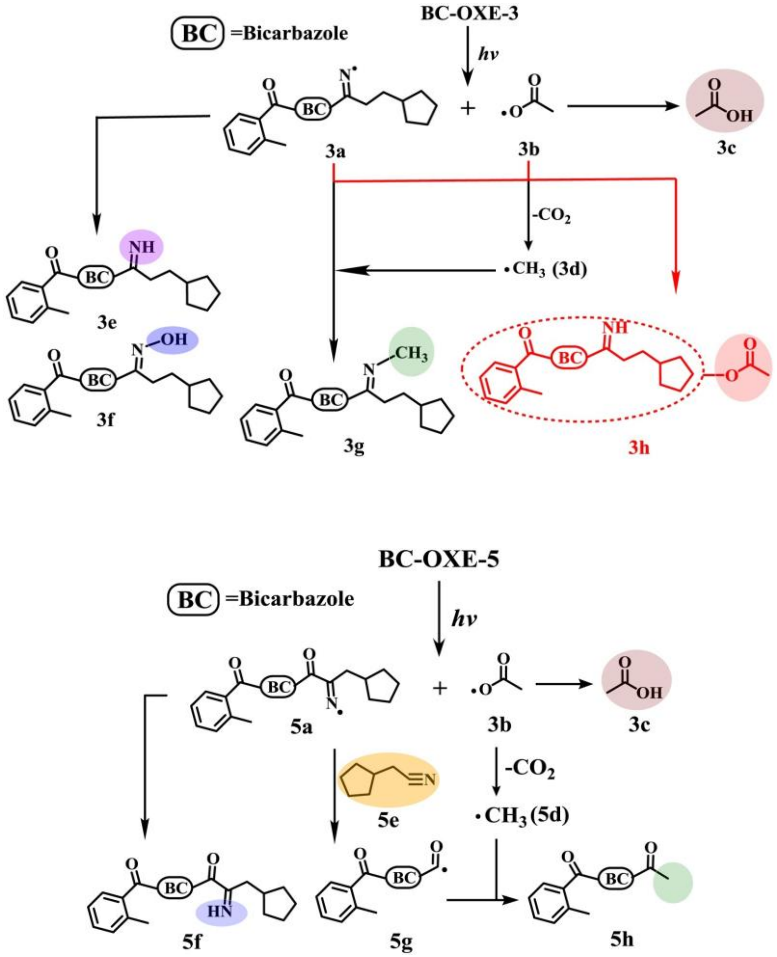


**Figure 10.** Photodegradation products formed during the photolysis of **BC-OXE-3** and **BC-OXE-5** identified by LC-MS and $^{1}$H NMR spectroscopy. Reproduced with permission of Ref.[262]

Photopolymerization experiments carried out for HDDA, TPGDA, and TMPTA upon irradiation at 365, 385, 405 and 425 nm (I = 45 mW/cm$^2$) revealed all *o*-acyl-*α*-oxooximes BC-OXE-4 and BC-OXE-5 to exhibit low photoinitiating abilities, irrespective of the irradiation wavelength. This counter-performance was assigned to photoinduced isomerization of the imine group adversely affecting their photoinitiating ability.[239] On the opposite, for *o*-acyloximes BC-OXE-1 - BC-OXE-3, photofragmentation of the N-O bond can undergo instead of the undesired photoisomerization. Except at 365 and 385 nm where OXE-02 could furnish monomer conversions on par with that of BC-OXE-3, a different situation was found at 405 nm, the conversion being reduced of 15% compared to BC-OXE-3 (See Figure 11). Overall, these different experiments revealed the detrimental impact of introducing *α*-carbonyl groups in *ortho*-position of the ketone group in BC-OXE-4 and BC-OXE-5 on the photoinitiating ability with regards to the performances obtained with their analogues BC-OXE-2 and BC-OXE-3.

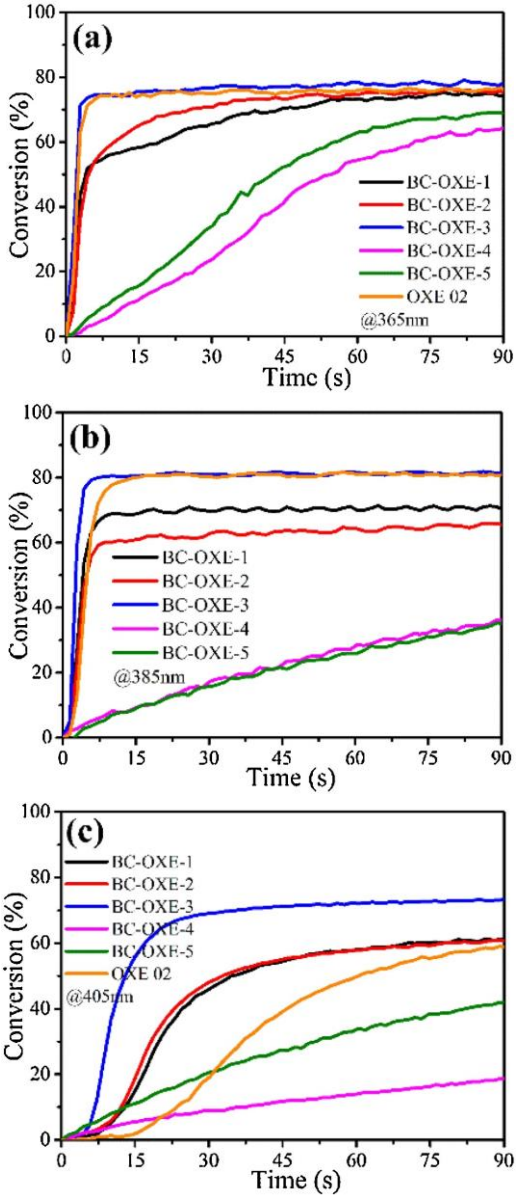


**Figure 11.** Photopolymerization performance of TPGDA in the presence of OXEs (1 wt%) upon irradiation at (a) 365, (b) 385, and (c) 405 nm. Reproduced with permission of Ref.[262]

In TMPTA, all OXEs could outperform OXE-02, irrespective of the irradiation wavelength. Logically, a reduction of the monomer conversions was observed for all OXEs by irradiation from 365 nm to 405 nm, consistent with a reduction of the molar extinction coefficients along with increasing the irradiation wavelength. Finally, due to the strongly redshifted absorption of BC-OXE-4 and BC-OXE-5 compared to the other oxime esters, these two OXE were the only ones capable to initiate a polymerization process at 425 and even 450 nm. Therefore, even if these two OXEs exhibit lower reactivity than the other BC-OXEs, polymerization processes at long irradiation wavelengths are still possible. Investigation of the stability of resins over time revealed the new OXE to give highly stable formulations. For these experiments, TMPTA was used as the monomer. Indeed, after seven months of storage in the dark, similar monomer conversions were obtained between the stored formulations and the freshly prepared formulations. By Differential Scanning Calorimetry (DCS) experiments, all resins showed a good stability until 150°C, no polymerization reaction being detected until this temperature.

By theoretical calculations, red-shifted absorptions of BC-OXE-4 and BC-OXE-5 compared to that of BC-OXE-1-BC-OXE-3 could be explained by mean of differences of electronic transitions involved in the main absorption peak. Thus, comparison of the HOMO energy levels of BC-OXE-3 and BC-OXE-5 revealed a similar electronic distribution mainly centered onto the bicarbazole structure. Conversely, major differences could be found concerning their LUMO and LUMO+1 energy levels since their respective electronic distributions were found in different subunits of the molecule, as shown in the Figure 12. Notably, upon introduction of the $\alpha$-carbonyl group in BC-OXE-5, a reduction of the LUMO and LUMO+1 energy levels were found compared to that of BC-OXE-3. Overall, a redshift of the absorption can be determined for BC-OXE-5, resulting from a decrease of the LUMO energy level.

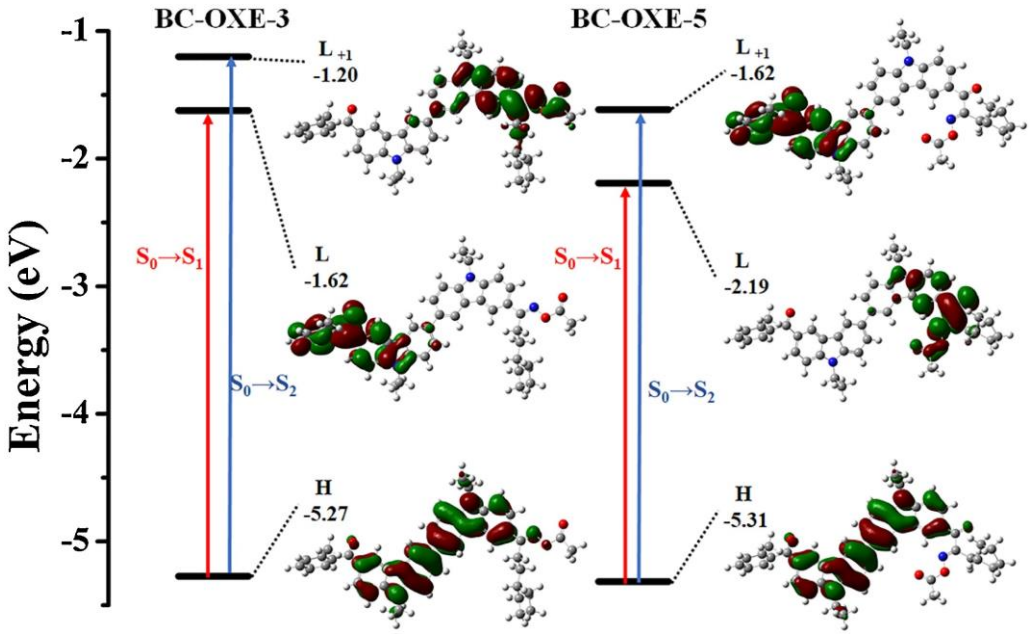


**Figure 12.** Frontier orbitals of BC-OXE-3 and BC-OXE-5.

Parallel to this, if the LUMO+1 orbital of BC-OXE-3 was mostly located onto the oxime ester group, an opposite situation was found for BC-OXE-5 and this is the LUMO energy level of BC-OXE-5 that was located on the cleavable group and not the LUMO+1 energy level as observed in BC-OXE-3. Based on the polymerization results, the lowest photoinitiating ability of BC-OXE-5 compared to that of BC-OXE-3 can be explained by different electronic repartitions of the LUMO and LUMO+1 energy levels, the two dyes exhibiting a similar electronic distribution for their HOMO energy levels.

In 2022, an original approach consisted in developing benzocarbazole-based oxime esters in order to redshift their absorption towards the visible range (See Figure 13).[264]

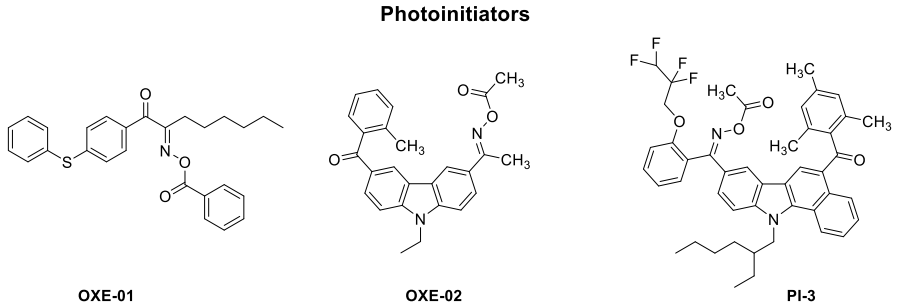


**Figure 13.** Chemical structure of PI-3 and reference compounds OXE-01 and OXE-02.

By extending the aromaticity of carbazole in PI-3, a redshift of the absorption of PI-3 could be obtained compared to the benchmark OXE-01 and OXE-02 (359 nm vs. 327 and 337 nm for OXE-01 and OXE-02 respectively) (See Figure 14). Interestingly, benzocarbazole derivative PI-3 showed a high sensitivity for the polymerization of black and blue resists. Notably, the redshifted absorption of PI-3 compared to that of OXE-01 and OXE-02 contributed to greatly increase the polymerization depth.

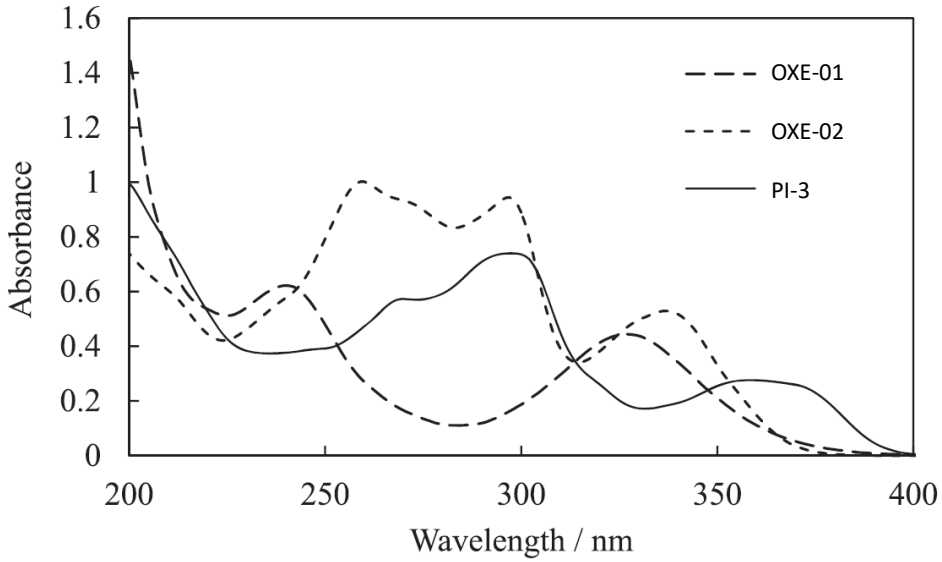


**Figure 14.** UV-visible absorption spectra of OXE-01, OXE-02 and PI-3 in acetonitrile. Reproduced with permission of Ref. [264]

### 1.2. Carbazole-phenothiazine hybrid oxime esters.

Even if OXE-02 proved to be efficient at 405 nm and thus in the visible range, the search for new structures exhibiting a high reactivity was intense. In 2017, a phenothiazine substituted by a carbazole moiety was proposed by the group of Tao Wang.[265] Interest for using a phenothiazine for the design of CZ-PTZ-OXE is directly related to the strong absorption of phenothiazine in the visible range, contrarily to carbazole which possesses a strongly UV-centered absorption.[181,266–268] Therefore, the design of visible dyes is strongly facilitated. To evidence the interest of introducing a carbazole substituent in CZ-PTZ-OXE, triphenylamine or more simply a phenyl ring were introduced in TPA-PTZ-OXE and Ph-PTZ-OXE for comparison respectively (See Figure 15). From the absorption viewpoint, the three oxime esters exhibited absorption spectra dominated by the contribution of the phenothiazine moiety so that the three dyes showed an absorption extending until 475 nm (See Figure 16). Thus, absorption maxima located at 378, 382 and 382 nm were respectively determined for Ph-PTZ-OXE, PA-PTZ-OXE and CZ-PTZ-OXE. These absorptions are greatly redshifted compared to that of BC-OXE-3 and OXE-04, their absorptions being centered at 337 and 329 nm respectively. Based on the absorptions of the different dyes, polymerization experiments of tripropylene glycol diacrylate (TPGDA) were carried out with laser diodes emitting at 405 nm (60 mW/cm²) and 455 nm (30 mW/cm²).

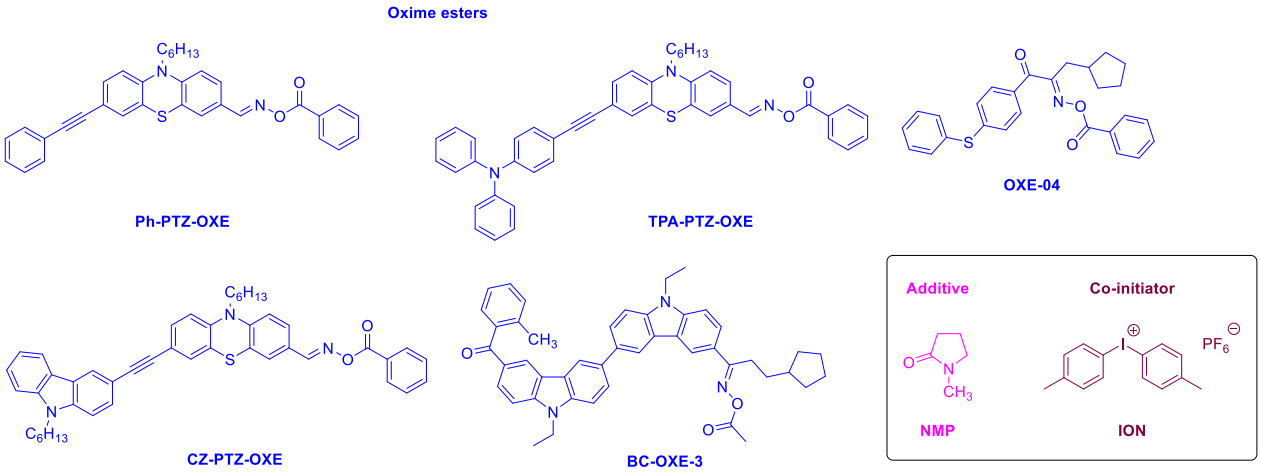


**Figure 15.** Chemical structures of CZ-PTZ-OXE, TPA-PTZ-OXE, Ph-PTZ-OXE, the reference compound OXE-04 and BC-OXE-3, different monomers and additives.

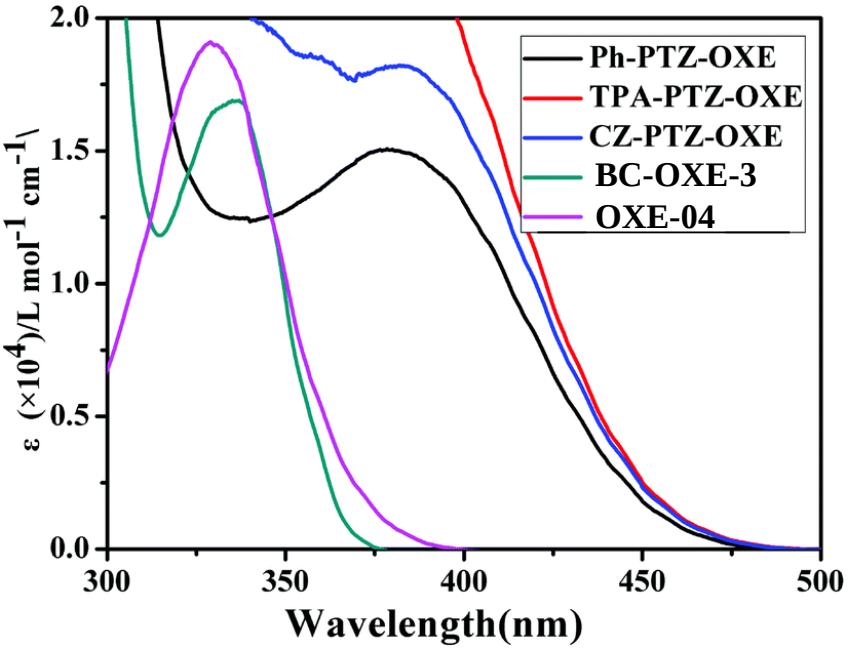


**Figure 16.** UV-visible absorption spectra of CZ-PTZ-OXE, TPA-PTZ-OXE and Ph-PTZ-OXE, BC-OXE-3 and OXE-04 in THF solutions ($10^{-4}$ mol.$L^{-1}$). Reproduced with permission of Ref.[265]

As shown in the Figure 17, at 405 nm, all oxime esters could furnish high final monomer conversions, the highest conversions being obtained for TPA-PTZ-OXE and CZ-PTZ-OXE (96 and 94% respectively after 50 s of irradiation). Comparison with the reference compounds BC-OXE-3 and OXE-04 revealed these two oxime esters to furnish TPGDA conversions as high as 91 and 96%, despites their extremely low molar extinction coefficients at 405 nm (See Figure 16). As previously mentioned for the different works done by Barner-Kowollik and coworkers,[258] no direct correlation could be established between the molar extinction coefficients of these oxime esters and the obtained monomer conversions. Noticeably, upon irradiation at 455 nm, no monomer conversion could be detected anymore for BC-OXE-3 and OXE-04, due to the lack of absorption at this wavelength. Concerning Ph-PTZ-OXE, TPA-PTZ-OXE and CZ-PTZ-OXE, monomer conversions of 62, 71 and 68% could be determined respectively after 100 s of irradiation. Comparison with the two-component camphorquinone (CQ)/triethanolamine (TEA) system and camphorquinone revealed the oxime esters to furnish higher final monomer conversions. Indeed, conversions of 52 and 10% were obtained with the reference systems CQ/TEA and CQ, far behind that of the oxime esters. Examination of the influence of the concentration revealed the optimum concentration to be between 0.3 and 1 wt%.

Finally, the authors examined the possibility to use the different oxime esters as Type II photoinitiators for the sensitization of an iodonium salt i.e. *bis*(4-methylphenyl)iodonium hexafluorophosphate (ION). At 405 nm, final monomer conversions around 90% could be obtained with the two-component OXE/ION (0.2%/2% w/w) systems. These conversions are slightly lower than that obtained for OXE alone (1 wt%). At 455 nm, only the two-component Ph-PTZ-OXE/ION, TPA-PTZ-OXE/ION (0.2%/2% w/w) systems could furnish higher monomer conversions than that obtained for the same dyes used as unimolecular

photoinitiating system (See Figure 18). Conversely, a severe reduction of the conversion was determined for the two-component CZ-PTZ-OXE/ION system. The reduced polymerization efficiencies obtained with oxime esters when tested as Type II photoinitiators can be assigned to less favorable rate constants of interaction of the photosensitizers with the iodonium salt compared to the sensitization of the photocleavage of the N-O bond, reducing the polymerization efficiency. This can also be assigned to a lower photoinitiator content (0.2 wt% in two-component systems), enabling the two-component photoinitiating system to generate less initiating radicals than when oxime esters are used as mono-component systems (1 wt%). Finally, examination of the thermal stability of oxime esters revealed OXE to be stable until 120°C, what is sufficient for numerous applications.

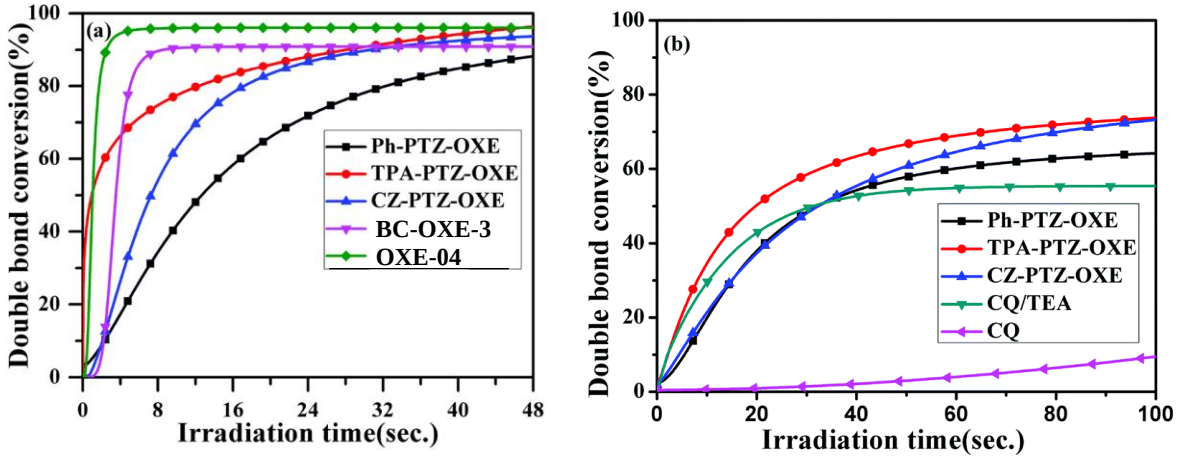


**Figure 17.** Photopolymerization profiles of TPGDA using different dyes (1.0 wt%) upon irradiation with a laser diode at 405 nm (a) and 455 nm (b). Reproduced with permission of Ref.[265]

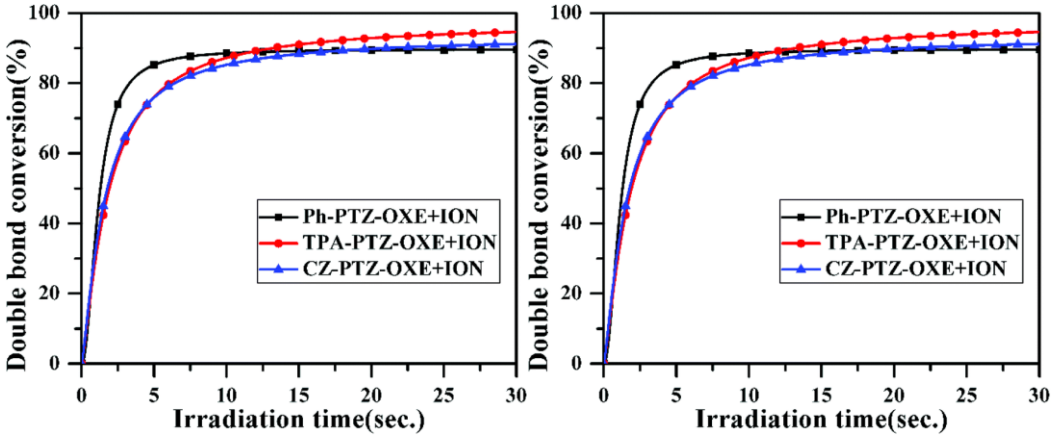


**Figure 18.** Photopolymerization profiles of TPGDA using the two-component OXE/ION (0.2%/2% w/w) systems upon irradiation with a laser diode at 405 nm (top) and 455 nm (bottom). Reproduced with permission of Ref.[265]

In 2019, another phenothiazine-based oxime ester PTZ-OXE-2 bearing a carbazole moiety was reported by the same group, differing from the previous ones by the position of the carbazole group with regards to the photocleavable group.[269] Here again, a

triphenylamine analogue i.e. TPA-OXE-1 was designed and synthesized for comparison (See Figure 19).

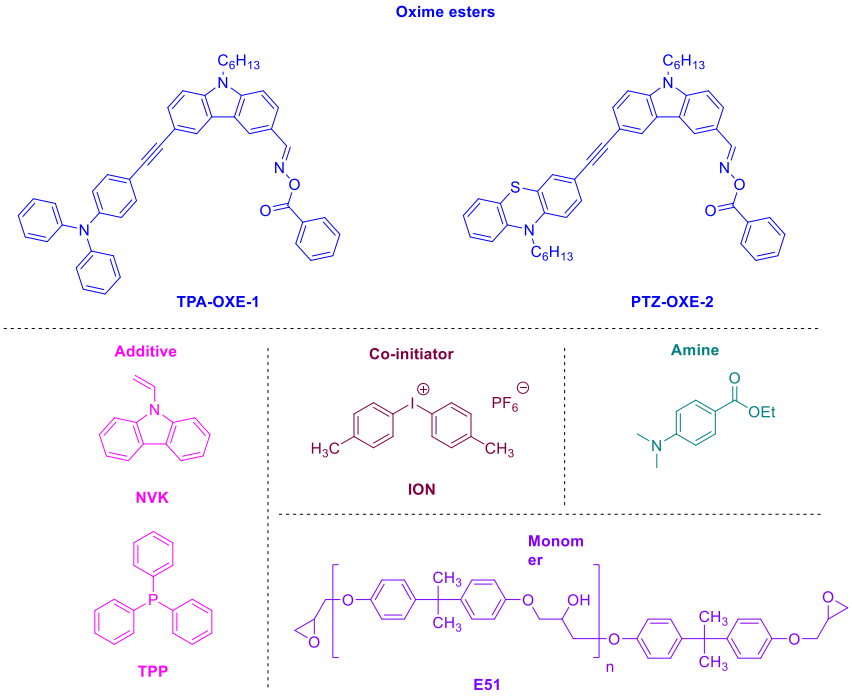


**Figure 19.** Chemical structures of oxime esters TPA-OXE-1 and PTZ-OXE-2, monomers and additives.

As shown in the Figure 20, if the two OXE exhibited almost similar absorption maxima (350 and 357 nm for TPA-OXE-1 and TPZ-OXE-2 respectively in THF), presence of the phenothiazine group enabled TPZ-OXE-2 to display an absorption extending until 450 nm. Conversely, for TPA-OXE-1, a more limited absorption could be determined, not extending beyond 420 nm.

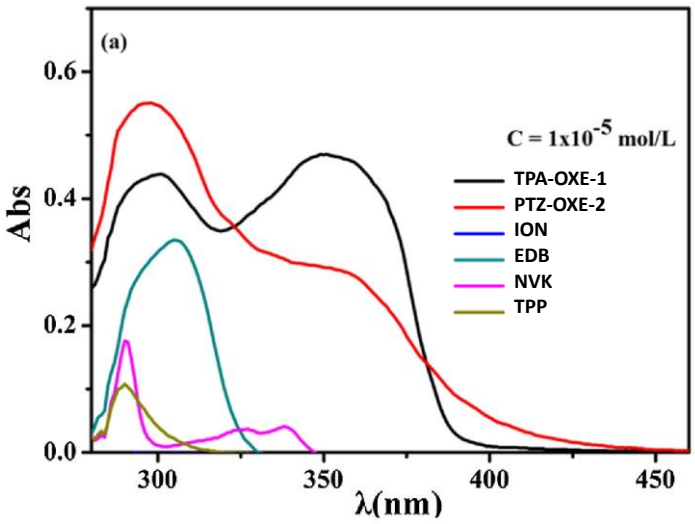


**Figure 20.** UV-visible absorption spectra of carbazole oxime esters and co-initiator in THF. Reproduced with permission of Ref. [269]

Considering that only few reports were available concerning the photoinitiating ability of OXE in multicomponent systems, TPA-OXE-1 and PTZ-OXE-2 were thus examined as photosensitizers for the sensitization of *bis*(4-methylphenyl)iodonium hexafluorophosphate (ION). Steady state photolysis experiments done in THF revealed the photolysis rate of the two-component OXE/ION (1.5%/1.5% w/w) system to be faster than that observed for OXE alone. It therefore indicates that an efficient electron transfer can occur between OXE and ION. Surprisingly, upon addition of a third component such as ethyl 4-dimethylaminobenzoate (EDB), triphenylphosphine (TPP) or *N*-vinylcarbazole (NVK), a remarkable decrease of the photolysis rate was detected. This unexpected behavior was assigned to secondary reactions occurring between the additives (EDB, TPP or NVK) and the different species formed in first step by photoinduced electron transfer between OXE and ION. Determination of the free energy change for TPA-OXE-1 ($\Delta G$ = - 1.53 eV) and PTZ-OXE-2 ($\Delta G$ = - 0.93 eV) revealed the electron transfer process between OXE and ION to be thermodynamically favorable from the singlet state. Similarly, the possibility of an electron transfer reaction between OXE and EDB was also determined, free energy changes of – 0.96 eV and – 0.68 eV being determined for the TPA-CZ-OXE/EDB and PTZ-CZ-OXE/EDB systems. Finally, NVK is an interesting additive for the design of three-component system as it allows to produce the highly reactive Ph-NVK$^{\bullet}$ radicals, by addition of NVK on the phenyl Ph$^{\bullet}$ radicals.[155,231] Therefore, the following mechanisms could be proposed, based on the EPR, steady state photolysis and cyclic voltammetry experiments (See Figure 21). In the case of the three-component dye/ION/EDB system, formation of Ph$^{\bullet}$ radicals is promoted by photoinduced electron transfer between the excited dye and the iodonium salt, generating radicals capable to initiate the free radical polymerization (FRP) of acrylates. Parallel to this, EDB can also react with the excited dye, inducing the formation of EDB$^{+\bullet}$ radical cations. These latter can interact with dye$^{\bullet-}$, which by hydrogen abstraction can form EDB$_{(-H)}^{\bullet}$ and dye-H$^{\bullet}$ radicals. Overall, three different types of radicals can be concomitantly formed. In the case of the three-component dye/ION/NVK system, Ph$^{\bullet}$ radicals can be advantageously converted to the more reactive Ph-NVK$^{\bullet}$ radicals, initiating the FRP process. These radicals can also react with ION, forming additional Ph$^{\bullet}$ radicals but also Ph-NVK$^{+}$ cations capable to initiate the cationic polymerization of epoxides.

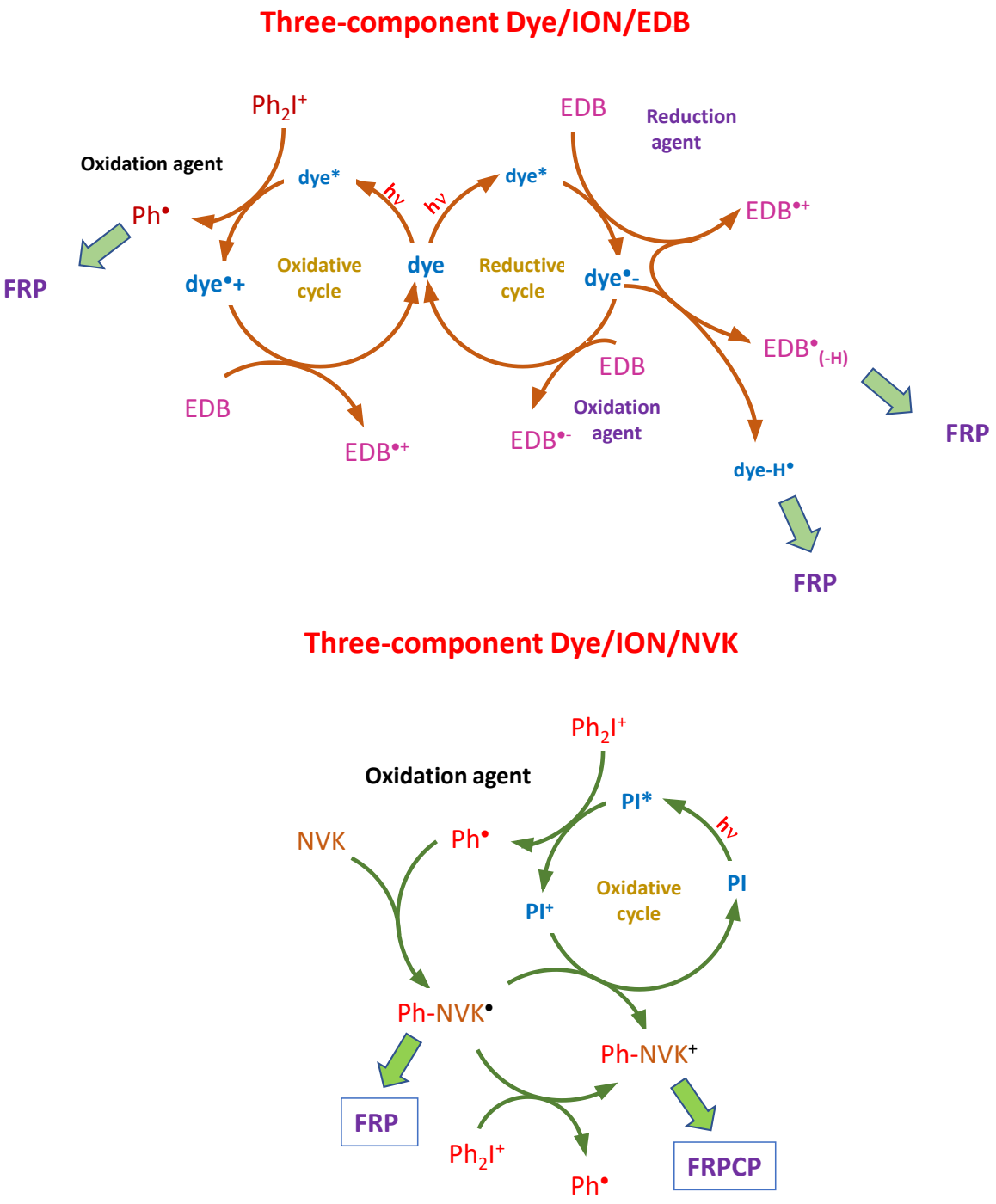


**Figure 21.** Photochemical mechanisms involved by two different three-component photoinitiating systems.

Polymerization tests of TPGDA carried out at 405 nm with the two-component OXE/ION (0.2%/1.0% w/w) and OXE/additives (1.0 wt%/1.0 wt%) revealed the two-component systems to furnish monomer conversions on par with that of OXE used alone. Among all systems investigated, only the OXE/ION combination could outperform the other photoinitiating systems and thus the unimolecular OXE system (See Figure 22). Addition of a third component enabled to improve the final monomer conversion by ca 10% compared to the previous two-component systems. Jointly, an improvement of the polymerization rates

could be observed (See Figure 23). It was thus concluded that a synergetic effect could be obtained by combining oxime esters with additives. In fact, due to the concomitant generation of initiating radicals by photodecomposition of oxime esters and the use of oxime esters as photosensitizers for the photodecomposition of the iodonium salt, the multiple generation of radicals contributed to improve the overall final monomer conversion.

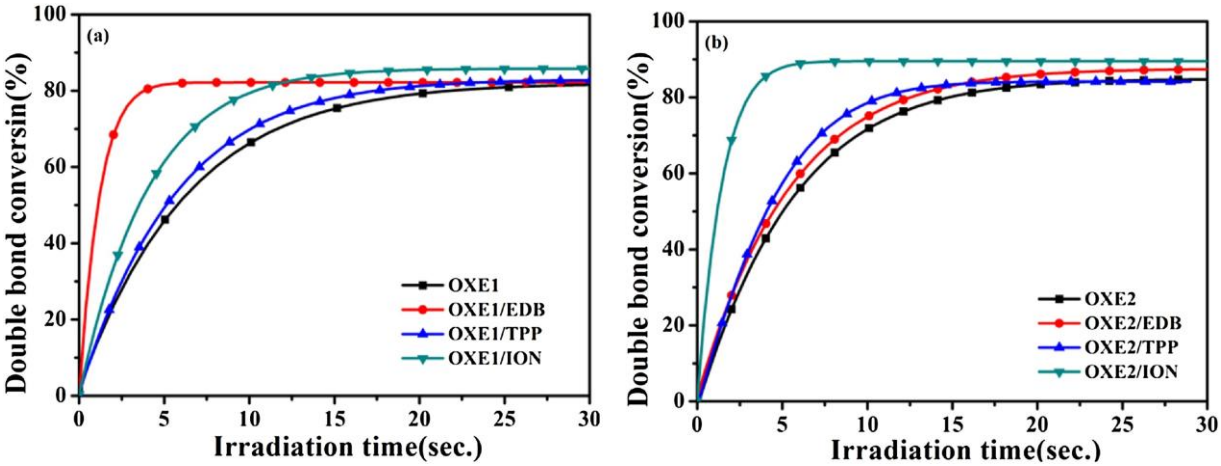


**Figure 22.** Polymerization profiles of TPGDA done at 405 nm using (a) TPA-OXE-1 (1.0 wt%), TPA-OXE-1/ION (0.2%/1.0% w/w), TPA-OXE-1/co-initiator (0.2%/1.0% w/w), (b) PTZ-OXE-2 (1.0 wt%) and PTZ-OXE-2/ION (0.2%/1.0% w/w) and PTZ-OXE-2/co-initiator (0.2%/1.0% w/w). Reproduced with permission of Ref. [269]

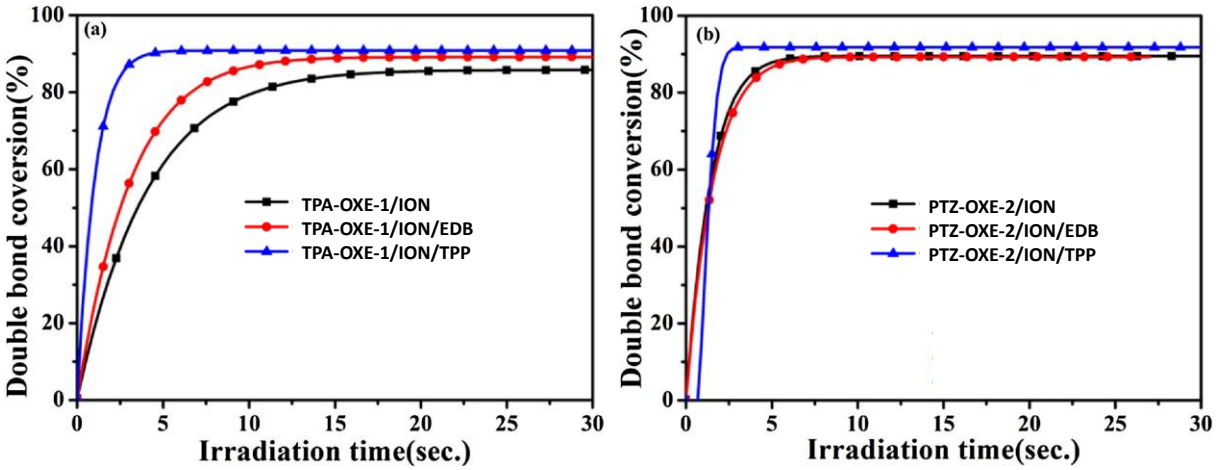


**Figure 23.** Polymerization profiles at 405 nm of TPGDA using (a) TPA-OXE-1/ION (0.2%/1.0% w/w) and TPA-OXE-1/ION/co-initiator (0.2%/1.0%/1.0% w/w/w), (b) PTZ-OXE-2/ION (0.2 %/1.0% w/w) and PTZ-OXE-2/ION/co-initiator (0.2%/1.0%/1.0% w/w/w). Reproduced with permission of Ref. [269]

Finally, the possibility to initiate a free radical promoted cationic polymerization of epoxides was examined with the polymerization of a bisphenol A epoxy resin i.e. E51. Using the three-component OXE/ION/NVK (0.2%/1.0%/1.0% w/w/w), final monomer conversions of 75% and 72% at 200 s could be obtained with TPA-OXE-1 and PTZ-OXE-2 (See Figure 24). These results are thus in agreement with the photochemical mechanism discussed above (See Figure 21).

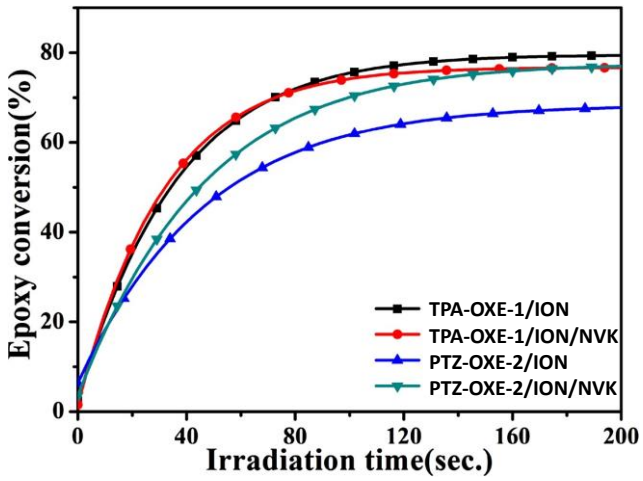


**Figure 24.** Photopolymerization profiles of E51 under air using OXE/ION(0.2%/1.0% w/w) and OXE/ION/NVK(0.2%/1.0%/1.0% w/w/w) upon irradiation at 405 nm. Reproduced with permission of Ref. [269]

### 1.3. Carbazole-based ether ring fused oxime esters.

In 2018, a series of ether ring-fused oxime esters was proposed by Tsuchimura and coworkers.[270] Introduction of ether rings at the periphery of the oxime function aimed at increasing the rigidity of the dye scaffold and to improve the radical generation quantum yield (See Figure 25).[271] Indeed, in order to improve the decomposition quantum efficiency of oxime esters, all processes of thermal inactivation enabling the dye to return from its excited state to its ground state have to be efficiently suppressed, what can be achieved by rigidifying the structure.

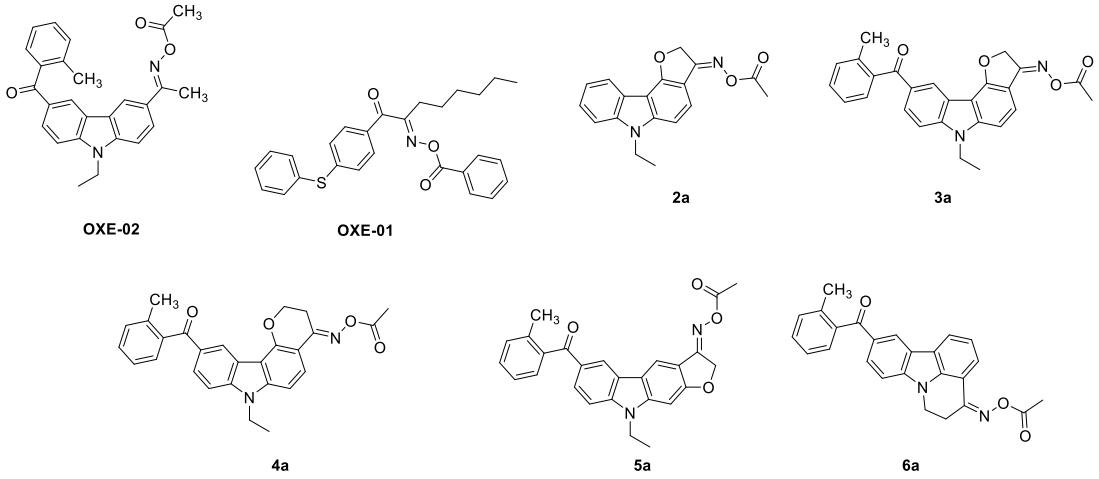


**Figure 25.** Chemical structures of ether ring-fused carbazole-based oxime esters.

From a mechanistic viewpoint, photodecomposition of oxime esters occurs after absorption of a photon of appropriate energy, so that oxime esters were promoted in the excited state (See Figure 26). By intersystem crossing, the electron transits from the singlet excited state to the triplet state. Upon decomposition, a biradical is formed by homolytic

cleavage of the N-O bond which evolves towards a carbon-centered radical acting as the initiating species.

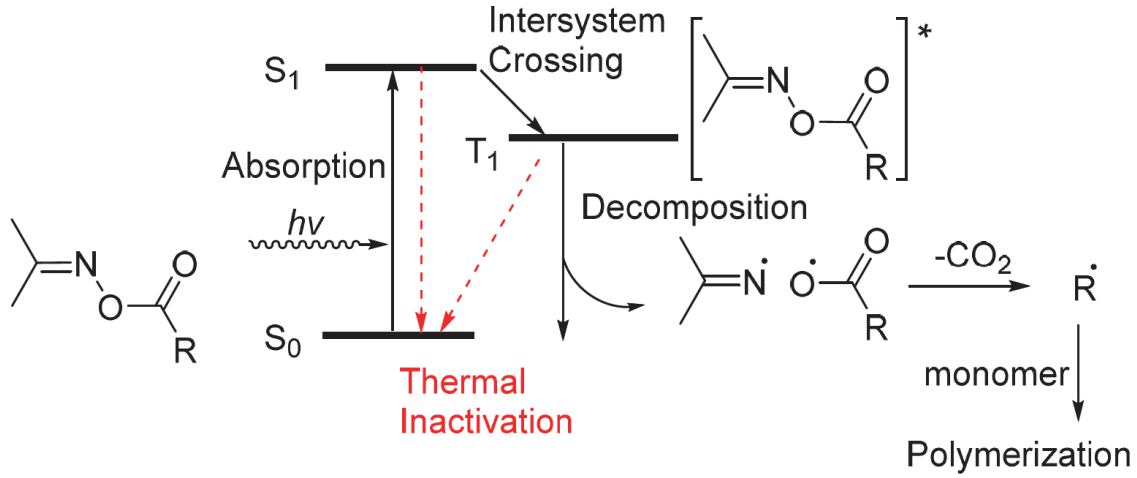


**Figure 26.** Mechanism of photocleavage of oxime esters.

Rigidification of the structures of 2a, 3a and 6a contributed to greatly improve the light absorption properties since a significant enhancement of the molar extinction coefficients could be determined, compared to OXE-02. Parallel to this, the more extended conjugation in 2a, 3a and 6a redshifted their absorptions to 360, 365 and 375 nm respectively (See Figure 27).

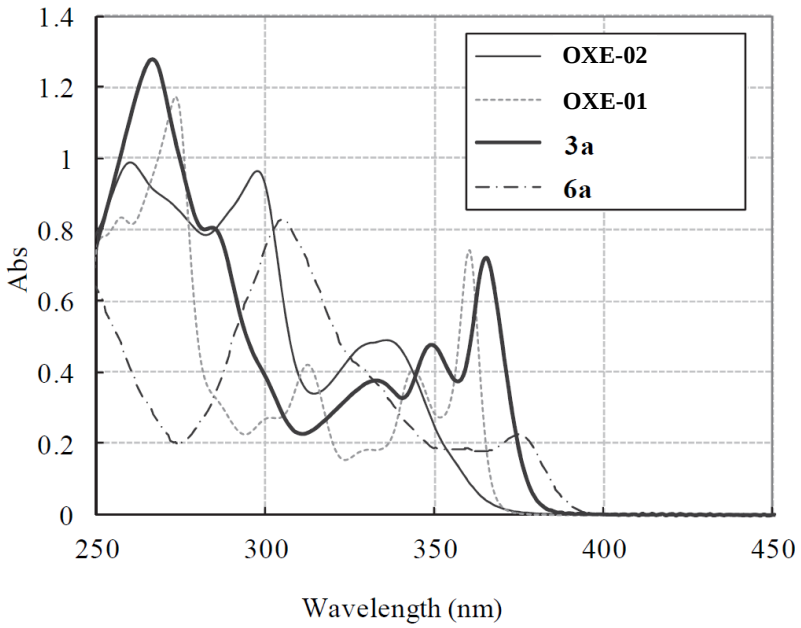


**Figure 27.** UV-visible absorption spectra of different oxime esters in ethyl acetate. Reproduced with permission of Ref.[270]

Photopolymerization experiments of HDDA at 365 nm revealed 2a and 6a to furnish lower monomer conversions than the reference compound OXE-02. An opposite situation was found for 3a, for which an enhancement of the monomer conversion by ca. 10% could be obtained compared to OXE-02 (See Figure 28).

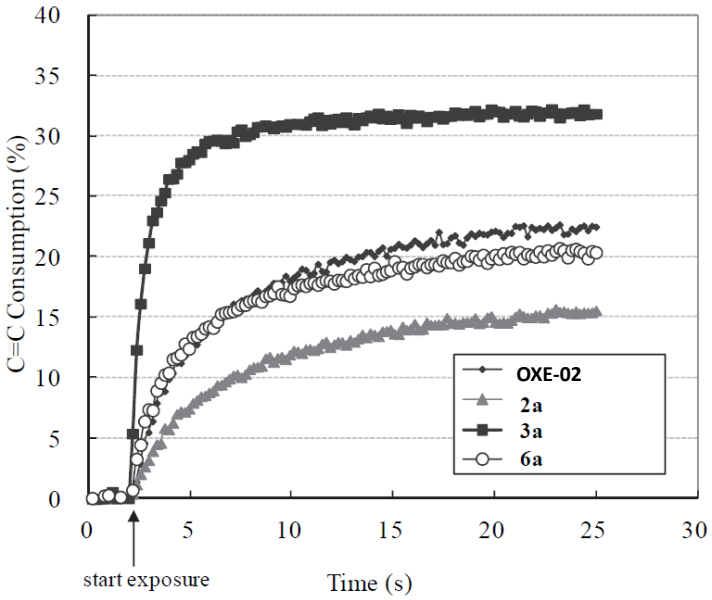


**Figure 28.** HDDA conversion obtained upon irradiation at 365 nm. Reproduced with permission of Ref.[270]

### 1.4. Nitrocarbazole-based oxime esters

Development of visible light photoinitiating system is an active research field and one efficient strategy to redshift the absorption of carbazole consists in introducing electron-withdrawing groups. This strategy was notably applied by Lalevée and coworkers who developed a series of three nitrocarbazole-based oxime esters (See Figure 29).[61] In this work, the authors demonstrated their nitrocarbazole-based oxime esters to exhibit a dual photochemical and thermal initiating ability.

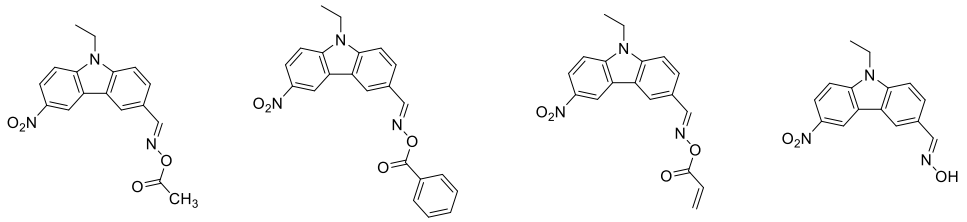


**Figure 29.** Chemical structures of nitrocarbazole-based oxime esters OXE-M, OXE-V, OXE-P and OXE-H

Interestingly, all carbazole dyes showed an absorption maximum located at 376 nm, no influence of the substitution pattern of the oxime ester group being detected. The highest molar extinction coefficient was determined for OXE-P (13 800 $M^{-1}.cm^{-1}$) due to the presence of the additional aromatic ring compared to OXE-M (13 000 $M^{-1}.cm^{-1}$) and OXE-V (12 400 $M^{-1}.cm^{-1}$). molar extinction coefficients of 4100, 3900, and 4100 $M^{-1}.cm^{-1}$ were respectively determined at 405 nm so that polymerization tests could be carried out at this wavelength. Photolysis experiments done in acetonitrile clearly evidenced the release of $CO_2$ during irradiation. Indeed, a new peak appearing at 2337 $cm^{-1}$ could be detected during the photolysis of oxime esters by real time Fourier transformed infrared spectroscopy (RT-FTIR) analyses during

irradiation.[272,273] Conversely, no release of $CO_2$ was detected for OXE-H, this oxime being not esterified and thus not capable to initiate any decarboxylation reaction upon irradiation. By theoretical calculations, the bond dissociation energy could be determined. Thus, N-O bond energies of 49.50, 48.62 and 48.07 kcal $mol^{-1}$ could be determined for OXE-V, OXE-M and OXE-P respectively. Markedly, energy of the triplet excited states of OXE-M, OXE-V, and OXE-P was determined by theoretical calculation and revealed the triplet state to be higher than their N-O bond dissociation energies, suggesting that photocleavage of oxime esters is favorable from the triplet excited state. Enthalpies of - 4.03, - 3.16 and -5.29 kcal $mol^{-1}$ were respectively calculated for the cleavage process of OXE-M, OXE-V, and OXE-P respectively. Photopolymerization experiments of TMPTA using the different OXEs at $2\times10^{-5}$ mol/g revealed OXE-M to overcome the final monomer conversion obtained with diphenyl(2,4,6-trimethylbenzoyl)phosphine (TPO) (69% vs 65% for TPO). This is directly related to the formation of methyl radicals after photocleavage. These radicals are the most reactive carbon-centered radicals.[274,275] This is the reason why the best monomer conversions were obtained with OXE-M. Conversely, lower monomer conversions were found for OXE-P and OXE-V (61 and 57% respectively). In this case, aryl and vinyl radicals exhibiting a lower reactivity that the methyl radicals are produced by decarboxylation, supporting the lower monomer conversions obtained with OXE-P and OXE-V. Finally, the lowest conversion was obtained for OXE-H (18%), consistent with the fact that OXE-H is not an oxime ester and can therefore not induce any photocleavage (See Figure 30). Higher monomer conversion obtained with OXE-M was assigned to the formation of methyl radicals which are more reactive than aryl radicals (formed by photodecomposition of OXE-P) or vinyl radicals (produced by OXE-V). This reactivity trend is consistent with previous results reported in the literature.[276]

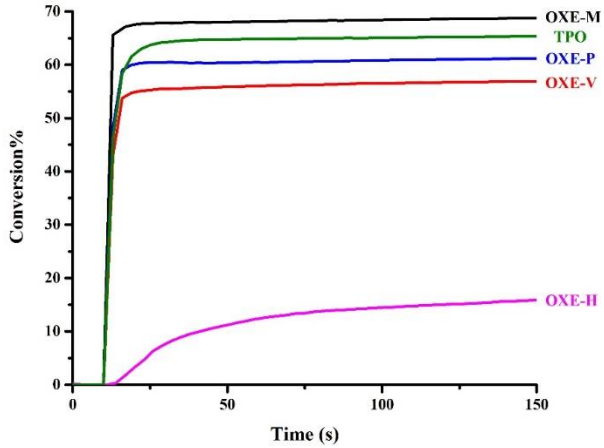


**Figure 30.** Photopolymerization profiles of TMPTA upon irradiation at 405 nm using OXE ($2 \times 10^{-5}$ mol/g). Reproduced with permission of Ref. [61]

Considering the high reactivity of OXE-M, direct laser write experiments but also 3D printing experiments were carried out (See Figure 31). In the two cases, patterns with a high spatial resolution could be obtained.

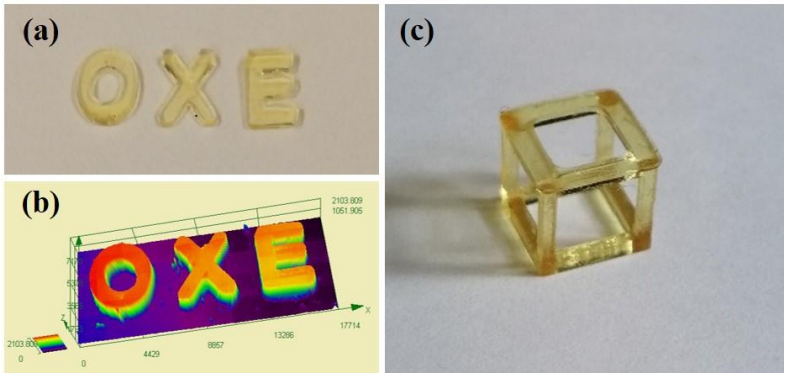


**Figure 31.** (a) The letter pattern "OXE" obtained by direct laser write; (b) Characterization of the letter pattern "OXE"; (c) 3D printed object of square frame (7×7×7 mm). Reproduced with permission of Ref. [61]

Finally, among the most interesting finding, OXE-M, OXE-V and OXE-P exhibited a dual photo/thermal initiating behavior. DSC experiments done in the dark revealed OXE-M to exhibit the lowest initiating temperature (113°C). For OXE-V and OXE-P, initiating temperatures higher than 150°C was determined. Due to the thermal initiation behavior of OXE-M, preparation of composites could be successfully achieved. By mixing TMPTA with 50% carbon fiber, prepregs were first irradiated at 395 nm to polymerize the surface then exposed to heat (150°C for 30 min.) to achieve a polymerization in depth. In turn, fully cured carbon fiber-based composites could be obtained (See Figure 32).

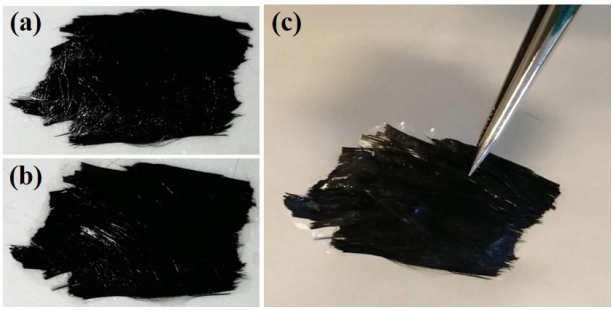


**Figure 32.** (a) Prepregs with resin/carbon fiber (50/50, wt%/wt%); (b) Surface cured prepregs; (c) Carbon fiber composite. Reproduced with permission of Ref. [61]

This year, the same authors examined a series of 50 nitrocarbazole-based oxime esters divided in five different series (See Figure 33).[63] In this work, influence of the oxime ester groups (acyloxy or aryloxy groups) on the photoinitiating ability, fine tuning of the solubility of oxime esters in resins by modifying the length of carbazole chains or the length of the lateral chains were examined in details. The key parameter to develop this large series of oxime esters was to use nitrocarbazole as the common scaffold for the design of all these dyes.

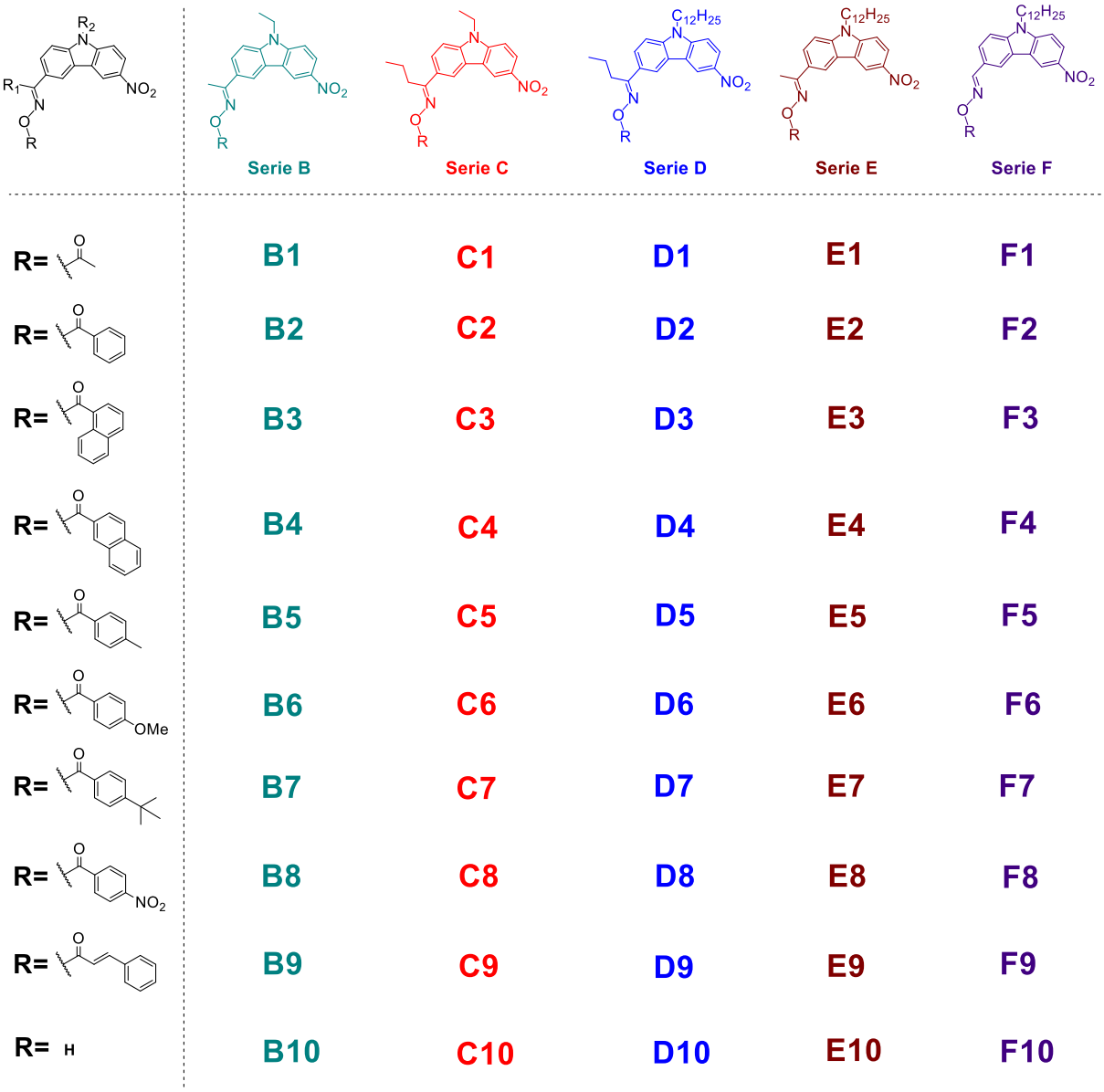


**Figure 33.** Chemical structures of nitrocarbazole-based oxime esters. Reproduced with permission of Ref. [63]

Interestingly, all oxime esters exhibited similar absorption maxima, ranging between 370 and 372 nm (See Figure 34 and Table 3). Considering that all dyes also possess comparable molar extinction coefficients, influence of the solubility, of the functionalizing groups used to form oxime esters on the photoinitiating ability could be examined in detail.

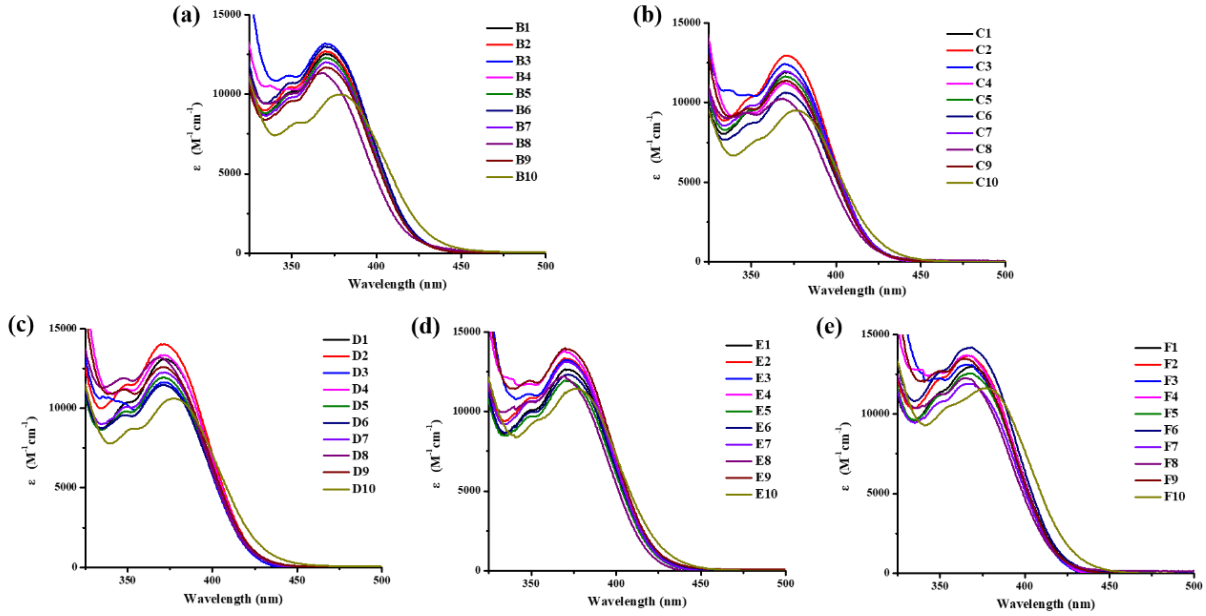


**Figure 34.** UV-visible absorption spectra of oxime esters in acetonitrile (a) OXEs based on Series B; (b) OXEs based on Series C; (c) OXEs based on Series D; (d) OXEs based on Series E; (e) OXEs based on Series F. Reproduced with permission of Ref. [63]

**Table 3.** Light absorption properties of some OXEs.

| PI | $\lambda_{max}$ (nm) | $\varepsilon_{max}$ ($M^{-1}cm^{-1}$) | $\varepsilon_{405\ nm}$ ($M^{-1}cm^{-1}$) |
|---|---|---|---|
| **B1** | 371 | 12500 | 4800 |
| **B2** | 371 | 12700 | 4700 |
| **C1** | 370 | 11900 | 4500 |
| **C2** | 370 | 12900 | 4600 |
| **D1** | 372 | 13000 | 5200 |
| **D2** | 372 | 14000 | 5400 |
| **E1** | 370 | 12700 | 5000 |
| **E2** | 370 | 13300 | 5100 |
| **F1** | 370 | 13000 | 4300 |
| **F2** | 370 | 13500 | 4200 |

Examination of the photoinitiating ability of oxime esters B1-B9, C1-C9, D1-D9, E1-E9 and F1-F9 was carried out by using TMPTA as the monomer and upon irradiation of the resins at 405 nm. As shown in the Table 4, oxime esters exhibiting the highest monomer conversions

were still OXEs 1 and 2 bearing acetyl or benzoyl groups. The worse monomer conversions were still obtained for OXEs 8 bearing a nitrobenzoyl group. In that case, the lower reactivity of the nitrobenzoyl radicals was assigned to the electron-withdrawing ability of the nitro group, deactivating the radicals. Noticeably, by comparing the different series, the best monomer conversions were obtained with the series D, bearing a dodecyl chain on carbazole and a butyryl group as the lateral chain. Overall, the best conversions were obtained for the carbazole derivatives bearing a maximum of solubilizing chains. Comparison of the monomer conversions of oxime esters with that of TPO (66% conversion) revealed that only OXEs bearing an acetyl substituent (B1, C1, D1, E1 and F1) could outperform the benchmark photoinitiator. Once again, C1, D1 and F1 are the oxime esters bearing the longest solubilizing chains of the five series. Some OXEs such as D4 and D5 showed remarkable performances compared to their analogues of the other series. Considering that all dyes have been designed to exhibit similar absorption properties, other parameters such as the decarboxylation reaction but also the reactivity of the generated radicals drastically impact the photoinitiation ability. Determination of the enthalpy for the decarboxylation reaction revealed the decarboxylation process to only be favorable for oxime esters bearing an acetyl group. For all the other, a less favorable decarboxylation process was evidenced, supporting the lower reactivity of the B/C/D/E/F 2-9 series compared to the B/C/D/E/F 1 series (See Table 5).

**Table 4.** The final function conversions (FCs) of TMPTA in the presence of OXEs.

| PI | **B1** | **B2** | **B3** | **B4** | **B5** | **B6** | **B7** | **B8** | **B9** | **B10** |
|---|---|---|---|---|---|---|---|---|---|---|
| FC (%) | 64 | 54 | 30 | 50 | 42 | 43 | 48 | 15 | 47 | 23 |
| PIs | **C1** | **C2** | **C3** | **C4** | **C5** | **C6** | **C7** | **C8** | **C9** | **C10** |
| FC (%) | 67 | 58 | 53 | 61 | 50 | 46 | 54 | 37 | 54 | 34 |
| PI | **D1** | **D2** | **D3** | **D4** | **D5** | **D6** | **D7** | **D8** | **D9** | **D10** |
| FC (%) | 68 | 62 | 56 | 61 | 59 | 58 | 58 | 41 | 55 | 35 |
| PI | **E1** | **E2** | **E3** | **E4** | **E5** | **E6** | **E7** | **E8** | **E9** | **E10** |
| FC (%) | 64 | 53 | 55 | 51 | 40 | 48 | 50 | 35 | 41 | 34 |
| PI | **F1** | **F2** | **F3** | **F4** | **F5** | **F6** | **F7** | **F8** | **F9** | **F10** |
| FC (%) | 68 | 56 | 54 | 58 | 45 | 51 | 53 | 36 | 57 | 38 |

**Table 5.** Enthalpies for the decarboxylation reactions for different acyloxy and aryloxy groups. Reproduced with permission of Ref. [63]

| Decarboxylation reactions | $\Delta H_{decarboxylation}$ (kcal $mol^{-1}$) |
|---|---|
| 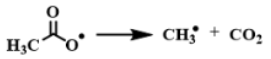 | -4.94 |
| 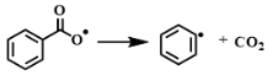 | 5.92 |
| 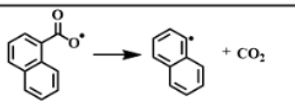 | 4.36 |
| 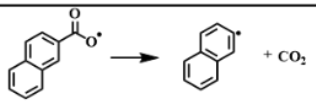 | 6.24 |
| 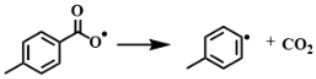 | 6.92 |
| 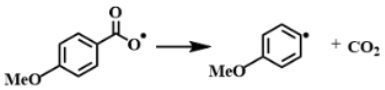 | 8.77 |
| 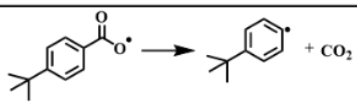 | 6.97 |
| 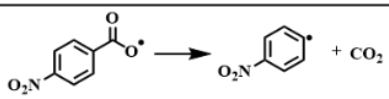 | 3.14 |
| 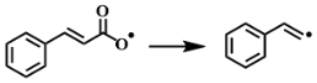 | 7.64 |

Examination of the thermal initiating ability of B1, C1, D1, E1 and F1 revealed B1 and D1 to exhibit low initial temperature of polymerization. Indeed, temperatures as low as 83 and 82°C were determined for B1 and D1 respectively. Overall, this series of 50 oxime esters exhibited an unprecedented dual thermal/photochemical initiating behavior.

**1.5. Carbazole-coumarins hybrid oxime esters.**

Carbazoles and coumarins have been extensively used for the design of Type II photoinitiators.[60,194] Their combination for the design of Type I photoinitiators was thus logical, what was done by Joyeux and coworkers.[277] Four coumarin-carbazole fused structures were designed, bearing an acetyl or a benzoyl group as functionalizing agents of oximes (See Figure 35). Noticeably, photodecomposition rate of oxime esters was clearly influenced by the group attached the carbon of the oxime group. Thus, by replacing an isopropyl by an ethyl group, higher photodecomposition rates were determined. Parallel to this, photoinitiating ability of OXE was mainly driven by the ester group of oximes. Thus, as

previously observed, replacement of the *O*-benzyl group by an *O*-acetyl group furnished radicals exhibiting a higher reactivity. Once again, photoinitiating efficiencies of OXEs largely departed from their absorption properties. Thus, photopolymerization performances increased by more than two orders of magnitude by shifting the irradiation wavelength from 365 nm by 425 nm.

Examination of the UV-visible absorption characteristics of the different OXEs in acetonitrile revealed the dyes to exhibit similar absorption properties, with absorption maxima at 374 nm. Logically, no influence of the lateral chains (ethyl or isopropyl) nor the functionalizing group of the oxime was found (See Figure 36). A long tail extending until 425 nm could be determined, enabling to perform polymerization tests in the visible range. In order to get insight into the photodissociation mechanism of OXEs, attempts to identify by-products and transient species formed during irradiation of oxime esters was carried out. By combining real-time $^{1}H$ NMR in $CDCl_3$ and ESR-ST experiments in *tert*-butylbenzene.

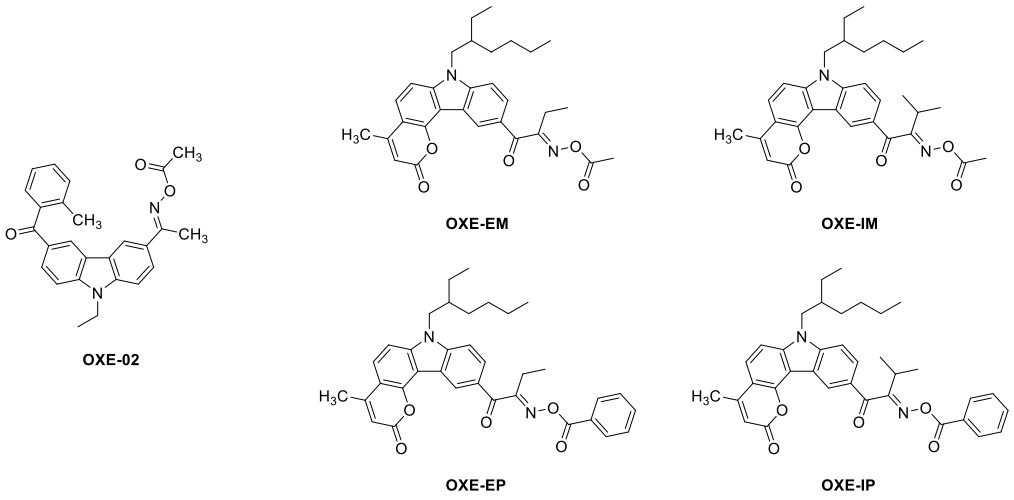


**Figure 35.** Chemical structures of coumarin-carbazole based oxime esters. From ref. [277]

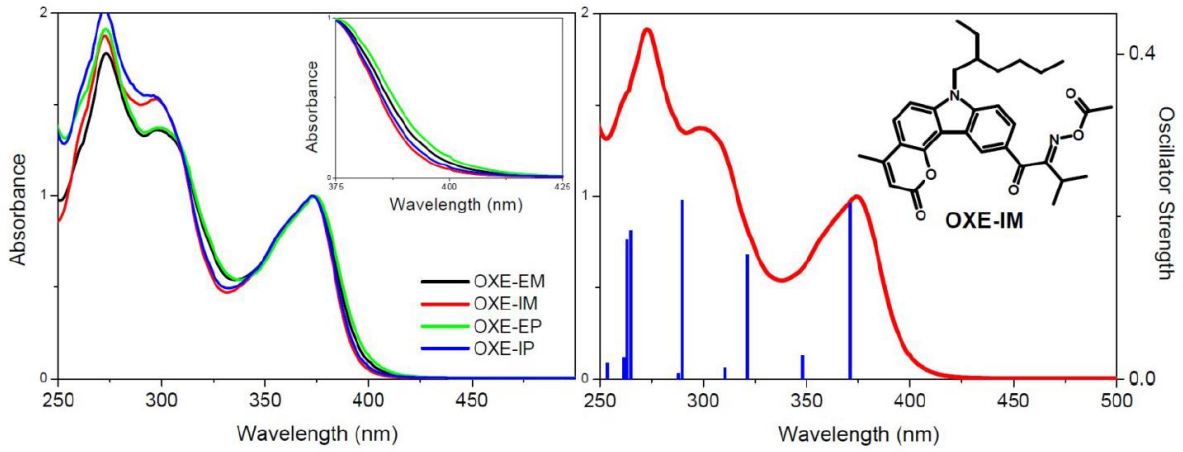


**Figure 36.** Left : Normalized UV-visible absorption spectra of carbazole-coumarin fused oxime esters in acetonitrile. Right : theoretical UV-visible absorption spectra. Reproduced with permission of Ref. [277]

Notably, formation of propanenitrile during irradiation could be evidenced. Parallel to this, identification of a product corresponding to the recombination of iminyl radicals and methyl radicals could be identified as another structure (See Scheme 1).

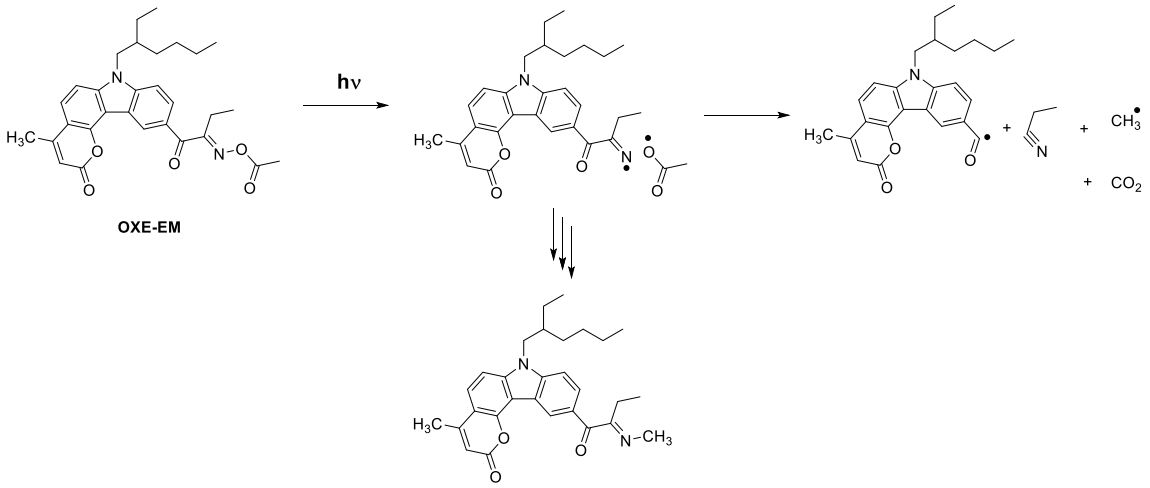


**Scheme 1.** By-products formed during irradiation of OXE-EM.

Free radical polymerization experiments of TPGDA carried out with the different OXEs revealed these oxime esters to act as thermal initiators. Thus, polymerization reactions could be heated at temperatures higher than 140°C. A remarkable stability of the resins could be evidenced. Thus, after several months of storage in the dark, similar final monomer conversions could be determined with the different dyes. Evaluation of the monomer conversions obtained upon irradiation of TMPTA at 365, 385, 405 and 425 nm (I = 5 mW/cm²) revealed a similar to that observed by Barner-Kowollic. Thus, the best monomer conversions were reached in spectral regions where oxime esters only hardly absorb.[258] Therefore, once again, a wavelength-dependent reactivity departing from the absorption properties of the different dyes was evidenced. Interestingly, if OXE-02 could outperform the different OXEs at

365 and 385 nm, an opposite trend was found at 405 and 425 nm for which no polymerization could be detected anymore for OXE-02. Therefore, interest for these carbazole-coumarin fused structures was clearly evidenced by enabling to initiate polymerization processes at 425 nm, at an irradiation wavelength where the benchmark OXE-02 does not operate anymore.

Analysis of the ground state properties of the different OXE by theoretical calculations revealed several interesting features. Thus, all compounds exhibited a planar conformation enabling an efficient π-electronic delocalization within the structures. Second, the C-C bond twist angles between the coumarin core and the adjacent ketone varied between 0.3 and 8.1°, letting the two groups almost co-planar. Third, the C-C bonds between the C=O and the C=N groups are clearly more twisted than the previous angles since a twist angle ranging between 19 and 23° for the ethyl derivatives. This value increased up to 43°C for all isopropyl derivatives (See Figure 37). Consequently, the important twist angle in OXE-EP and OXE-IP precludes any electronic coupling with the rest of the molecules, adversely affecting their photoinitiating abilities.

| PI | $\Theta_1$ | $\Theta_2$ |
|---|---|---|
| **OXE-EM** | 7.6° | 19.4° |
| **OXE-IM** | 0.3° | 43.1° |
| **OXE-EP** | 8.1° | 23.1° |
| **OXE-IP** | 1.7° | 42.7° |

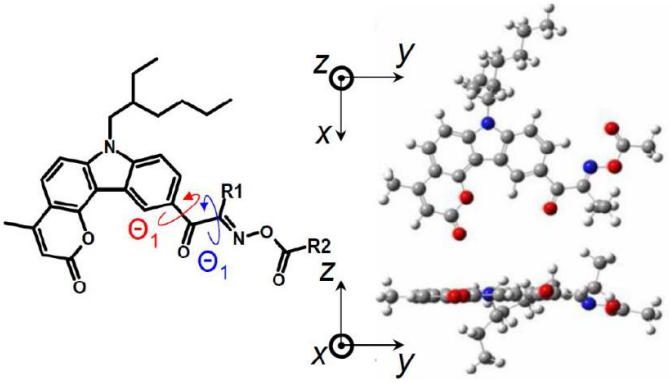


**Figure 37.** Twist angles determined by theoretical calculations for the different carbazole-fused coumarins. Reproduced with permission of Ref. [277]

By theoretical calculations, absorption band detected at low energy was determined as encompassing two electronic transitions. Thus, the $S_0 \rightarrow S_1$ was determined as mainly arising from a HOMO-LUMO transition admixed with a charge transfer character. Notably, a ππ*-delocalization from the coumarin core towards the oxime ester group was found. Parallel to this, the $S_0 \rightarrow S_2$ transition exhibited a nπ* character and was mainly located onto the oxime ester group.

After cleavage of the N-O bond, an iminyl and an acyloyl group are produced. Crucial role of the imine-based transient species which can react with the acrylic monomer was also evidenced, promoting an alternative competing reaction sequence to polymerization. Notably, photolysis experiments revealed OXE-EM to exhibit similar photobleaching rates when irradiated at 365 nm or 405 nm. An opposite situation was found in the presence of methyl methacrylate (MMA) and divergent photolysis behaviors could be detected, depending of the irradiation wavelength. Thus, formation of an imine-based derivative could be determined at 405 nm, with an absorption band located in the 320-400 nm range. Conversely, upon irradiation at 365 nm, no apparent formation of this imine derivative could be detected.

Photolysis experiments of OXE-EM at 405 nm revealed two distinctive regimes corresponding first to a rapid production of imines in first step followed in second step by a progressive decrease of this by-product in the presence of MMA, resulting from its consumption. Overall, both reactants and imine byproducts can induce additional reaction pathways compared to that observed at 365 nm that can strongly impact the polymerization process and therefore the final monomer conversions. Indeed, at 405 nm, both reactants and imine byproducts strongly absorb, contributing to photopolymerization whereas the imine byproducts only weakly absorb at 365 nm. At 365 nm, imine-based transient species can also promote an alternative photoinduced reaction to the detriment of the photoinitiation step, adversely affecting the polymerization efficiency.

**1.6. Carbazole-based oxime esters.**

With aim at developing original carbazole-based oxime esters, several groups examined the possibility to introduce the oxime ester moiety at other positions of carbazole than the usual 3 and 6-positions. Thus, the group of Zhiquan Li examined two families of oxime esters differing by the position of oxime functions at the 3,6- or 2,7-positions with regards to the carbazole central group (See Figure 38).[278] In order to redshift the absorption spectra of oxime esters, a A-π-D-π-A structure was employed. These structures reported in 2020 were also the first examples of bifunctional oxime esters to be reported. Noticeably, by changing the position of the π-bridge from the 3,6-positions to the 2,7-positions, a redshift of the absorption spectra was found for 4c and 4d compared to their analogues 4a and 4b. Besides, no major change was found for the positions of the absorption maxima, ranging from 377 nm for 4a and 4b to 371 nm for 4c and 4d. As a result of this redshift, higher molar extinction coefficients were found for 4c and 4d at 405 nm (42 and 38 × $10^3$ $M^{-1}.cm^{-1}$) compared to 4a and 4b (7 and 6 × $10^3$ $M^{-1}.cm^{-1}$) (See Figure 39).

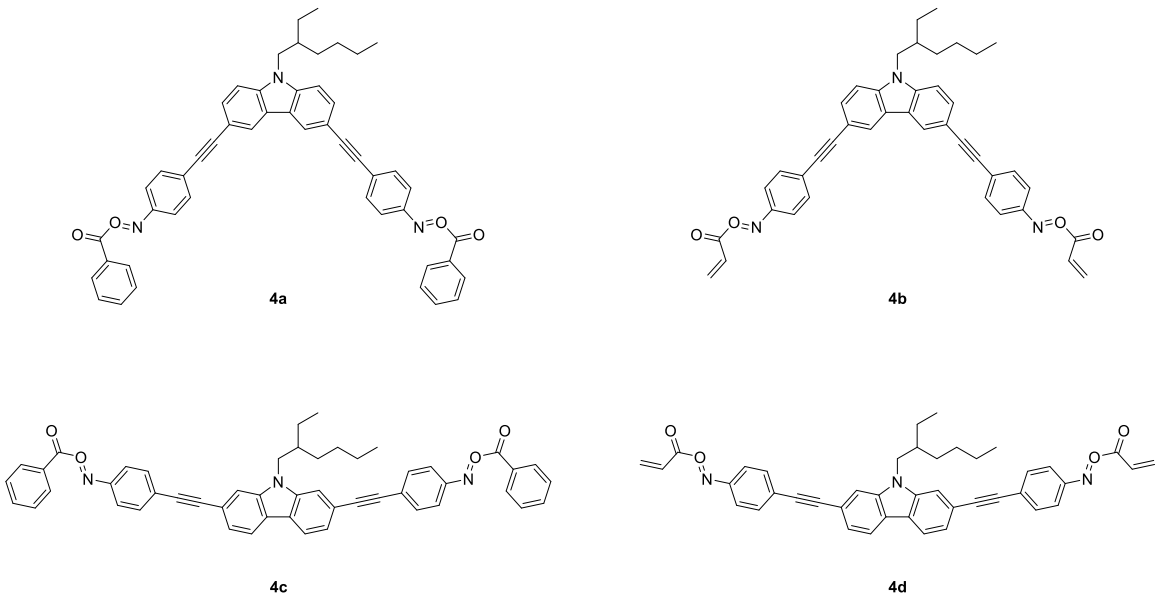


**Figure 38.** Chemical structures of oxime esters developed by Li and coworkers. From ref. [278]

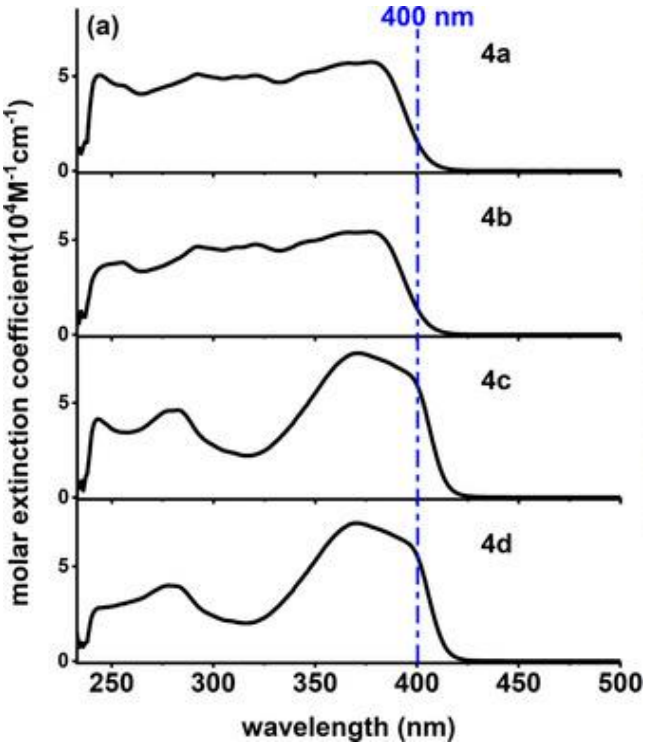


**Figure 39.** UV-visible absorption spectra of oxime esters in chloroform. Reproduced with permission of Ref. [278]

As observed for the previous oxime esters detailed in this review, photolysis of Type I photoinitiators resulted in a blueshift of their absorptions together with a significant decrease of the optical density in the visible range, what is beneficial for the polymerization depth. Polymerization tests carried out at 405 nm using TMPTMA as the resin revealed 4c to be unable to initiate any polymerization due to the lack of solubility in resins. Replacement of the benzoyl group in 4a by a vinyl group in 4b greatly improved the monomer conversion from 40 to 57% after 300 s of irradiation. This trend is consistent with the results obtained by other groups for which none-aromatic radicals are more inclined to add on the carbon-carbon bond of monomers. Noticeably, on a marginal improvement of the monomer conversion was observed by changing the π-bridge from the 3,6-position in 4b to the 2,7-position in 4d. Comparisons with the reference compound TPO revealed the different carbazole derivatives to give lower monomer conversions (See Figure 40). Considering that 4d is the most efficient oxime ester, 3D printing experiments were carried out, giving 3D patterns with an excellent spatial resolution, even at very low photoinitiator content (0.5 wt%).

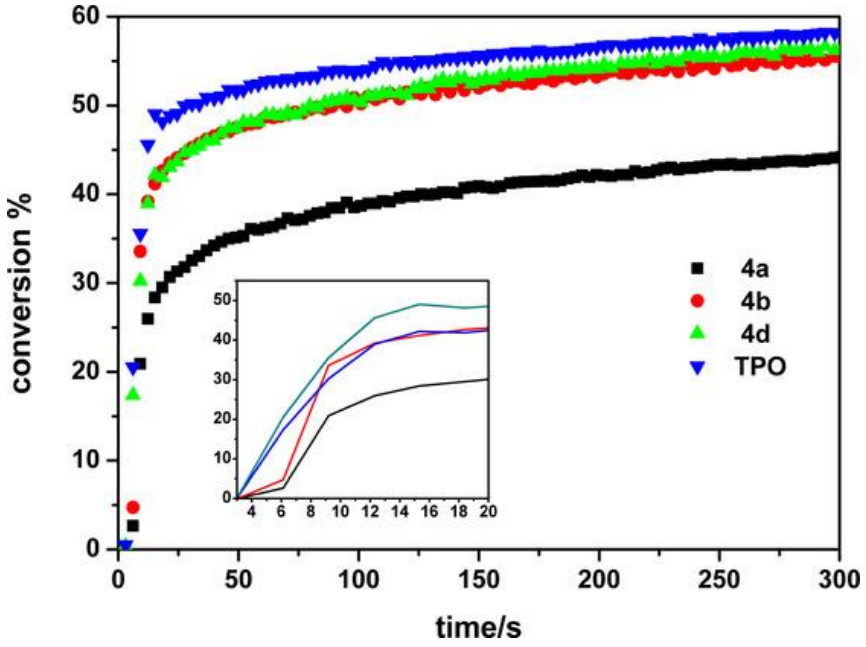


**Figure 40.** Polymerization profiles of TMPTMA upon irradiation at 405 nm and using the different OXE at 1.3 × $10^{-6}$ mol/g resin. Reproduced with permission of Ref. [278]

From a mechanistic viewpoint, occurrence of a triplet photodecomposition pathway was proposed for the different photoinitiators. Thus, theoretical calculations revealed the $S_1$ and $T_1$ excited states to be populated by a HOMO-LUMO $\pi\pi^*$-electron excitation (where HOMO and LUMO respectively stand for highest occupied molecular orbital and lowest unoccupied molecular orbital). Noticeably, examination of the electronic distribution on the different molecules revealed the HOMO energy level to be located onto the carbazole moiety whereas the LUMO energy level was centered onto the oxime moiety. Upon excitation of the molecule, one electron is promoted in the singlet excited state and by intersystem crossing, the triplet excited state can be populated. By structural relaxation and molecular geometry rearrangement, the $T_1$ state can undergo a relaxation resulting from electron distribution changes induced by the excitation. The relaxed triplet state can thus undergo an exergonic formation of reactive radicals capable to start polymerizations (See Figure 31). Notably, a bond dissociation energy of 63 kJ/mol from the triplet state and an enthalpy of decarboxylation of 39 kJ/mol could be determined by theoretical calculations.

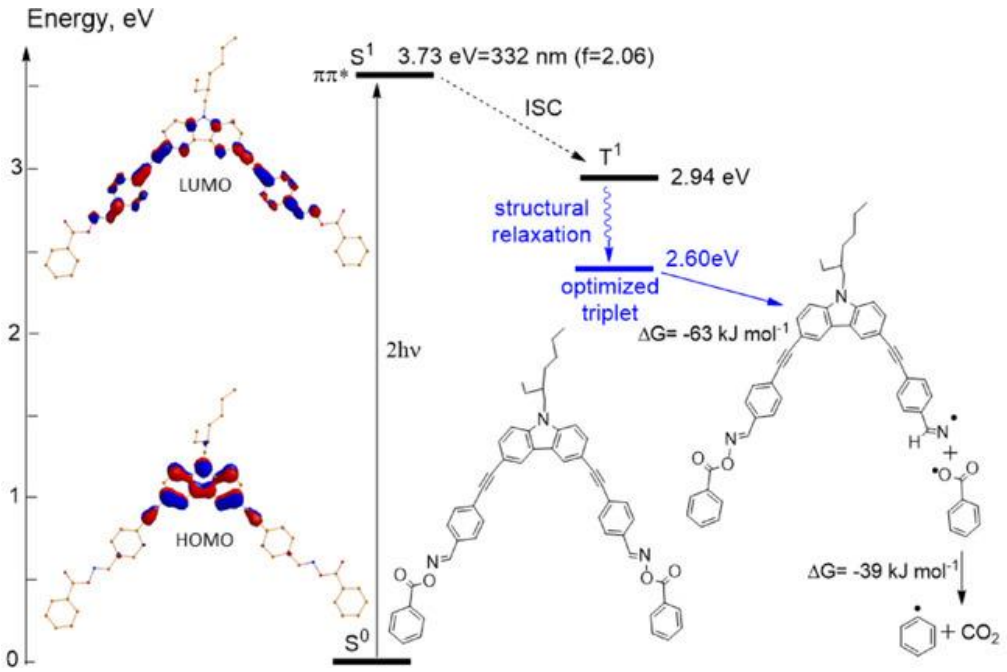


**Figure 41.** Reaction pathway enabling the formation of initiating species. Calculated in acetonitrile at the TDM06-2X/6-31G(d,p)/PBF level. Reproduced with permission of Ref. [278]

Finally, the different dyes proved also to be excellent candidates for two-photon polymerization. Following this work, the same authors investigated another family of carbazole where the oxime function was connected to carbazole by mean of the nitrogen atom (See Figure 42).[279]

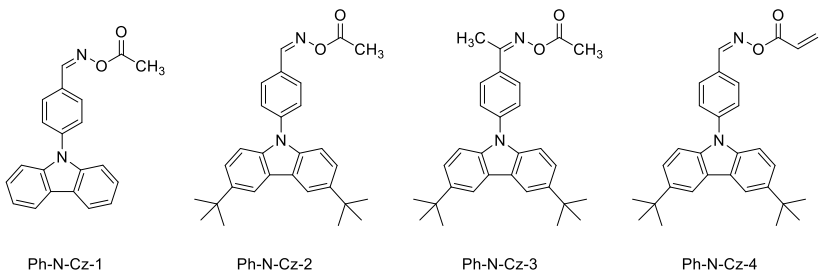


**Figure 42.** Chemical structures of Ph-N-Cz-1- Ph-N-Cz-4.

Among the most interesting findings, Ph-N-CZ-2 clearly outperformed Ph-N-CZ-3 during the FRP of TMPTA. As the main difference, Ph-N-CZ-2 has been prepared starting from an aldehyde whereas Ph-N-CZ-3 was obtained from a ketone. Parallel to this, the higher reactivity of the methyl radicals compared to the vinyl radicals was confirmed in this work. Comparison with OXE-02 and TPO also revealed Ph-N-CZ-2 to give lower monomer conversions than the reference compounds (See Figure 43). Besides, it has to be noticed that TPO can produce simultaneously four radicals contrarily to carbazole-based OXEs that can only produce one. Therefore, the only 10% reduction of the monomer conversion for the carbazole-based OXEs highlight their high reactivities.

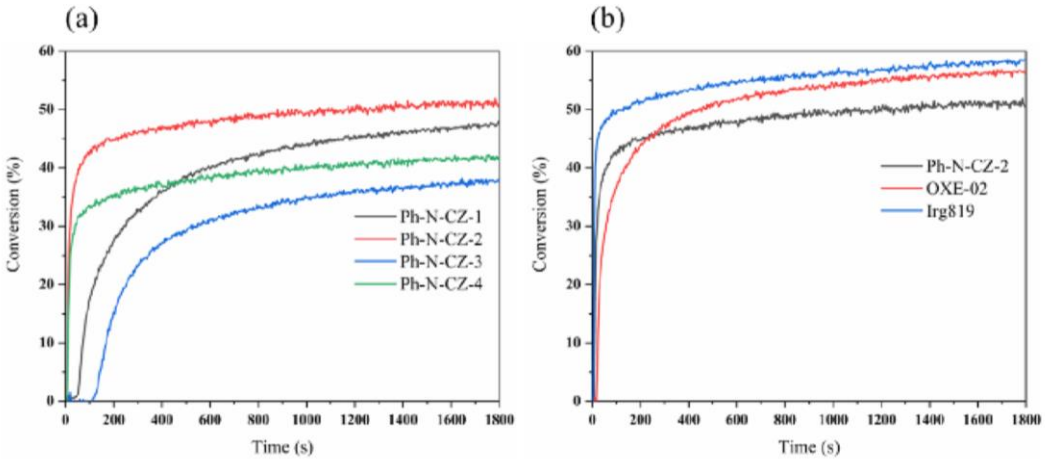


**Figure 43.** Polymerization profiles of TMPTA obtained with the carbazole based photoinitiators (a) and the reference compounds (b) upon irradiation at 405 nm (I = 10 mW/cm²). Reproduced with permission of Ref. [279]

Calculated frontier orbitals of photoinitiators revealed a good coplanarity between the carbazole moiety and the cleavable groups. As shown in the Figure 44, the substitution pattern of the oxime function did not significantly influence the electronic distribution of the frontier orbitals. Noticeably, theoretical calculations revealed the electronic cloud initially distributed onto the carbazole moiety to be shifted towards the oxime group after excitation, facilitating the cleavage of the N-O bond. Introduction of *tert*-butyl groups at the 3,6-positions of carbazole significantly reduced the energy required for the HOMO-LUMO transition in Ph-N-CZ-2 and Ph-N-CZ-4, rendering these two oxime esters to be more prone to photocleavage than the others.

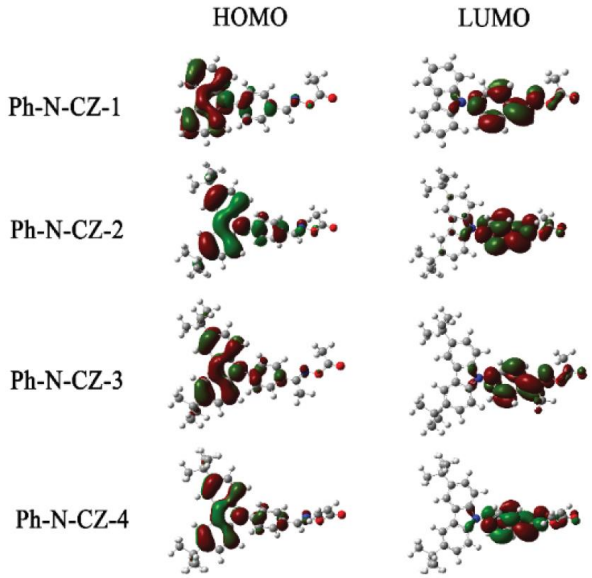


**Figure 44**. Frontier orbitals of Ph-N-CZ-1-Ph-N-CZ-4. Reproduced with permission of Ref. [279]

### 1.6. *Bis*-carbazole-based oxime esters.

This year, improvement of the molar extinction coefficients in the visible range could be obtained by fusing carbazole units together.[280] In this work reported by Lalevée and coworkers, a series of nine structures were designed, differing by the substitution of the oxime ester function (See Figure 45). Thus, *O*-acyloxy or *O*-benzoyloxy derivatives were designed and synthesized. It has to be noticed that if the 5,12-dialkyl-5,12-dihydroindolo[3,2-*a*]carbazole has been reported for the first time in 2019,[281] only few works were devoted to investigate the chemistry of this interesting building block, and especially to asymmetrize the substitution of this *bis*-carbazole structure.[62,64] From the absorption viewpoint, all oxime esters exhibit similar absorption properties, enabling to determine exactly the reactivity of the different groups attached to the oxime function (See Figure 46). Thus, for all dyes, absorption maxima located at 379 nm could be determined. All dyes showed a long tail extending in the visible range. Especially, the best absorption was found for the nitrobenzoyl derivatives (dye 9), outperforming the other dyes in terms of molar extinction coefficients (See Table 5). Based on their absorption at 405 nm, polymerization tests could be carried out at this wavelength. Solubility of photoinitiators is a major issue in photopolymerization as it can adversely affect the monomer conversion. For this reason, a second series of compounds 2′-10′ was designed, differing from the series 2-10 by the length of the alkyl chain (a methyl chain for 2′-10′ vs. a hexyl chain for 2-10). No modification of the absorption spectra was found between the 2-20 and 2′-10′ series.

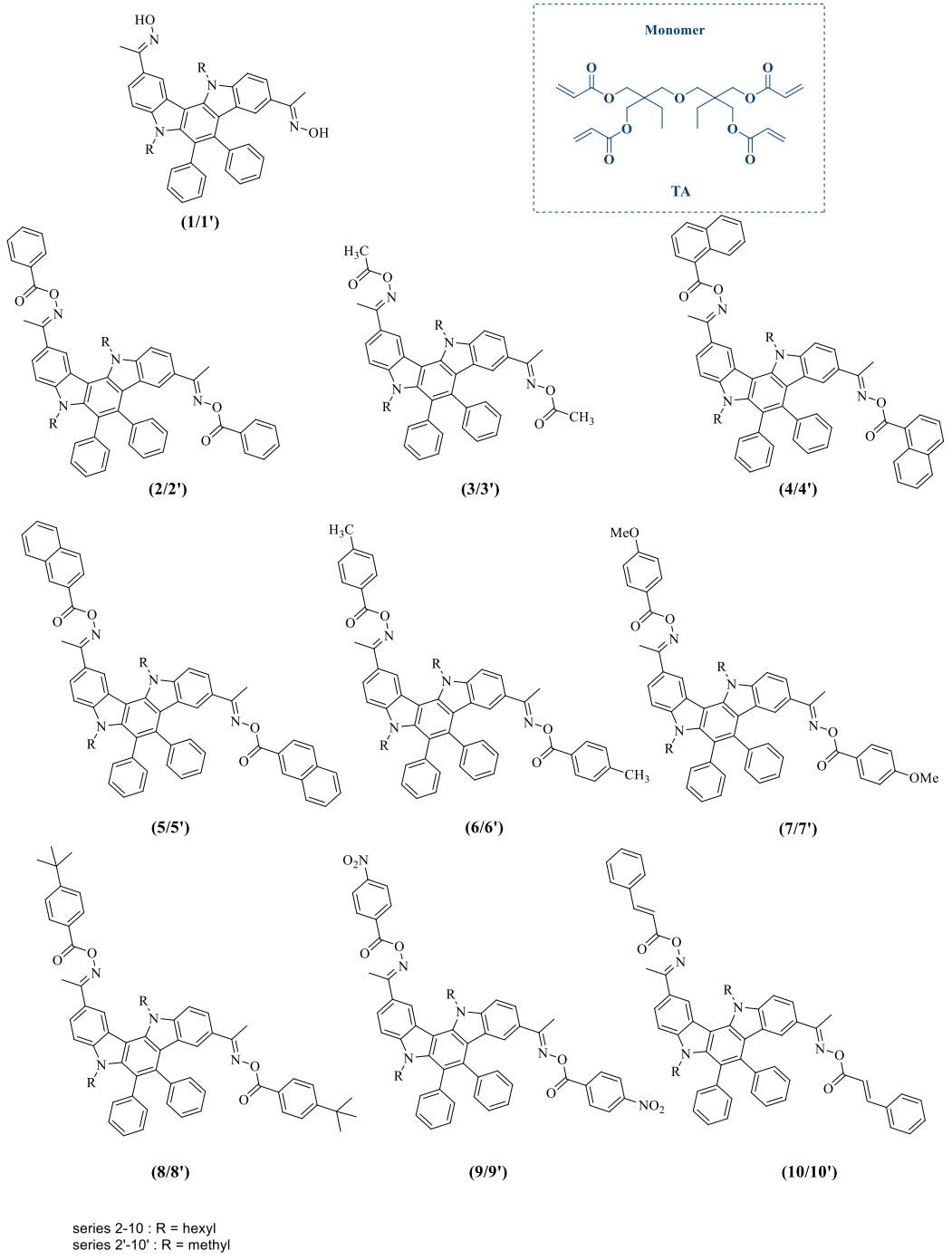


**Figure 45.** Chemical structures of 5,12-dialkyl-5,12-dihydroindolo[3,2-*a*]carbazole-derived oxime esters 2-10 and 2'-10' and the monomer (TA). From ref. [280]

Polymerization tests carried out in TMPTA upon irradiation with a LED emitting at 405 nm confirmed the superiority of the methyl radicals over the others in thick and thin films. As shown in the Figure 47, an improvement of ca 20% of the TMPTA conversion could be obtained with dye 3 (See Table 6). The lowest TMPTA conversions were obtained for 7/7' and 9/9', bearing respectively an electron-withdrawing or an electron-releasing group.

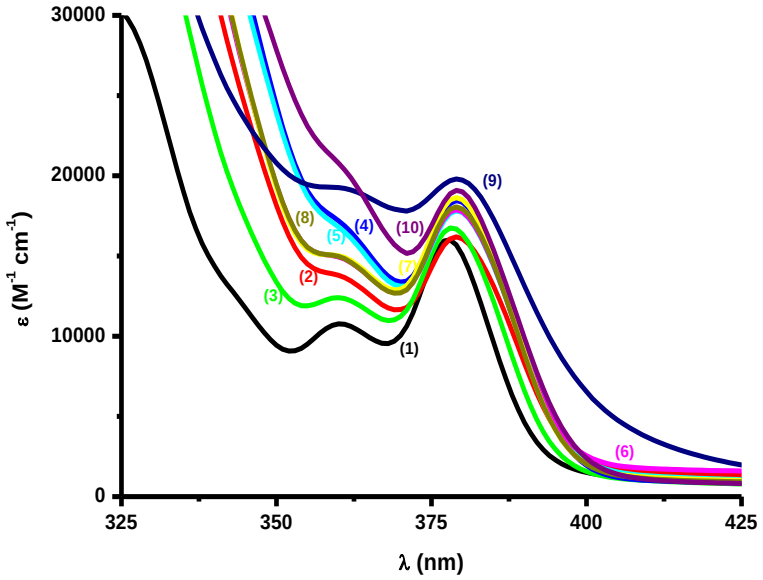


**Figure 46.** UV-visible absorption spectra of oxime-esters **(1)-(10)** in toluene. Reproduced with permission of Ref. [280]

**Table 5.** Light absorption properties of the proposed structures **(1)-(10)**; maximum absorption wavelengths ($\lambda_{max}$), extinction coefficients at $\varepsilon_{max}$ and extinction coefficients at 405 nm.

| PI | $\lambda_{max}$ (nm) | $\varepsilon_{max}$ ($M^{-1}$ $cm^{-1}$) | $\varepsilon_{(405nm)}$ ($M^{-1}.cm^{-1}$) |
|---|---|---|---|
| **(1)** | 378 | 16000 | 1260 |
| **(2)** | 379 | 16200 | 1720 |
| **(3)** | 378 | 16700 | 1145 |
| **(4)** | 379 | 18450 | 1200 |
| **(5)** | 379 | 17800 | 1535 |
| **(6)** | 379 | 17900 | 1930 |
| **(7)** | 379 | 18650 | 1400 |
| **(8)** | 379 | 18000 | 1335 |
| **(9)** | 379 | 19800 | 4780 |
| **(10)** | 379 | 19000 | 1395 |

As anticipated, reduction of the solubilizing chain in 2′-10′ resulted in a severe reduction of the monomer conversion, demonstrating once again that the reactivity is governed by the solubility of oxime esters in resins.

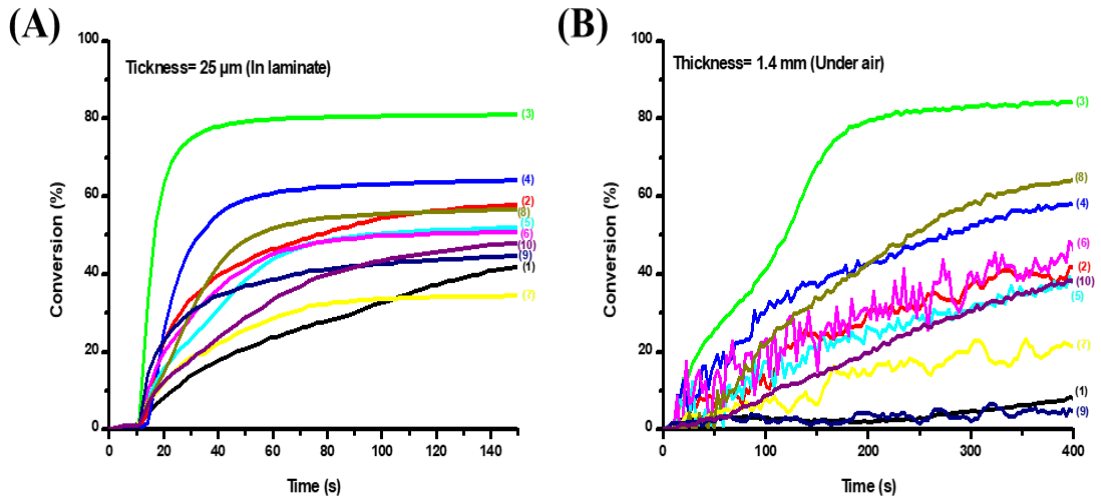


**Figure 47.** (A) Polymerization profiles of oxime esters **(1)-(10)** (0.5% w) in TMPTA in laminate (thickness = 25 µm) upon exposure to LED light $\lambda$ = 405 nm using OXE (0.5% w). (B) Polymerization profiles of oxime esters **(1)-(10)** (0.5% w) in TMPTA under air (thickness = 1.4 mm) upon exposure to LED light $\lambda$ = 405 nm using OXE (0.5% w). Reproduced with permission of Ref. [280]

**Table 6.** Final acrylate function conversions (FCs) and polymerization rates for TMPTA using one component (0.5% w) photoinitiators after irradiation with LED light (◎= 405 nm).

| OXE | Thin sample (25 µm) in laminate | OXE | Thin sample (25 µm) in laminate | OXE | Thick sample (1.4 mm) under air | OXE | Thick sample (1.4 mm) under air |
|---|---|---|---|---|---|---|---|
| **(1)** | 42% | **(1′)** | 29% | **(1)** | 8% | **(1′)** | 15% |
| **(2)** | 58% | **(2′)** | 38% | **(2)** | 50% | **(2′)** | 61% |
| **(3)** | 81% | **(3′)** | 82% | **(3)** | 84% | **(3′)** | 81% |
| **(4)** | 64% | **(4′)** | 66% | **(4)** | 58% | **(4′)** | 38% |
| **(5)** | 52% | **(5′)** | 49% | **(5)** | 39% | **(5′)** | 34% |
| **(6)** | 51% | **(6′)** | 41% | **(6)** | 45% | **(6′)** | 58% |
| **(7)** | 35% | **(7′)** | 47% | **(7)** | 21% | **(7′)** | 35% |
| **(8)** | 57% | **(8′)** | 54% | **(8)** | 65% | **(8′)** | 54% |
| **(9)** | 45% | **(9′)** | 28% | **(9)** | 5% | **(9′)** | 19% |
| **(10)** | 48% | **(10′)** | 49% | **(10)** | 39% | **(10′)** | 41% |

For all oxime esters, a bond dissociation energy around 41-43 kcal/mol were determined by theoretical calculations for the N-O bond. Determination of the enthalpy of cleavage also revealed the photocleavage to occur from the singlet excited state, the process being unfavorable from the triplet excited state (See Table 7).

**Table 7.** Parameters characterizing the investigated OXEs **(1)-(10)**. Some parameters were calculated by molecular modelling: the bond dissociation energy BDE (N-O), the triplet state energy $E_{T1}$ and the enthalpy $\Delta H_{cleavage\ T1}$ for the cleavage from $T_1$. The singlet excited state energy $E_{S1}$, the enthalpy $\Delta H_{cleavage\ S1}$ for the cleavage from $S_1$, and the fluorescence lifetime of the OXEs were measured experimentally.

| OXE | BDE (N-O) (kcal.mol$^{-1}$) | $E_{S1}$ (kcal mol$^{-1}$) | $\Delta H_{cleavage\ S1}$ (kcal mol$^{-1}$) | $E_{T1}$ (kcal mol$^{-1}$) | $\Delta H_{cleavage\ T1}$ (kcal mol$^{-1}$) |
|---|---|---|---|---|---|
| **(1)** | - | 74.25 | - | 62.21 | - |
| **(2)** | 41.55 | 73.1 | -31.55 | 62.22 | -20.67 |
| **(3)** | 47.02 | 73.56 | -26.54 | 52.15 | -5.13 |
| **(4)** | 40.56 | 72.87 | -32.31 | 58.09 | -17.53 |
| **(5)** | 41.35 | 73.33 | -31.98 | 52.14 | -10.79 |
| **(6)** | 41.28 | 73.33 | -32.05 | 62.16 | -20.88 |
| **(7)** | 40.88 | 73.33 | -32.45 | 62.15 | -21.27 |
| **(8)** | 41.25 | 73.1 | -31.85 | 62.20 | -20.95 |
| **(9)** | 43.71 | - | - | 62.07 | -18.36 |
| **(10)** | 42.97 | 66.88 | -23.91 | 52.45 | -9.48 |

## Conclusion

The design of carbazole-based oxime esters is an active research field since more than 100 structures have been proposed during the last three years. Various combinations have been examined including fused carbazole/coumarins, fused *bis*-carbazole structures or carbazole/phenothiazine structures. Noticeably, in these different works, the higher reactivity of the aliphatic radicals with regards to the aryl radicals has been clearly demonstrated. If numerous high-performance photoinitiating systems have been designed, the solubility issue has adversely affected the photoinitiating ability of numerous dyes. At present, oxime esters only exhibiting absorption in the 450-500 nm range were reported. With aim at getting an improved light penetration within the photocurable resins, future works will consist in designing oxime esters with absorptions more redshifted than that achieved at present. Future works will also consist in developing oxime esters exhibiting this dual thermal/photochemical initiating ability. By combining the two polymerization processes, a good conversion at the surface of the sample could be obtained photochemically whereas the thermal polymerization

could allow to get a good monomer conversion in depth where the light penetration is more limited. After years of optimization, influence of the distance between the photocleavable group and the chromophore has been clearly evidenced and future works will consist in getting a deeper insight into this point. At present, no water-soluble oxime esters have been reported in the literature, what constitutes a real challenge for developing greener polymerization processes.

**Acknowledgments**

Aix Marseille University and the Centre National de la Recherche Scientifique (CNRS) are acknowledged for financial supports.

**Conflicts of Interest**

The authors declare no conflict of interest.

**References**

[1] J. Lalevée, H. Mokbel, J.-P. Fouassier, Recent Developments of Versatile Photoinitiating Systems for Cationic Ring Opening Polymerization Operating at Any Wavelengths and under Low Light Intensity Sources, Molecules. 20 (2015) 7201–7221. https://doi.org/10.3390/molecules20047201.

[2] M.A. Tehfe, F. Louradour, J. Lalevée, J.-P. Fouassier, Photopolymerization Reactions: On the Way to a Green and Sustainable Chemistry, Applied Sciences. 3 (2013) 490–514. https://doi.org/10.3390/app3020490.

[3] P. Xiao, J. Zhang, F. Dumur, M.A. Tehfe, F. Morlet-Savary, B. Graff, D. Gigmes, J.P. Fouassier, J. Lalevée, Visible light sensitive photoinitiating systems: Recent progress in cationic and radical photopolymerization reactions under soft conditions, Progress in Polymer Science. 41 (2015) 32–66. https://doi.org/10.1016/j.progpolymsci.2014.09.001.

[4] K. Sun, P. Xiao, F. Dumur, J. Lalevée, Organic dye-based photoinitiating systems for visible-light-induced photopolymerization, Journal of Polymer Science. 59 (2021) 1338–1389. https://doi.org/10.1002/pol.20210225.

[5] J. Lalevée, S. Telitel, P. Xiao, M. Lepeltier, F. Dumur, F. Morlet-Savary, D. Gigmes, J.-P. Fouassier, Metal and metal-free photocatalysts: mechanistic approach and application as photoinitiators of photopolymerization, Beilstein J. Org. Chem. 10 (2014) 863–876. https://doi.org/10.3762/bjoc.10.83.

[6] P. Xiao, F. Dumur, B. Graff, J.P. Fouassier, D. Gigmes, J. Lalevée, Cationic and Thiol–Ene Photopolymerization upon Red Lights Using Anthraquinone Derivatives as Photoinitiators, Macromolecules. 46 (2013) 6744–6750. https://doi.org/10.1021/ma401513b.

[7] M.-A. Tehfe, D. Gigmes, F. Dumur, D. Bertin, F. Morlet-Savary, B. Graff, J. Lalevée, J.-P. Fouassier, Cationic photosensitive formulations based on silyl radical chemistry for green and red diode laser exposure, Polym. Chem. 3 (2012) 1899–1902. https://doi.org/10.1039/C1PY00460C.

[8] P. Garra, C. Dietlin, F. Morlet-Savary, F. Dumur, D. Gigmes, J.-P. Fouassier, J. Lalevée, Redox two-component initiated free radical and cationic polymerizations: Concepts, reactions and applications, Progress in Polymer Science. 94 (2019) 33–56. https://doi.org/10.1016/j.progpolymsci.2019.04.003.
[9] Y. Zhang, Y. Xu, A. Simon-Masseron, J. Lalevée, Radical photoinitiation with LEDs and applications in the 3D printing of composites, Chem. Soc. Rev. 50 (2021) 3824–3841. https://doi.org/10.1039/D0CS01411G.
[10] F. Dumur, Recent Advances on Visible Light Metal-Based Photocatalysts for Polymerization under Low Light Intensity, Catalysts. 9 (2019). https://doi.org/10.3390/catal9090736.
[11] C. Pigot, G. Noirbent, D. Brunel, F. Dumur, Recent advances on push–pull organic dyes as visible light photoinitiators of polymerization, European Polymer Journal. 133 (2020) 109797. https://doi.org/10.1016/j.eurpolymj.2020.109797.
[12] P. Garra, C. Dietlin, F. Morlet-Savary, F. Dumur, D. Gigmes, J.-P. Fouassier, J. Lalevée, Photopolymerization processes of thick films and in shadow areas: a review for the access to composites, Polym. Chem. 8 (2017) 7088–7101. https://doi.org/10.1039/C7PY01778B.
[13] W. Tomal, J. Ortyl, Water-Soluble Photoinitiators in Biomedical Applications, Polymers. 12 (2020) 1073. https://doi.org/10.3390/polym12051073.
[14] N. Corrigan, J. Yeow, P. Judzewitsch, J. Xu, C. Boyer, Seeing the Light: Advancing Materials Chemistry through Photopolymerization, Angewandte Chemie International Edition. 58 (2019) 5170–5189. https://doi.org/10.1002/anie.201805473.
[15] A. Banerji, K. Jin, K. Liu, M.K. Mahanthappa, C.J. Ellison, Cross-Linked Nonwoven Fibers by Room-Temperature Cure Blowing and in Situ Photopolymerization, Macromolecules. 52 (2019) 6662–6672. https://doi.org/10.1021/acs.macromol.9b01002.
[16] G. Yilmaz, Y. Yagci, Light-induced step-growth polymerization, Progress in Polymer Science. 100 (2020) 101178. https://doi.org/10.1016/j.progpolymsci.2019.101178.
[17] M. Layani, X. Wang, S. Magdassi, Novel Materials for 3D Printing by Photopolymerization, Advanced Materials. 30 (2018) 1706344. https://doi.org/10.1002/adma.201706344.
[18] C. Dietlin, S. Schweizer, P. Xiao, J. Zhang, F. Morlet-Savary, B. Graff, J.-P. Fouassier, J. Lalevée, Photopolymerization upon LEDs: new photoinitiating systems and strategies, Polym. Chem. 6 (2015) 3895–3912. https://doi.org/10.1039/C5PY00258C.
[19] S. Shanmugam, J. Xu, C. Boyer, Photocontrolled Living Polymerization Systems with Reversible Deactivations through Electron and Energy Transfer, Macromolecular Rapid Communications. 38 (2017) 1700143. https://doi.org/10.1002/marc.201700143.
[20] F. Jasinski, P.B. Zetterlund, A.M. Braun, A. Chemtob, Photopolymerization in dispersed systems, Progress in Polymer Science. 84 (2018) 47–88. https://doi.org/10.1016/j.progpolymsci.2018.06.006.
[21] C. Noè, M. Hakkarainen, M. Sangermano, Cationic UV-Curing of Epoxidized Biobased Resins, Polymers. 13 (2021) 89. https://doi.org/10.3390/polym13010089.
[22] Y. Yuan, C. Li, R. Zhang, R. Liu, J. Liu, Low volume shrinkage photopolymerization system using hydrogen-bond-based monomers, Progress in Organic Coatings. 137 (2019) 105308. https://doi.org/10.1016/j.porgcoat.2019.105308.
[23] I.V. Khudyakov, J.C. Legg, M.B. Purvis, B.J. Overton, Kinetics of Photopolymerization of Acrylates with Functionality of 1−6, Ind. Eng. Chem. Res. 38 (1999) 3353–3359. https://doi.org/10.1021/ie990306i.

[24] S.H. Dickens, J.W. Stansbury, K.M. Choi, C.J.E. Floyd, Photopolymerization Kinetics of Methacrylate Dental Resins, Macromolecules. 36 (2003) 6043–6053. https://doi.org/10.1021/ma021675k.
[25] A. Maffezzoli, A.D. Pietra, S. Rengo, L. Nicolais, G. Valletta, Photopolymerization of dental composite matrices, Biomaterials. 15 (1994) 1221–1228. https://doi.org/10.1016/0142-9612(94)90273-9.
[26] T. Dikova, J. Maximov, V. Todorov, G. Georgiev, V. Panov, Optimization of Photopolymerization Process of Dental Composites, Processes. 9 (2021) 779. https://doi.org/10.3390/pr9050779.
[27] A. Andreu, P.-C. Su, J.-H. Kim, C.S. Ng, S. Kim, I. Kim, J. Lee, J. Noh, A.S. Subramanian, Y.-J. Yoon, 4D printing materials for vat photopolymerization, Additive Manufacturing. 44 (2021) 102024. https://doi.org/10.1016/j.addma.2021.102024.
[28] H. Chen, G. Noirbent, Y. Zhang, K. Sun, S. Liu, D. Brunel, D. Gigmes, B. Graff, F. Morlet-Savary, P. Xiao, F. Dumur, J. Lalevée, Photopolymerization and 3D/4D applications using newly developed dyes: Search around the natural chalcone scaffold in photoinitiating systems, Dyes and Pigments. 188 (2021) 109213. https://doi.org/10.1016/j.dyepig.2021.109213.
[29] A. Bagheri, J. Jin, Photopolymerization in 3D Printing, ACS Appl. Polym. Mater. 1 (2019) 593–611. https://doi.org/10.1021/acsapm.8b00165.
[30] B.K. Armstrong, A. Kricker, The epidemiology of UV induced skin cancer, Journal of Photochemistry and Photobiology B: Biology. 63 (2001) 8–18. https://doi.org/10.1016/S1011-1344(01)00198-1.
[31] F.R. de Gruijl, Skin cancer and solar UV radiation, European Journal of Cancer. 35 (1999) 2003–2009. https://doi.org/10.1016/S0959-8049(99)00283-X.
[32] D.L. Narayanan, R.N. Saladi, J.L. Fox, Review: Ultraviolet radiation and skin cancer, International Journal of Dermatology. 49 (2010) 978–986. https://doi.org/10.1111/j.1365-4632.2010.04474.x.
[33] J. Shao, Y. Huang, Q. Fan, Visible light initiating systems for photopolymerization: status, development and challenges, Polym. Chem. 5 (2014) 4195–4210. https://doi.org/10.1039/C4PY00072B.
[34] F. Petko, A. Świeży, J. Ortyl, Photoinitiating systems and kinetics of frontal photopolymerization processes – the prospects for efficient preparation of composites and thick 3D structures, Polym. Chem. 12 (2021) 4593–4612. https://doi.org/10.1039/D1PY00596K.
[35] A.H. Bonardi, F. Dumur, T.M. Grant, G. Noirbent, D. Gigmes, B.H. Lessard, J.-P. Fouassier, J. Lalevée, High Performance Near-Infrared (NIR) Photoinitiating Systems Operating under Low Light Intensity and in the Presence of Oxygen, Macromolecules. 51 (2018) 1314–1324. https://doi.org/10.1021/acs.macromol.8b00051.
[36] M.-A. Tehfe, F. Dumur, B. Graff, J.-L. Clément, D. Gigmes, F. Morlet-Savary, J.-P. Fouassier, J. Lalevée, New Cleavable Photoinitiator Architecture with Huge Molar Extinction Coefficients for Polymerization in the 340–450 nm Range., Macromolecules. 46 (2013) 736–746. https://doi.org/10.1021/ma3024359.
[37] P. Xiao, F. Dumur, J. Zhang, J.P. Fouassier, D. Gigmes, J. Lalevée, Copper Complexes in Radical Photoinitiating Systems: Applications to Free Radical and Cationic Polymerization upon Visible LEDs, Macromolecules. 47 (2014) 3837–3844. https://doi.org/10.1021/ma5006793.

[38] P. Xiao, F. Dumur, J. Zhang, D. Gigmes, J.P. Fouassier, J. Lalevée, Copper complexes: the effect of ligands on their photoinitiation efficiencies in radical polymerization reactions under visible light, Polym. Chem. 5 (2014) 6350–6357. https://doi.org/10.1039/C4PY00925H.
[39] P. Xiao, J. Zhang, D. Campolo, F. Dumur, D. Gigmes, J.P. Fouassier, J. Lalevée, Copper and iron complexes as visible-light-sensitive photoinitiators of polymerization, Journal of Polymer Science Part A: Polymer Chemistry. 53 (2015) 2673–2684. https://doi.org/10.1002/pola.27762.
[40] P. Garra, M. Carré, F. Dumur, F. Morlet-Savary, C. Dietlin, D. Gigmes, J.-P. Fouassier, J. Lalevée, Copper-Based (Photo)redox Initiating Systems as Highly Efficient Systems for Interpenetrating Polymer Network Preparation, Macromolecules. 51 (2018) 679–688. https://doi.org/10.1021/acs.macromol.7b02491.
[41] P. Garra, F. Dumur, F. Morlet-Savary, C. Dietlin, D. Gigmes, J.P. Fouassier, J. Lalevée, Mechanosynthesis of a Copper complex for redox initiating systems with a unique near infrared light activation, Journal of Polymer Science Part A: Polymer Chemistry. 55 (2017) 3646–3655. https://doi.org/10.1002/pola.28750.
[42] P. Garra, F. Dumur, A.A. Mousawi, B. Graff, D. Gigmes, F. Morlet-Savary, C. Dietlin, J.P. Fouassier, J. Lalevée, Mechanosynthesized copper(I) complex based initiating systems for redox polymerization: towards upgraded oxidizing and reducing agents, Polym. Chem. 8 (2017) 5884–5896. https://doi.org/10.1039/C7PY01244F.
[43] H. Mokbel, D. Anderson, R. Plenderleith, C. Dietlin, F. Morlet-Savary, F. Dumur, D. Gigmes, J.-P. Fouassier, J. Lalevée, Copper photoredox catalyst "G1": a new high performance photoinitiator for near-UV and visible LEDs, Polym. Chem. 8 (2017) 5580–5592. https://doi.org/10.1039/C7PY01016H.
[44] H. Mokbel, D. Anderson, R. Plenderleith, C. Dietlin, F. Morlet-Savary, F. Dumur, D. Gigmes, J.P. Fouassier, J. Lalevée, Simultaneous initiation of radical and cationic polymerization reactions using the "G1" copper complex as photoredox catalyst: Applications of free radical/cationic hybrid photopolymerization in the composites and 3D printing fields, Progress in Organic Coatings. 132 (2019) 50–61. https://doi.org/10.1016/j.porgcoat.2019.02.044.
[45] A.A. Mousawi, A. Kermagoret, D.-L. Versace, J. Toufaily, T. Hamieh, B. Graff, F. Dumur, D. Gigmes, J.P. Fouassier, J. Lalevée, Copper photoredox catalysts for polymerization upon near UV or visible light: structure/reactivity/efficiency relationships and use in LED projector 3D printing resins, Polym. Chem. 8 (2017) 568–580. https://doi.org/10.1039/C6PY01958G.
[46] A. Mau, G. Noirbent, C. Dietlin, B. Graff, D. Gigmes, F. Dumur, J. Lalevée, Panchromatic Copper Complexes for Visible Light Photopolymerization, Photochem. 1 (2021). https://doi.org/10.3390/photochem1020010.
[47] A. Mau, C. Dietlin, F. Dumur, J. Lalevée, Concomitant initiation of radical and cationic polymerisations using new copper complexes as photoinitiators: Synthesis and characterisation of acrylate/epoxy interpenetrated polymer networks, European Polymer Journal. 152 (2021) 110457. https://doi.org/10.1016/j.eurpolymj.2021.110457.
[48] P. Garra, F. Dumur, D. Gigmes, A. Al Mousawi, F. Morlet-Savary, C. Dietlin, J.P. Fouassier, J. Lalevée, Copper (Photo)redox Catalyst for Radical Photopolymerization in Shadowed Areas and Access to Thick and Filled Samples, Macromolecules. 50 (2017) 3761–3771. https://doi.org/10.1021/acs.macromol.7b00622.

[49] P. Garra, F. Dumur, F. Morlet-Savary, C. Dietlin, J.P. Fouassier, J. Lalevée, A New Highly Efficient Amine-Free and Peroxide-Free Redox System for Free Radical Polymerization under Air with Possible Light Activation, Macromolecules. 49 (2016) 6296–6309. https://doi.org/10.1021/acs.macromol.6b01615.
[50] P. Garra, A. Kermagoret, A.A. Mousawi, F. Dumur, D. Gigmes, F. Morlet-Savary, C. Dietlin, J.P. Fouassier, J. Lalevée, New copper(I) complex based initiating systems in redox polymerization and comparison with the amine/benzoyl peroxide reference, Polym. Chem. 8 (2017) 4088–4097. https://doi.org/10.1039/C7PY00726D.
[51] G. Noirbent, F. Dumur, Recent Advances on Copper Complexes as Visible Light Photoinitiators and (Photo) Redox Initiators of Polymerization, Catalysts. 10 (2020). https://doi.org/10.3390/catal10090953.
[52] T. Borjigin, G. Noirbent, D. Gigmes, P. Xiao, F. Dumur, J. Lalevée, The new LED-Sensitive photoinitiators of Polymerization: Copper complexes in free radical and cationic photoinitiating systems and application in 3D printing, European Polymer Journal. 162 (2022) 110885. https://doi.org/10.1016/j.eurpolymj.2021.110885.
[53] M. Rahal, G. Noirbent, B. Graff, J. Toufaily, T. Hamieh, D. Gigmes, F. Dumur, J. Lalevée, Novel Copper Complexes as Visible Light Photoinitiators for the Synthesis of Interpenetrating Polymer Networks (IPNs), Polymers. 14 (2022). https://doi.org/10.3390/polym14101998.
[54] J. Zhang, D. Campolo, F. Dumur, P. Xiao, D. Gigmes, J.P. Fouassier, J. Lalevée, The carbazole-bound ferrocenium salt as a specific cationic photoinitiator upon near-UV and visible LEDs (365–405 nm), Polym. Bull. 73 (2016) 493–507. https://doi.org/10.1007/s00289-015-1506-1.
[55] A. Al Mousawi, F. Dumur, P. Garra, J. Toufaily, T. Hamieh, B. Graff, D. Gigmes, J.P. Fouassier, J. Lalevée, Carbazole Scaffold Based Photoinitiator/Photoredox Catalysts: Toward New High Performance Photoinitiating Systems and Application in LED Projector 3D Printing Resins, Macromolecules. 50 (2017) 2747–2758. https://doi.org/10.1021/acs.macromol.7b00210.
[56] A. Al Mousawi, D.M. Lara, G. Noirbent, F. Dumur, J. Toufaily, T. Hamieh, T.-T. Bui, F. Goubard, B. Graff, D. Gigmes, J.P. Fouassier, J. Lalevée, Carbazole Derivatives with Thermally Activated Delayed Fluorescence Property as Photoinitiators/Photoredox Catalysts for LED 3D Printing Technology, Macromolecules. 50 (2017) 4913–4926. https://doi.org/10.1021/acs.macromol.7b01114.
[57] A. Al Mousawi, P. Garra, F. Dumur, T.-T. Bui, F. Goubard, J. Toufaily, T. Hamieh, B. Graff, D. Gigmes, J.P. Fouassier, J. Lalevée, Novel Carbazole Skeleton-Based Photoinitiators for LED Polymerization and LED Projector 3D Printing, Molecules. 22 (2017) 2143. https://doi.org/10.3390/molecules22122143.
[58] A.A. Mousawi, A. Arar, M. Ibrahim-Ouali, S. Duval, F. Dumur, P. Garra, J. Toufaily, T. Hamieh, B. Graff, D. Gigmes, J.-P. Fouassier, J. Lalevée, Carbazole-based compounds as photoinitiators for free radical and cationic polymerization upon near visible light illumination, Photochem. Photobiol. Sci. 17 (2018) 578–585. https://doi.org/10.1039/C7PP00400A.
[59] M. Abdallah, D. Magaldi, A. Hijazi, B. Graff, F. Dumur, J.-P. Fouassier, T.-T. Bui, F. Goubard, J. Lalevée, Development of new high-performance visible light photoinitiators based on carbazole scaffold and their applications in 3d printing and photocomposite synthesis, Journal of Polymer Science Part A: Polymer Chemistry. 57 (2019) 2081–2092. https://doi.org/10.1002/pola.29471.

[60] F. Dumur, Recent advances on carbazole-based photoinitiators of polymerization, European Polymer Journal. 125 (2020) 109503. https://doi.org/10.1016/j.eurpolymj.2020.109503.
[61] S. Liu, B. Graff, P. Xiao, F. Dumur, J. Lalevée, Nitro-Carbazole Based Oxime Esters as Dual Photo/Thermal Initiators for 3D Printing and Composite Preparation, Macromolecular Rapid Communications. 42 (2021) 2100207. https://doi.org/10.1002/marc.202100207.
[62] F. Hammoud, A. Hijazi, S. Duval, J. Lalevée, F. Dumur, 5,12-Dihydroindolo[3,2-a]carbazole: A promising scaffold for the design of visible light photoinitiators of polymerization, European Polymer Journal. 162 (2022) 110880. https://doi.org/10.1016/j.eurpolymj.2021.110880.
[63] S. Liu, N. Giacoletto, M. Schmitt, M. Nechab, B. Graff, F. Morlet-Savary, P. Xiao, F. Dumur, J. Lalevée, Effect of Decarboxylation on the Photoinitiation Behavior of Nitrocarbazole-Based Oxime Esters, Macromolecules. 55 (2022) 2475–2485. https://doi.org/10.1021/acs.macromol.2c00294.
[64] F. Hammoud, A. Hijazi, M. Ibrahim-Ouali, J. Lalevée, F. Dumur, Chemical engineering around the 5,12-dihydroindolo[3,2-a]carbazole scaffold : Fine tuning of the optical properties of visible light photoinitiators of polymerization, European Polymer Journal. (2022) 111218. https://doi.org/10.1016/j.eurpolymj.2022.111218.
[65] C. Xu, S. Gong, X. Wu, Y. Wu, Q. Liao, Y. Xiong, Z. Li, H. Tang, High-efficient carbazole-based photo-bleachable dyes as free radical initiators for visible light polymerization, Dyes and Pigments. 198 (2022) 110039. https://doi.org/10.1016/j.dyepig.2021.110039.
[66] H. Chen, G. Noirbent, K. Sun, D. Brunel, D. Gigmes, F. Morlet-Savary, Y. Zhang, S. Liu, P. Xiao, F. Dumur, J. Lalevée, Photoinitiators derived from natural product scaffolds: monochalcones in three-component photoinitiating systems and their applications in 3D printing, Polym. Chem. 11 (2020) 4647–4659. https://doi.org/10.1039/D0PY00568A.
[67] L. Tang, J. Nie, X. Zhu, A high performance phenyl-free LED photoinitiator for cationic or hybrid photopolymerization and its application in LED cationic 3D printing, Polym. Chem. 11 (2020) 2855–2863. https://doi.org/10.1039/D0PY00142B.
[68] Y. Xu, G. Noirbent, D. Brunel, Z. Ding, D. Gigmes, B. Graff, P. Xiao, F. Dumur, J. Lalevée, Allyloxy ketones as efficient photoinitiators with high migration stability in free radical polymerization and 3D printing, Dyes and Pigments. 185 (2021) 108900. https://doi.org/10.1016/j.dyepig.2020.108900.
[69] Y. Xu, Z. Ding, H. Zhu, B. Graff, S. Knopf, P. Xiao, F. Dumur, J. Lalevée, Design of ketone derivatives as highly efficient photoinitiators for free radical and cationic photopolymerizations and application in 3D printing of composites, Journal of Polymer Science. 58 (2020) 3432–3445. https://doi.org/10.1002/pol.20200658.
[70] H. Chen, G. Noirbent, S. Liu, D. Brunel, B. Graff, D. Gigmes, Y. Zhang, K. Sun, F. Morlet-Savary, P. Xiao, F. Dumur, J. Lalevée, Bis-chalcone derivatives derived from natural products as near-UV/visible light sensitive photoinitiators for 3D/4D printing, Mater. Chem. Front. 5 (2021) 901–916. https://doi.org/10.1039/D0QM00755B.
[71] S. Liu, Y. Zhang, K. Sun, B. Graff, P. Xiao, F. Dumur, J. Lalevée, Design of photoinitiating systems based on the chalcone-anthracene scaffold for LED cationic photopolymerization and application in 3D printing, European Polymer Journal. 147 (2021) 110300. https://doi.org/10.1016/j.eurpolymj.2021.110300.

[72] N. Giacoletto, F. Dumur, Recent Advances in bis-Chalcone-Based Photoinitiators of Polymerization: From Mechanistic Investigations to Applications, Molecules. 26 (2021) 3192. https://doi.org/10.3390/molecules26113192.
[73] M. Ibrahim-Ouali, F. Dumur, Recent Advances on Chalcone-based Photoinitiators of Polymerization, European Polymer Journal. (2021) 110688. https://doi.org/10.1016/j.eurpolymj.2021.110688.
[74] H. Chen, G. Noirbent, S. Liu, Y. Zhang, K. Sun, F. Morlet-Savary, D. Gigmes, P. Xiao, F. Dumur, J. Lalevée, In situ generation of Ag nanoparticles during photopolymerization by using newly developed dyes-based three-component photoinitiating systems and the related 3D printing applications and their shape change behavior, Journal of Polymer Science. 59 (2021) 843–859. https://doi.org/10.1002/pol.20210154.
[75] H. Chen, M. Vahdati, P. Xiao, F. Dumur, J. Lalevée, Water-Soluble Visible Light Sensitive Photoinitiating System Based on Charge Transfer Complexes for the 3D Printing of Hydrogels, Polymers. 13 (2021). https://doi.org/10.3390/polym13183195.
[76] M.-A. Tehfe, F. Dumur, P. Xiao, M. Delgove, B. Graff, J.-P. Fouassier, D. Gigmes, J. Lalevée, Chalcone derivatives as highly versatile photoinitiators for radical, cationic, thiol–ene and IPN polymerization reactions upon exposure to visible light, Polym. Chem. 5 (2014) 382–390. https://doi.org/10.1039/C3PY00922J.
[77] K. Sun, Y. Xu, F. Dumur, F. Morlet-Savary, H. Chen, C. Dietlin, B. Graff, J. Lalevée, P. Xiao, In silico rational design by molecular modeling of new ketones as photoinitiators in three-component photoinitiating systems: application in 3D printing, Polym. Chem. 11 (2020) 2230–2242. https://doi.org/10.1039/C9PY01874C.
[78] H. Chen, C. Regeard, H. Salmi, F. Morlet-Savary, N. Giacoletto, M. Nechab, P. Xiao, F. Dumur, J. Lalevée, Interpenetrating polymer network hydrogels using natural based dyes initiating systems: antibacterial activity and 3D/4D performance, European Polymer Journal. (2022) 111042. https://doi.org/10.1016/j.eurpolymj.2022.111042.
[79] M.-A. Tehfe, F. Dumur, S. Telitel, D. Gigmes, E. Contal, D. Bertin, F. Morlet-Savary, B. Graff, J.-P. Fouassier, J. Lalevée, Zinc-based metal complexes as new photocatalysts in polymerization initiating systems, European Polymer Journal. 49 (2013) 1040–1049. https://doi.org/10.1016/j.eurpolymj.2013.01.023.
[80] M. Abdallah, H. Le, A. Hijazi, M. Schmitt, B. Graff, F. Dumur, T.-T. Bui, F. Goubard, J.-P. Fouassier, J. Lalevée, Acridone derivatives as high performance visible light photoinitiators for cationic and radical photosensitive resins for 3D printing technology and for low migration photopolymer property, Polymer. 159 (2018) 47–58. https://doi.org/10.1016/j.polymer.2018.11.021.
[81] J. Zhang, F. Dumur, M. Bouzrati, P. Xiao, C. Dietlin, F. Morlet-Savary, B. Graff, D. Gigmes, J.P. Fouassier, J. Lalevée, Novel panchromatic photopolymerizable matrices: N,N′-dibutylquinacridone as an efficient and versatile photoinitiator, Journal of Polymer Science Part A: Polymer Chemistry. 53 (2015) 1719–1727. https://doi.org/10.1002/pola.27615.
[82] J. Lalevée, M. Peter, F. Dumur, D. Gigmes, N. Blanchard, M.-A. Tehfe, F. Morlet-Savary, J.P. Fouassier, Subtle Ligand Effects in Oxidative Photocatalysis with Iridium Complexes: Application to Photopolymerization, Chemistry – A European Journal. 17 (2011) 15027–15031. https://doi.org/10.1002/chem.201101445.
[83] J. Lalevée, M.-A. Tehfe, F. Dumur, D. Gigmes, N. Blanchard, F. Morlet-Savary, J.P. Fouassier, Iridium Photocatalysts in Free Radical Photopolymerization under Visible Lights, ACS Macro Lett. 1 (2012) 286–290. https://doi.org/10.1021/mz2001753.

[84] J. Lalevée, F. Dumur, C.R. Mayer, D. Gigmes, G. Nasr, M.-A. Tehfe, S. Telitel, F. Morlet-Savary, B. Graff, J.P. Fouassier, Photopolymerization of N-Vinylcarbazole Using Visible-Light Harvesting Iridium Complexes as Photoinitiators, Macromolecules. 45 (2012) 4134–4141. https://doi.org/10.1021/ma3005229.
[85] M.-A. Tehfe, M. Lepeltier, F. Dumur, D. Gigmes, J.-P. Fouassier, J. Lalevée, Structural Effects in the Iridium Complex Series: Photoredox Catalysis and Photoinitiation of Polymerization Reactions under Visible Lights, Macromolecular Chemistry and Physics. 218 (2017) 1700192. https://doi.org/10.1002/macp.201700192.
[86] S. Telitel, F. Dumur, S. Telitel, O. Soppera, M. Lepeltier, Y. Guillaneuf, J. Poly, F. Morlet-Savary, P. Fioux, J.-P. Fouassier, D. Gigmes, J. Lalevée, Photoredox catalysis using a new iridium complex as an efficient toolbox for radical, cationic and controlled polymerizations under soft blue to green lights, Polym. Chem. 6 (2014) 613–624. https://doi.org/10.1039/C4PY01358A.
[87] S. Telitel, F. Dumur, M. Lepeltier, D. Gigmes, J.-P. Fouassier, J. Lalevée, Photoredox process induced polymerization reactions: Iridium complexes for panchromatic photoinitiating systems, Comptes Rendus Chimie. 19 (2016) 71–78. https://doi.org/10.1016/j.crci.2015.06.016.
[88] F. Dumur, D. Bertin, D. Gigmes, Iridium (III) complexes as promising emitters for solid–state Light–Emitting Electrochemical Cells (LECs), International Journal of Nanotechnology. 9 (2012) 377–395. https://doi.org/10.1504/IJNT.2012.045343.
[89] F. Dumur, G. Nasr, G. Wantz, C.R. Mayer, E. Dumas, A. Guerlin, F. Miomandre, G. Clavier, D. Bertin, D. Gigmes, Cationic iridium complex for the design of soft salt-based phosphorescent OLEDs and color-tunable light-emitting electrochemical cells, Organic Electronics. 12 (2011) 1683–1694. https://doi.org/10.1016/j.orgel.2011.06.014.
[90] H. Mokbel, F. Dumur, J. Lalevée, On demand NIR activated photopolyaddition reactions, Polym. Chem. 11 (2020) 4250–4259. https://doi.org/10.1039/D0PY00639D.
[91] H. Mokbel, B. Graff, F. Dumur, J. Lalevée, NIR Sensitizer Operating under Long Wavelength (1064 nm) for Free Radical Photopolymerization Processes, Macromolecular Rapid Communications. 41 (2020) 2000289. https://doi.org/10.1002/marc.202000289.
[92] V. Launay, F. Dumur, D. Gigmes, J. Lalevée, Near-infrared light for polymer re-shaping and re-processing applications, Journal of Polymer Science. 59 (2021) 2193–2200. https://doi.org/10.1002/pol.20210450.
[93] A. Caron, G. Noirbent, D. Gigmes, F. Dumur, J. Lalevée, Near-Infrared PhotoInitiating Systems: Photothermal versus Triplet–Triplet Annihilation-Based Upconversion Polymerization, Macromolecular Rapid Communications. 42 (2021) 2100047. https://doi.org/10.1002/marc.202100047.
[94] A.-H. Bonardi, F. Bonardi, F. Morlet-Savary, C. Dietlin, G. Noirbent, T.M. Grant, J.-P. Fouassier, F. Dumur, B.H. Lessard, D. Gigmes, J. Lalevée, Photoinduced Thermal Polymerization Reactions, Macromolecules. 51 (2018) 8808–8820. https://doi.org/10.1021/acs.macromol.8b01741.
[95] V. Launay, F. Dumur, L. Pieuchot, J. Lalevée, Safe near infrared light for fast polymers surface sterilization using organic heaters, Mater. Chem. Front. 6 (2022) 1172–1179. https://doi.org/10.1039/D1QM01609A.
[96] M.-A. Tehfe, F. Dumur, P. Xiao, J. Zhang, B. Graff, F. Morlet-Savary, D. Gigmes, J.-P. Fouassier, J. Lalevée, Photoinitiators based on a phenazine scaffold: High performance

systems upon near-UV or visible LED (385, 395 and 405 nm) irradiations, Polymer. 55 (2014) 2285–2293. https://doi.org/10.1016/j.polymer.2014.04.005.
[97] P. Garra, D. Brunel, G. Noirbent, B. Graff, F. Morlet-Savary, C. Dietlin, V.F. Sidorkin, F. Dumur, D. Duché, D. Gigmes, J.-P. Fouassier, J. Lalevée, Ferrocene-based (photo)redox polymerization under long wavelengths, Polym. Chem. 10 (2019) 1431–1441. https://doi.org/10.1039/C9PY00059C.
[98] M.-A. Tehfe, A. Zein-Fakih, J. Lalevée, F. Dumur, D. Gigmes, B. Graff, F. Morlet-Savary, T. Hamieh, J.-P. Fouassier, New pyridinium salts as versatile compounds for dye sensitized photopolymerization, European Polymer Journal. 49 (2013) 567–574. https://doi.org/10.1016/j.eurpolymj.2012.10.010.
[99] P. Xiao, M. Frigoli, F. Dumur, B. Graff, D. Gigmes, J.P. Fouassier, J. Lalevée, Julolidine or Fluorenone Based Push–Pull Dyes for Polymerization upon Soft Polychromatic Visible Light or Green Light., Macromolecules. 47 (2014) 106–112. https://doi.org/10.1021/ma402196p.
[100] H. Mokbel, F. Dumur, B. Graff, C.R. Mayer, D. Gigmes, J. Toufaily, T. Hamieh, J.-P. Fouassier, J. Lalevée, Michler's Ketone as an Interesting Scaffold for the Design of High-Performance Dyes in Photoinitiating Systems Upon Visible Light, Macromolecular Chemistry and Physics. 215 (2014) 783–790. https://doi.org/10.1002/macp.201300779.
[101] M.-A. Tehfe, F. Dumur, B. Graff, F. Morlet-Savary, J.-P. Fouassier, D. Gigmes, J. Lalevée, New Push–Pull Dyes Derived from Michler's Ketone For Polymerization Reactions Upon Visible Lights., Macromolecules. 46 (2013) 3761–3770. https://doi.org/10.1021/ma400766z.
[102] H. Mokbel, F. Dumur, C.R. Mayer, F. Morlet-Savary, B. Graff, D. Gigmes, J. Toufaily, T. Hamieh, J.-P. Fouassier, J. Lalevée, End capped polyenic structures as visible light sensitive photoinitiators for polymerization of vinylethers, Dyes and Pigments. 105 (2014) 121–129. https://doi.org/10.1016/j.dyepig.2014.02.002.
[103] S. Telitel, F. Dumur, T. Kavalli, B. Graff, F. Morlet-Savary, D. Gigmes, J.-P. Fouassier, J. Lalevée, The 1,3-bis(dicyanomethylidene)indane skeleton as a (photo) initiator in thermal ring opening polymerization at RT and radical or cationic photopolymerization, RSC Adv. 4 (2014) 15930–15936. https://doi.org/10.1039/C3RA42819B.
[104] P. Xiao, F. Dumur, B. Graff, F. Morlet-Savary, L. Vidal, D. Gigmes, J.P. Fouassier, J. Lalevée, Structural Effects in the Indanedione Skeleton for the Design of Low Intensity 300–500 nm Light Sensitive Initiators., Macromolecules. 47 (2014) 26–34. https://doi.org/10.1021/ma402149g.
[105] K. Sun, S. Liu, C. Pigot, D. Brunel, B. Graff, M. Nechab, D. Gigmes, F. Morlet-Savary, Y. Zhang, P. Xiao, F. Dumur, J. Lalevée, Novel Push–Pull Dyes Derived from 1H-cyclopenta[b]naphthalene-1,3(2H)-dione as Versatile Photoinitiators for Photopolymerization and Their Related Applications: 3D Printing and Fabrication of Photocomposites, Catalysts. 10 (2020) 1196. https://doi.org/10.3390/catal10101196.
[106] K. Sun, S. Liu, H. Chen, F. Morlet-Savary, B. Graff, C. Pigot, M. Nechab, P. Xiao, F. Dumur, J. Lalevée, N-ethyl carbazole-1-allylidene-based push-pull dyes as efficient light harvesting photoinitiators for sunlight induced polymerization, European Polymer Journal. 147 (2021) 110331. https://doi.org/10.1016/j.eurpolymj.2021.110331.
[107] M.-A. Tehfe, F. Dumur, B. Graff, F. Morlet-Savary, D. Gigmes, J.-P. Fouassier, J. Lalevée, Push–pull (thio)barbituric acid derivatives in dye photosensitized radical and cationic

polymerization reactions under 457/473 nm laser beams or blue LEDs, Polym. Chem. 4 (2013) 3866–3875. https://doi.org/10.1039/C3PY00372H.
[108] K. Sun, H. Chen, Y. Zhang, F. Morlet-Savary, B. Graff, P. Xiao, F. Dumur, J. Lalevée, High-performance sunlight induced polymerization using novel push-pull dyes with high light absorption properties, European Polymer Journal. 151 (2021) 110410. https://doi.org/10.1016/j.eurpolymj.2021.110410.
[109] H. Mokbel, F. Dumur, S. Telitel, L. Vidal, P. Xiao, D.-L. Versace, M.-A. Tehfe, F. Morlet-Savary, B. Graff, J.-P. Fouassier, D. Gigmes, J. Toufaily, T. Hamieh, J. Lalevée, Photoinitiating systems of polymerization and in situ incorporation of metal nanoparticles into polymer matrices upon exposure to visible light: push–pull malonate and malononitrile based dyes, Polym. Chem. 4 (2013) 5679–5687. https://doi.org/10.1039/C3PY00846K.
[110] S. Helmy, S. Oh, F.A. Leibfarth, C.J. Hawker, J. Read de Alaniz, Design and Synthesis of Donor–Acceptor Stenhouse Adducts: A Visible Light Photoswitch Derived from Furfural, J. Org. Chem. 79 (2014) 11316–11329. https://doi.org/10.1021/jo502206g.
[111] K. Sun, C. Pigot, Y. Zhang, T. Borjigin, F. Morlet-Savary, B. Graff, M. Nechab, P. Xiao, F. Dumur, J. Lalevée, Sunlight Induced Polymerization Photoinitiated by Novel Push–Pull Dyes: Indane-1,3-Dione, 1H-Cyclopenta[b]Naphthalene-1,3(2H)-Dione and 4-Dimethoxyphenyl-1-Allylidene Derivatives, Macromolecular Chemistry and Physics. n/a (2022) 2100439. https://doi.org/10.1002/macp.202100439.
[112] F. Dumur, Recent Advances on Anthracene-based Photoinitiators of Polymerization, European Polymer Journal. (2022) 111139. https://doi.org/10.1016/j.eurpolymj.2022.111139.
[113] A. Al Mousawi, C. Poriel, F. Dumur, J. Toufaily, T. Hamieh, J.P. Fouassier, J. Lalevée, Zinc Tetraphenylporphyrin as High Performance Visible Light Photoinitiator of Cationic Photosensitive Resins for LED Projector 3D Printing Applications, Macromolecules. 50 (2017) 746–753. https://doi.org/10.1021/acs.macromol.6b02596.
[114] G. Noirbent, Y. Xu, A.-H. Bonardi, D. Gigmes, J. Lalevée, F. Dumur, Metalated porphyrins as versatile visible light and NIR photoinitiators of polymerization, European Polymer Journal. 139 (2020) 110019. https://doi.org/10.1016/j.eurpolymj.2020.110019.
[115] F. Dumur, Recent advances on visible light Triphenylamine-based photoinitiators of polymerization, European Polymer Journal. 166 (2022) 111036. https://doi.org/10.1016/j.eurpolymj.2022.111036.
[116] N. Karaca, N. Ocal, N. Arsu, S. Jockusch, Thioxanthone-benzothiophenes as photoinitiator for free radical polymerization, Journal of Photochemistry and Photobiology A: Chemistry. 331 (2016) 22–28. https://doi.org/10.1016/j.jphotochem.2016.01.017.
[117] D.K. Balta, N. Cetiner, G. Temel, Z. Turgut, N. Arsu, An annelated thioxanthone as a new Type II initiator, Journal of Photochemistry and Photobiology A: Chemistry. 199 (2008) 316–321. https://doi.org/10.1016/j.jphotochem.2008.06.008.
[118] D.K. Balta, G. Temel, G. Goksu, N. Ocal, N. Arsu, Thioxanthone–Diphenyl Anthracene: Visible Light Photoinitiator, Macromolecules. 45 (2012) 119–125. https://doi.org/10.1021/ma202168m.
[119] S. Dadashi-Silab, C. Aydogan, Y. Yagci, Shining a light on an adaptable photoinitiator: advances in photopolymerizations initiated by thioxanthones, Polym. Chem. 6 (2015) 6595–6615. https://doi.org/10.1039/C5PY01004G.

[120] T.N. Eren, N. Yasar, V. Aviyente, F. Morlet-Savary, B. Graff, J.P. Fouassier, J. Lalevee, D. Avci, Photophysical and Photochemical Studies of Novel Thioxanthone-Functionalized Methacrylates through LED Excitation, Macromolecular Chemistry and Physics. 217 (2016) 1501–1512. https://doi.org/10.1002/macp.201600051.
[121] J. Qiu, J. Wei, Thioxanthone photoinitiator containing polymerizable N-aromatic maleimide for photopolymerization, J Polym Res. 21 (2014) 559. https://doi.org/10.1007/s10965-014-0559-4.
[122] H. Tar, D. Sevinc Esen, M. Aydin, C. Ley, N. Arsu, X. Allonas, Panchromatic Type II Photoinitiator for Free Radical Polymerization Based on Thioxanthone Derivative, Macromolecules. 46 (2013) 3266–3272. https://doi.org/10.1021/ma302641d.
[123] Q. Wu, X. Wang, Y. Xiong, J. Yang, H. Tang, Thioxanthone based one-component polymerizable visible light photoinitiator for free radical polymerization, RSC Adv. 6 (2016) 66098–66107. https://doi.org/10.1039/C6RA15349F.
[124] Q. Wu, K. Tang, Y. Xiong, X. Wang, J. Yang, H. Tang, High-Performance and Low Migration One-Component Thioxanthone Visible Light Photoinitiators, Macromolecular Chemistry and Physics. 218 (2017) 1600484. https://doi.org/10.1002/macp.201600484.
[125] X. Wu, M. Jin, J.-P. Malval, D. Wan, H. Pu, Visible light-emitting diode-sensitive thioxanthone derivatives used in versatile photoinitiating systems for photopolymerizations, Journal of Polymer Science Part A: Polymer Chemistry. 55 (2017) 4037–4045. https://doi.org/10.1002/pola.28871.
[126] J. Lalevée, M.-A. Tehfe, F. Dumur, D. Gigmes, B. Graff, F. Morlet-Savary, J.-P. Fouassier, Light-Harvesting Organic Photoinitiators of Polymerization, Macromolecular Rapid Communications. 34 (2013) 239–245. https://doi.org/10.1002/marc.201200578.
[127] D.S. Esen, F. Karasu, N. Arsu, The investigation of photoinitiated polymerization of multifunctional acrylates with TX-BT by Photo-DSC and RT-FTIR, Progress in Organic Coatings. 70 (2011) 102–107. https://doi.org/10.1016/j.porgcoat.2010.10.010.
[128] J. Lalevée, N. Blanchard, M.A. Tehfe, C. Fries, F. Morlet-Savary, D. Gigmes, J.P. Fouassier, New thioxanthone and xanthone photoinitiators based on silyl radical chemistry, Polym. Chem. 2 (2011) 1077–1084. https://doi.org/10.1039/C0PY00392A.
[129] J. Zhang, J. Lalevée, J. Zhao, B. Graff, M.H. Stenzel, P. Xiao, Dihydroxyanthraquinone derivatives: natural dyes as blue-light-sensitive versatile photoinitiators of photopolymerization, Polym. Chem. 7 (2016) 7316–7324. https://doi.org/10.1039/C6PY01550F.
[130] C. Brahmi, M. Benltifa, C. Vaulot, L. Michelin, F. Dumur, F. Millange, M. Frigoli, A. Airoudj, F. Morlet-Savary, L. Bousselmi, J. Lalevée, New hybrid MOF/polymer composites for the photodegradation of organic dyes, European Polymer Journal. 154 (2021) 110560. https://doi.org/10.1016/j.eurpolymj.2021.110560.
[131] J. Zhang, F. Dumur, P. Horcajada, C. Livage, P. Xiao, J.P. Fouassier, D. Gigmes, J. Lalevée, Iron-Based Metal-Organic Frameworks (MOF) as Photocatalysts for Radical and Cationic Polymerizations under Near UV and Visible LEDs (385–405 nm), Macromolecular Chemistry and Physics. 217 (2016) 2534–2540. https://doi.org/10.1002/macp.201600352.
[132] C. Brahmi, M. Benltifa, C. Vaulot, L. Michelin, F. Dumur, E. Gkaniatsou, C. Sicard, A. Airoudj, F. Morlet-Savary, L. Bousselmi, J. Lalevée, New Hybrid Fe-based MOFs/Polymer Composites for the Photodegradation of Organic Dyes, ChemistrySelect. 6 (2021) 8120–8132. https://doi.org/10.1002/slct.202102194.

[133] J. Zhang, N. Zivic, F. Dumur, C. Guo, Y. Li, P. Xiao, B. Graff, D. Gigmes, J.P. Fouassier, J. Lalevée, Panchromatic photoinitiators for radical, cationic and thiol-ene polymerization reactions: A search in the diketopyrrolopyrrole or indigo dye series, Materials Today Communications. 4 (2015) 101–108. https://doi.org/10.1016/j.mtcomm.2015.06.007.
[134] P. Xiao, W. Hong, Y. Li, F. Dumur, B. Graff, J.P. Fouassier, D. Gigmes, J. Lalevée, Diketopyrrolopyrrole dyes: Structure/reactivity/efficiency relationship in photoinitiating systems upon visible lights, Polymer. 55 (2014) 746–751. https://doi.org/10.1016/j.polymer.2014.01.003.
[135] P. Xiao, W. Hong, Y. Li, F. Dumur, B. Graff, J.P. Fouassier, D. Gigmes, J. Lalevée, Green light sensitive diketopyrrolopyrrole derivatives used in versatile photoinitiating systems for photopolymerizations, Polym. Chem. 5 (2014) 2293–2300. https://doi.org/10.1039/C3PY01599H.
[136] M.-A. Tehfe, F. Dumur, E. Contal, B. Graff, F. Morlet-Savary, D. Gigmes, J.-P. Fouassier, J. Lalevée, New insights into radical and cationic polymerizations upon visible light exposure: role of novel photoinitiator systems based on the pyrene chromophore, Polym. Chem. 4 (2013) 1625–1634. https://doi.org/10.1039/C2PY20950K.
[137] S. Telitel, F. Dumur, T. Faury, B. Graff, M.-A. Tehfe, D. Gigmes, J.-P. Fouassier, J. Lalevée, New core-pyrene π structure organophotocatalysts usable as highly efficient photoinitiators, Beilstein J. Org. Chem. 9 (2013) 877–890. https://doi.org/10.3762/bjoc.9.101.
[138] N. Uchida, H. Nakano, T. Igarashi, T. Sakurai, Nonsalt 1-(arylmethyloxy)pyrene photoinitiators capable of initiating cationic polymerization, Journal of Applied Polymer Science. 131 (2014). https://doi.org/10.1002/app.40510.
[139] A. Mishra, S. Daswal, 1-(Bromoacetyl)pyrene, a novel photoinitiator for the copolymerization of styrene and methylmethacrylate, Radiation Physics and Chemistry. 75 (2006) 1093–1100. https://doi.org/10.1016/j.radphyschem.2006.01.013.
[140] M.-A. Tehfe, F. Dumur, B. Graff, F. Morlet-Savary, D. Gigmes, J.-P. Fouassier, J. Lalevée, Design of new Type I and Type II photoinitiators possessing highly coupled pyrene–ketone moieties, Polym. Chem. 4 (2013) 2313–2324. https://doi.org/10.1039/C3PY21079K.
[141] F. Dumur, Recent advances on pyrene-based photoinitiators of polymerization, European Polymer Journal. 126 (2020) 109564. https://doi.org/10.1016/j.eurpolymj.2020.109564.
[142] M.-A. Tehfe, F. Dumur, N. Vilà, B. Graff, C.R. Mayer, J.P. Fouassier, D. Gigmes, J. Lalevée, A Multicolor Photoinitiator for Cationic Polymerization and Interpenetrated Polymer Network Synthesis: 2,7-Di-tert-butyldimethyldihydropyrene, Macromolecular Rapid Communications. 34 (2013) 1104–1109. https://doi.org/10.1002/marc.201300302.
[143] S. Telitel, F. Dumur, D. Gigmes, B. Graff, J.P. Fouassier, J. Lalevée, New functionalized aromatic ketones as photoinitiating systems for near visible and visible light induced polymerizations, Polymer. 54 (2013) 2857–2864. https://doi.org/10.1016/j.polymer.2013.03.062.
[144] M.-A. Tehfe, J. Lalevée, S. Telitel, E. Contal, F. Dumur, D. Gigmes, D. Bertin, M. Nechab, B. Graff, F. Morlet-Savary, J.-P. Fouassier, Polyaromatic Structures as Organo-Photoinitiator Catalysts for Efficient Visible Light Induced Dual Radical/Cationic Photopolymerization and Interpenetrated Polymer Networks Synthesis, Macromolecules. 45 (2012) 4454–4460. https://doi.org/10.1021/ma300760c.

[145] C. Brahmi, M. Benltifa, C. Vaulot, L. Michelin, F. Dumur, A. Airoudj, F. Morlet-Savary, B. Raveau, L. Bousselmi, J. Lalevée, New hybrid perovskites/polymer composites for the photodegradation of organic dyes, European Polymer Journal. 157 (2021) 110641. https://doi.org/10.1016/j.eurpolymj.2021.110641.
[146] H. Mokbel, F. Dumur, B. Raveau, F. Morlet-Savary, C. Simonnet-Jégat, D. Gigmes, J. Toufaily, T. Hamieh, J.P. Fouassier, J. Lalevée, Perovskites as new radical photoinitiators for radical and cationic polymerizations, Tetrahedron. 72 (2016) 7686–7690. https://doi.org/10.1016/j.tet.2016.03.057.
[147] M.-A. Tehfe, F. Dumur, E. Contal, B. Graff, D. Gigmes, J.-P. Fouassier, J. Lalevée, Novel Highly Efficient Organophotocatalysts: Truxene–Acridine-1,8-diones as Photoinitiators of Polymerization, Macromolecular Chemistry and Physics. 214 (2013) 2189–2201. https://doi.org/10.1002/macp.201300362.
[148] P. Xiao, F. Dumur, M.-A. Tehfe, B. Graff, D. Gigmes, J.P. Fouassier, J. Lalevée, Difunctional acridinediones as photoinitiators of polymerization under UV and visible lights: Structural effects, Polymer. 54 (2013) 3458–3466. https://doi.org/10.1016/j.polymer.2013.04.055.
[149] P. Xiao, F. Dumur, M.-A. Tehfe, B. Graff, D. Gigmes, J.P. Fouassier, J. Lalevée, Acridinediones: Effect of Substituents on Their Photoinitiating Abilities in Radical and Cationic Photopolymerization, Macromolecular Chemistry and Physics. 214 (2013) 2276–2282. https://doi.org/10.1002/macp.201300363.
[150] P. Xiao, F. Dumur, M. Frigoli, B. Graff, F. Morlet-Savary, G. Wantz, H. Bock, J.P. Fouassier, D. Gigmes, J. Lalevée, Perylene derivatives as photoinitiators in blue light sensitive cationic or radical curable films and panchromatic thiol-ene polymerizable films, European Polymer Journal. 53 (2014) 215–222. https://doi.org/10.1016/j.eurpolymj.2014.01.024.
[151] P. Xiao, F. Dumur, B. Graff, D. Gigmes, J.P. Fouassier, J. Lalevée, Red-Light-Induced Cationic Photopolymerization: Perylene Derivatives as Efficient Photoinitiators, Macromolecular Rapid Communications. 34 (2013) 1452–1458. https://doi.org/10.1002/marc.201300383.
[152] F. Dumur, Recent advances on perylene-based photoinitiators of polymerization, European Polymer Journal. 159 (2021) 110734. https://doi.org/10.1016/j.eurpolymj.2021.110734.
[153] M.-A. Tehfe, F. Dumur, B. Graff, D. Gigmes, J.-P. Fouassier, J. Lalevée, Green-Light-Induced Cationic Ring Opening Polymerization Reactions: Perylene-3,4:9,10-bis(Dicarboximide) as Efficient Photosensitizers, Macromolecular Chemistry and Physics. 214 (2013) 1052–1060. https://doi.org/10.1002/macp.201200728.
[154] A. Al Mousawi, P. Garra, X. Sallenave, F. Dumur, J. Toufaily, T. Hamieh, B. Graff, D. Gigmes, J.P. Fouassier, J. Lalevée, π-Conjugated Dithienophosphole Derivatives as High Performance Photoinitiators for 3D Printing Resins, Macromolecules. 51 (2018) 1811–1821. https://doi.org/10.1021/acs.macromol.8b00044.
[155] F. Dumur, D. Gigmes, J.-P. Fouassier, J. Lalevée, Organic Electronics: An El Dorado in the Quest of New Photocatalysts for Polymerization Reactions, Acc. Chem. Res. 49 (2016) 1980–1989. https://doi.org/10.1021/acs.accounts.6b00227.
[156] N. Zivic, M. Bouzrati-Zerrelli, S. Villotte, F. Morlet-Savary, C. Dietlin, F. Dumur, D. Gigmes, J.P. Fouassier, J. Lalevée, A novel naphthalimide scaffold based iodonium salt as a one-component photoacid/photoinitiator for cationic and radical polymerization

under LED exposure, Polym. Chem. 7 (2016) 5873–5879. https://doi.org/10.1039/C6PY01306F.
[157] H. Mokbel, J. Toufaily, T. Hamieh, F. Dumur, D. Campolo, D. Gigmes, J.P. Fouassier, J. Ortyl, J. Lalevée, Specific cationic photoinitiators for near UV and visible LEDs: Iodonium versus ferrocenium structures, Journal of Applied Polymer Science. 132 (2015). https://doi.org/10.1002/app.42759.
[158] S. Villotte, D. Gigmes, F. Dumur, J. Lalevée, Design of Iodonium Salts for UV or Near-UV LEDs for Photoacid Generator and Polymerization Purposes, Molecules. 25 (2020) 149. https://doi.org/10.3390/molecules25010149.
[159] M.A. Tasdelen, V. Kumbaraci, S. Jockusch, N.J. Turro, N. Talinli, Y. Yagci, Photoacid Generation by Stepwise Two-Photon Absorption: Photoinitiated Cationic Polymerization of Cyclohexene Oxide by Using Benzodioxinone in the Presence of Iodonium Salt, Macromolecules. 41 (2008) 295–297. https://doi.org/10.1021/ma7023649.
[160] J.V. Crivello, J.H.W. Lam, Diaryliodonium Salts. A New Class of Photoinitiators for Cationic Polymerization, Macromolecules. 10 (1977) 1307–1315. https://doi.org/10.1021/ma60060a028.
[161] Y. He, W. Zhou, F. Wu, M. Li, E. Wang, Photoreaction and photopolymerization studies on squaraine dyes/iodonium salts combination, Journal of Photochemistry and Photobiology A: Chemistry. 162 (2004) 463–471. https://doi.org/10.1016/S1010-6030(03)00390-3.
[162] L.I. Jun, L.I. Miaozhen, S. Huaihai, Y. Yongyuan, W. Erjian, Photopolymerization Initiated by Dimethylaminochalcone/Diphenyliodonium Salt Combination System Sensitive to Visible Light, Chinese J. Polym. Sci. 11 (1993) 163–170.
[163] N. Zivic, P.K. Kuroishi, F. Dumur, D. Gigmes, A.P. Dove, H. Sardon, Recent Advances and Challenges in the Design of Organic Photoacid and Photobase Generators for Polymerizations, Angewandte Chemie International Edition. 58 (2019) 10410–10422. https://doi.org/10.1002/anie.201810118.
[164] S. Telitel, F. Dumur, D. Campolo, J. Poly, D. Gigmes, J.P. Fouassier, J. Lalevée, Iron complexes as potential photocatalysts for controlled radical photopolymerizations: A tool for modifications and patterning of surfaces, Journal of Polymer Science Part A: Polymer Chemistry. 54 (2016) 702–713. https://doi.org/10.1002/pola.27896.
[165] J. Zhang, D. Campolo, F. Dumur, P. Xiao, J.P. Fouassier, D. Gigmes, J. Lalevée, Iron complexes as photoinitiators for radical and cationic polymerization through photoredox catalysis processes, Journal of Polymer Science Part A: Polymer Chemistry. 53 (2015) 42–49. https://doi.org/10.1002/pola.27435.
[166] J. Zhang, D. Campolo, F. Dumur, P. Xiao, J.P. Fouassier, D. Gigmes, J. Lalevée, Visible-light-sensitive photoredox catalysis by iron complexes: Applications in cationic and radical polymerization reactions, Journal of Polymer Science Part A: Polymer Chemistry. 54 (2016) 2247–2253. https://doi.org/10.1002/pola.28098.
[167] J. Zhang, D. Campolo, F. Dumur, P. Xiao, J.P. Fouassier, D. Gigmes, J. Lalevée, Iron Complexes in Visible-Light-Sensitive Photoredox Catalysis: Effect of Ligands on Their Photoinitiation Efficiencies, ChemCatChem. 8 (2016) 2227–2233. https://doi.org/10.1002/cctc.201600320.
[168] F. Dumur, Recent advances on ferrocene-based photoinitiating systems, European Polymer Journal. 147 (2021) 110328. https://doi.org/10.1016/j.eurpolymj.2021.110328.
[169] F. Dumur, Recent advances on iron-based photoinitiators of polymerization, European Polymer Journal. 139 (2020) 110026. https://doi.org/10.1016/j.eurpolymj.2020.110026.

[170] A.A. Mousawi, F. Dumur, P. Garra, J. Toufaily, T. Hamieh, F. Goubard, T.-T. Bui, B. Graff, D. Gigmes, J.P. Fouassier, J. Lalevée, Azahelicenes as visible light photoinitiators for cationic and radical polymerization: Preparation of photoluminescent polymers and use in high performance LED projector 3D printing resins, Journal of Polymer Science Part A: Polymer Chemistry. 55 (2017) 1189–1199. https://doi.org/10.1002/pola.28476.
[171] A. Al Mousawi, M. Schmitt, F. Dumur, J. Ouyang, L. Favereau, V. Dorcet, N. Vanthuyne, P. Garra, J. Toufaily, T. Hamieh, B. Graff, J.P. Fouassier, D. Gigmes, J. Crassous, J. Lalevée, Visible Light Chiral Photoinitiator for Radical Polymerization and Synthesis of Polymeric Films with Strong Chiroptical Activity, Macromolecules. 51 (2018) 5628–5637. https://doi.org/10.1021/acs.macromol.8b01085.
[172] F. Dumur, Recent advances on visible light pyrrole-derived photoinitiators of polymerization, European Polymer Journal. 173 (2022) 111254. https://doi.org/10.1016/j.eurpolymj.2022.111254.
[173] B. Corakci, S.O. Hacioglu, L. Toppare, U. Bulut, Long wavelength photosensitizers in photoinitiated cationic polymerization: The effect of quinoxaline derivatives on photopolymerization, Polymer. 54 (2013) 3182–3187. https://doi.org/10.1016/j.polymer.2013.04.008.
[174] P. Xiao, F. Dumur, D. Thirion, S. Fagour, A. Vacher, X. Sallenave, F. Morlet-Savary, B. Graff, J.P. Fouassier, D. Gigmes, J. Lalevée, Multicolor Photoinitiators for Radical and Cationic Polymerization: Monofunctional vs Polyfunctional Thiophene Derivatives, Macromolecules. 46 (2013) 6786–6793. https://doi.org/10.1021/ma401389t.
[175] F. Dumur, Recent Advances on Visible Light Thiophene-based Photoinitiators of Polymerization, European Polymer Journal. (2022) 111120. https://doi.org/10.1016/j.eurpolymj.2022.111120.
[176] M. Ghali, M. Benltifa, C. Brahmi, L. Elbassi, F. Dumur, C. Simonnet-Jégat, L. Bousselmi, J. Lalevée, LED and solar photodecomposition of erythrosine B and rose Bengal using H3PMo12O40/polymer photocatalyst, European Polymer Journal. 159 (2021) 110743. https://doi.org/10.1016/j.eurpolymj.2021.110743.
[177] C. Brahmi, M. Benltifa, M. Ghali, F. Dumur, C. Simonnet-Jégat, M. Valérie, F. Morlet-Savary, L. Bousselmi, J. Lalevée, Performance improvement of the photocatalytic process for the degradation of pharmaceutical compounds using new POM/polymer photocatalysts, Journal of Environmental Chemical Engineering. 9 (2021) 106015. https://doi.org/10.1016/j.jece.2021.106015.
[178] C. Brahmi, M. Benltifa, M. Ghali, F. Dumur, C. Simonnet-Jégat, V. Monnier, F. Morlet-Savary, L. Bousselmi, J. Lalevée, Polyoxometalates/polymer composites for the photodegradation of bisphenol-A, Journal of Applied Polymer Science. 138 (2021) 50864. https://doi.org/10.1002/app.50864.
[179] E.A. Kamoun, A. Winkel, M. Eisenburger, H. Menzel, Carboxylated camphorquinone as visible-light photoinitiator for biomedical application: Synthesis, characterization, and application, Arabian Journal of Chemistry. 9 (2016) 745–754. https://doi.org/10.1016/j.arabjc.2014.03.008.
[180] A. Santini, I.T. Gallegos, C.M. Felix, Photoinitiators in Dentistry: A Review, Prim Dent J. 2 (2013) 30–33. https://doi.org/10.1308/205016814809859563.
[181] F. Dumur, Recent advances on visible light Phenothiazine-based photoinitiators of polymerization, European Polymer Journal. 165 (2022) 110999. https://doi.org/10.1016/j.eurpolymj.2022.110999.

[182] J. Lalevée, F. Dumur, M.-A. Tehfe, A. Zein-Fakih, D. Gigmes, F. Morlet-Savary, B. Graff, J.-P. Fouassier, Dye photosensitized cationic ring-opening polymerization: Search for new dye skeletons, Polymer. 53 (2012) 4947–4954. https://doi.org/10.1016/j.polymer.2012.08.067.
[183] M. Abdallah, A. Hijazi, B. Graff, J.-P. Fouassier, G. Rodeghiero, A. Gualandi, F. Dumur, P.G. Cozzi, J. Lalevée, Coumarin derivatives as versatile photoinitiators for 3D printing, polymerization in water and photocomposite synthesis, Polym. Chem. 10 (2019) 872–884. https://doi.org/10.1039/C8PY01708E.
[184] M. Abdallah, F. Dumur, A. Hijazi, G. Rodeghiero, A. Gualandi, P.G. Cozzi, J. Lalevée, Keto-coumarin scaffold for photoinitiators for 3D printing and photocomposites, Journal of Polymer Science. 58 (2020) 1115–1129. https://doi.org/10.1002/pol.20190290.
[185] M. Abdallah, A. Hijazi, F. Dumur, J. Lalevée, Coumarins as Powerful Photosensitizers for the Cationic Polymerization of Epoxy-Silicones under Near-UV and Visible Light and Applications for 3D Printing Technology, Molecules. 25 (2020) 2063. https://doi.org/10.3390/molecules25092063.
[186] M. Abdallah, A. Hijazi, P.G. Cozzi, A. Gualandi, F. Dumur, J. Lalevée, Boron Compounds as Additives for the Cationic Polymerization Using Coumarin Derivatives in Epoxy Silicones, Macromolecular Chemistry and Physics. 222 (2021) 2000404. https://doi.org/10.1002/macp.202000404.
[187] Q. Chen, Q. Yang, P. Gao, B. Chi, J. Nie, Y. He, Photopolymerization of Coumarin-Containing Reversible Photoresponsive Materials Based on Wavelength Selectivity, Ind. Eng. Chem. Res. 58 (2019) 2970–2975. https://doi.org/10.1021/acs.iecr.8b05164.
[188] Z. Li, X. Zou, G. Zhu, X. Liu, R. Liu, Coumarin-Based Oxime Esters: Photobleachable and Versatile Unimolecular Initiators for Acrylate and Thiol-Based Click Photopolymerization under Visible Light-Emitting Diode Light Irradiation, ACS Appl. Mater. Interfaces. 10 (2018) 16113–16123. https://doi.org/10.1021/acsami.8b01767.
[189] M. Rahal, H. Mokbel, B. Graff, J. Toufaily, T. Hamieh, F. Dumur, J. Lalevée, Mono vs. Difunctional Coumarin as Photoinitiators in Photocomposite Synthesis and 3D Printing, Catalysts. 10 (2020) 1202. https://doi.org/10.3390/catal10101202.
[190] M. Rajeshirke, M.C. Sreenath, S. Chitrambalam, I.H. Joe, N. Sekar, Enhancement of NLO Properties in OBO Fluorophores Derived from Carbazole–Coumarin Chalcones Containing Carboxylic Acid at the N-Alykl Terminal End, J. Phys. Chem. C. 122 (2018) 14313–14325. https://doi.org/10.1021/acs.jpcc.8b02937.
[191] M. Rahal, B. Graff, J. Toufaily, T. Hamieh, F. Dumur, J. Lalevée, Design of keto-coumarin based photoinitiator for Free Radical Photopolymerization: Towards 3D printing and photocomposites applications, European Polymer Journal. 154 (2021) 110559. https://doi.org/10.1016/j.eurpolymj.2021.110559.
[192] M. Rahal, B. Graff, J. Toufaily, T. Hamieh, G. Noirbent, D. Gigmes, F. Dumur, J. Lalevée, 3-Carboxylic Acid and Formyl-Derived Coumarins as Photoinitiators in Photo-Oxidation or Photo-Reduction Processes for Photopolymerization upon Visible Light: Photocomposite Synthesis and 3D Printing Applications, Molecules. 26 (2021). https://doi.org/10.3390/molecules26061753.
[193] F. Hammoud, N. Giacoletto, G. Noirbent, B. Graff, A. Hijazi, M. Nechab, D. Gigmes, F. Dumur, J. Lalevée, Substituent effects on the photoinitiation ability of coumarin-based oxime-ester photoinitiators for free radical photopolymerization, Mater. Chem. Front. 5 (2021) 8361–8370. https://doi.org/10.1039/D1QM01310F.

[194] F. Dumur, Recent advances on coumarin-based photoinitiators of polymerization, European Polymer Journal. 163 (2022) 110962. https://doi.org/10.1016/j.eurpolymj.2021.110962.
[195] A.-H. Bonardi, S. Zahouily, C. Dietlin, B. Graff, F. Morlet-Savary, M. Ibrahim-Ouali, D. Gigmes, N. Hoffmann, F. Dumur, J. Lalevée, New 1,8-Naphthalimide Derivatives as Photoinitiators for Free-Radical Polymerization Upon Visible Light, Catalysts. 9 (2019) 637. https://doi.org/10.3390/catal9080637.
[196] J. Zhang, N. Zivic, F. Dumur, P. Xiao, B. Graff, J.P. Fouassier, D. Gigmes, J. Lalevée, Naphthalimide-Tertiary Amine Derivatives as Blue-Light-Sensitive Photoinitiators, ChemPhotoChem. 2 (2018) 481–489. https://doi.org/10.1002/cptc.201800006.
[197] P. Xiao, F. Dumur, J. Zhang, B. Graff, D. Gigmes, J.P. Fouassier, J. Lalevée, Naphthalimide Derivatives: Substituent Effects on the Photoinitiating Ability in Polymerizations under Near UV, Purple, White and Blue LEDs (385, 395, 405, 455, or 470 nm), Macromolecular Chemistry and Physics. 216 (2015) 1782–1790. https://doi.org/10.1002/macp.201500150.
[198] P. Xiao, F. Dumur, J. Zhang, B. Graff, D. Gigmes, J.P. Fouassier, J. Lalevée, Naphthalimide-phthalimide derivative based photoinitiating systems for polymerization reactions under blue lights, Journal of Polymer Science Part A: Polymer Chemistry. 53 (2015) 665–674. https://doi.org/10.1002/pola.27490.
[199] J. Zhang, N. Zivic, F. Dumur, P. Xiao, B. Graff, D. Gigmes, J.P. Fouassier, J. Lalevée, A benzophenone-naphthalimide derivative as versatile photoinitiator of polymerization under near UV and visible lights, Journal of Polymer Science Part A: Polymer Chemistry. 53 (2015) 445–451. https://doi.org/10.1002/pola.27451.
[200] J. Zhang, N. Zivic, F. Dumur, P. Xiao, B. Graff, J.P. Fouassier, D. Gigmes, J. Lalevée, N-[2-(Dimethylamino)ethyl]-1,8-naphthalimide derivatives as photoinitiators under LEDs, Polym. Chem. 9 (2018) 994–1003. https://doi.org/10.1039/C8PY00055G.
[201] J. Zhang, F. Dumur, P. Xiao, B. Graff, D. Bardelang, D. Gigmes, J.P. Fouassier, J. Lalevée, Structure Design of Naphthalimide Derivatives: Toward Versatile Photoinitiators for Near-UV/Visible LEDs, 3D Printing, and Water-Soluble Photoinitiating Systems, Macromolecules. 48 (2015) 2054–2063. https://doi.org/10.1021/acs.macromol.5b00201.
[202] J. Zhang, N. Zivic, F. Dumur, P. Xiao, B. Graff, J.P. Fouassier, D. Gigmes, J. Lalevée, UV-violet-blue LED induced polymerizations: Specific photoinitiating systems at 365, 385, 395 and 405 nm, Polymer. 55 (2014) 6641–6648. https://doi.org/10.1016/j.polymer.2014.11.002.
[203] P. Xiao, F. Dumur, B. Graff, D. Gigmes, J.P. Fouassier, J. Lalevée, Blue Light Sensitive Dyes for Various Photopolymerization Reactions: Naphthalimide and Naphthalic Anhydride Derivatives., Macromolecules. 47 (2014) 601–608. https://doi.org/10.1021/ma402376x.
[204] P. Xiao, F. Dumur, M. Frigoli, M.-A. Tehfe, B. Graff, J.P. Fouassier, D. Gigmes, J. Lalevée, Naphthalimide based methacrylated photoinitiators in radical and cationic photopolymerization under visible light, Polym. Chem. 4 (2013) 5440–5448. https://doi.org/10.1039/C3PY00766A.
[205] G. Noirbent, F. Dumur, Recent advances on naphthalic anhydrides and 1,8-naphthalimide-based photoinitiators of polymerization, European Polymer Journal. 132 (2020) 109702. https://doi.org/10.1016/j.eurpolymj.2020.109702.
[206] M. Rahal, H. Mokbel, B. Graff, V. Pertici, D. Gigmes, J. Toufaily, T. Hamieh, F. Dumur, J. Lalevée, Naphthalimide-Based Dyes as Photoinitiators under Visible Light Irradiation

and their Applications: Photocomposite Synthesis, 3D printing and Polymerization in Water, ChemPhotoChem. 5 (2021) 476–490. https://doi.org/10.1002/cptc.202000306.
[207] M. Rahal, B. Graff, J. Toufaily, T. Hamieh, M. Ibrahim-Ouali, F. Dumur, J. Lalevée, Naphthyl-Naphthalimides as High-Performance Visible Light Photoinitiators for 3D Printing and Photocomposites Synthesis, Catalysts. 11 (2021). https://doi.org/10.3390/catal11111269.
[208] N. Zivic, J. Zhang, D. Bardelang, F. Dumur, P. Xiao, T. Jet, D.-L. Versace, C. Dietlin, F. Morlet-Savary, B. Graff, J.P. Fouassier, D. Gigmes, J. Lalevée, Novel naphthalimide–amine based photoinitiators operating under violet and blue LEDs and usable for various polymerization reactions and synthesis of hydrogels, Polym. Chem. 7 (2015) 418–429. https://doi.org/10.1039/C5PY01617G.
[209] P. Xiao, F. Dumur, B. Graff, F. Morlet-Savary, D. Gigmes, J.P. Fouassier, J. Lalevée, Design of High Performance Photoinitiators at 385–405 nm: Search around the Naphthalene Scaffold, Macromolecules. 47 (2014) 973–978. https://doi.org/10.1021/ma402622v.
[210] P. Xiao, F. Dumur, J. Zhang, B. Graff, D. Gigmes, J.P. Fouassier, J. Lalevée, Amino and nitro substituted 2-amino-1H-benzo[de]isoquinoline-1,3(2H)-diones: as versatile photoinitiators of polymerization from violet-blue LED absorption to a panchromatic behavior, Polym. Chem. 6 (2015) 1171–1179. https://doi.org/10.1039/C4PY01409J.
[211] H. Chen, L. Pieuchot, P. Xiao, F. Dumur, J. Lalevée, Water-soluble/visible-light-sensitive naphthalimide derivative-based photoinitiating systems: 3D printing of antibacterial hydrogels, Polym. Chem. 13 (2022) 2918–2932. https://doi.org/10.1039/D2PY00417H.
[212] M.-A. Tehfe, F. Dumur, P. Xiao, B. Graff, F. Morlet-Savary, J.-P. Fouassier, D. Gigmes, J. Lalevée, New chromone based photoinitiators for polymerization reactions under visible light, Polym. Chem. 4 (2013) 4234–4244. https://doi.org/10.1039/C3PY00536D.
[213] J. You, H. Fu, D. Zhao, T. Hu, J. Nie, T. Wang, Flavonol dyes with different substituents in photopolymerization, Journal of Photochemistry and Photobiology A: Chemistry. 386 (2020) 112097. https://doi.org/10.1016/j.jphotochem.2019.112097.
[214] A. Al Mousawi, P. Garra, M. Schmitt, J. Toufaily, T. Hamieh, B. Graff, J.P. Fouassier, F. Dumur, J. Lalevée, 3-Hydroxyflavone and N-Phenylglycine in High Performance Photoinitiating Systems for 3D Printing and Photocomposites Synthesis, Macromolecules. 51 (2018) 4633–4641. https://doi.org/10.1021/acs.macromol.8b00979.
[215] J. Zhao, J. Lalevée, H. Lu, R. MacQueen, S.H. Kable, T.W. Schmidt, M.H. Stenzel, P. Xiao, A new role of curcumin: as a multicolor photoinitiator for polymer fabrication under household UV to red LED bulbs, Polym. Chem. 6 (2015) 5053–5061. https://doi.org/10.1039/C5PY00661A.
[216] J.V. Crivello, U. Bulut, Curcumin: A naturally occurring long-wavelength photosensitizer for diaryliodonium salts, Journal of Polymer Science Part A: Polymer Chemistry. 43 (2005) 5217–5231. https://doi.org/10.1002/pola.21017.
[217] W. Han, H. Fu, T. Xue, T. Liu, Y. Wang, T. Wang, Facilely prepared blue-green light sensitive curcuminoids with excellent bleaching properties as high performance photosensitizers in cationic and free radical photopolymerization, Polym. Chem. 9 (2018) 1787–1798. https://doi.org/10.1039/C8PY00166A.
[218] A. Mishra, S. Daswal, Curcumin, A Novel Natural Photoinitiator for the Copolymerization of Styrene and Methylmethacrylate, Null. 42 (2005) 1667–1678. https://doi.org/10.1080/10601320500246974.

[219] N. Giacoletto, M. Ibrahim-Ouali, F. Dumur, Recent advances on squaraine-based photoinitiators of polymerization, European Polymer Journal. 150 (2021) 110427. https://doi.org/10.1016/j.eurpolymj.2021.110427.
[220] P. Xiao, F. Dumur, T.T. Bui, F. Goubard, B. Graff, F. Morlet-Savary, J.P. Fouassier, D. Gigmes, J. Lalevée, Panchromatic Photopolymerizable Cationic Films Using Indoline and Squaraine Dye Based Photoinitiating Systems, ACS Macro Lett. 2 (2013) 736–740. https://doi.org/10.1021/mz400316y.
[221] V. Launay, A. Caron, G. Noirbent, D. Gigmes, F. Dumur, J. Lalevée, NIR Organic Dyes as Innovative Tools for Reprocessing/Recycling of Plastics: Benefits of the Photothermal Activation in the Near-Infrared Range, Advanced Functional Materials. 31 (2021) 2006324. https://doi.org/10.1002/adfm.202006324.
[222] A. Bonardi, F. Bonardi, G. Noirbent, F. Dumur, C. Dietlin, D. Gigmes, J.-P. Fouassier, J. Lalevée, Different NIR dye scaffolds for polymerization reactions under NIR light, Polym. Chem. 10 (2019) 6505–6514. https://doi.org/10.1039/C9PY01447K.
[223] S. Liu, H. Chen, Y. Zhang, K. Sun, Y. Xu, F. Morlet-Savary, B. Graff, G. Noirbent, C. Pigot, D. Brunel, M. Nechab, D. Gigmes, P. Xiao, F. Dumur, J. Lalevée, Monocomponent Photoinitiators based on Benzophenone-Carbazole Structure for LED Photoinitiating Systems and Application on 3D Printing, Polymers. 12 (2020) 1394. https://doi.org/10.3390/polym12061394.
[224] P. Xiao, F. Dumur, B. Graff, D. Gigmes, J.P. Fouassier, J. Lalevée, Variations on the Benzophenone Skeleton: Novel High Performance Blue Light Sensitive Photoinitiating Systems, Macromolecules. 46 (2013) 7661–7667. https://doi.org/10.1021/ma401766v.
[225] J. Zhang, M. Frigoli, F. Dumur, P. Xiao, L. Ronchi, B. Graff, F. Morlet-Savary, J.P. Fouassier, D. Gigmes, J. Lalevée, Design of Novel Photoinitiators for Radical and Cationic Photopolymerizations under Near UV and Visible LEDs (385, 395, and 405 nm)., Macromolecules. 47 (2014) 2811–2819. https://doi.org/10.1021/ma500612x.
[226] S. Liu, D. Brunel, G. Noirbent, A. Mau, H. Chen, F. Morlet-Savary, B. Graff, D. Gigmes, P. Xiao, F. Dumur, J. Lalevée, New multifunctional benzophenone-based photoinitiators with high migration stability and their applications in 3D printing, Mater. Chem. Front. 5 (2021) 1982–1994. https://doi.org/10.1039/D0QM00885K.
[227] S. Liu, D. Brunel, K. Sun, Y. Zhang, H. Chen, P. Xiao, F. Dumur, J. Lalevée, Novel Photoinitiators Based on Benzophenone-Triphenylamine Hybrid Structure for LED Photopolymerization, Macromolecular Rapid Communications. 41 (2020) 2000460. https://doi.org/10.1002/marc.202000460.
[228] S. Liu, D. Brunel, K. Sun, Y. Xu, F. Morlet-Savary, B. Graff, P. Xiao, F. Dumur, J. Lalevée, A monocomponent bifunctional benzophenone–carbazole type II photoinitiator for LED photoinitiating systems, Polym. Chem. 11 (2020) 3551–3556. https://doi.org/10.1039/D0PY00644K.
[229] M.-A. Tehfe, F. Dumur, B. Graff, F. Morlet-Savary, J.-P. Fouassier, D. Gigmes, J. Lalevée, Trifunctional Photoinitiators Based on a Triazine Skeleton for Visible Light Source and UV LED Induced Polymerizations, Macromolecules. 45 (2012) 8639–8647. https://doi.org/10.1021/ma301931p.
[230] J.-T. Lin, J. Lalevee, Efficacy Modeling of New Multi-Functional Benzophenone-Based System for Free-Radical/Cationic Hybrid Photopolymerization Using 405 nm LED, (2021). https://doi.org/10.20944/preprints202106.0502.v1.
[231] J. Zhang, P. Xiao, F. Dumur, C. Guo, W. Hong, Y. Li, D. Gigmes, B. Graff, J.-P. Fouassier, J. Lalevée, Polymeric Photoinitiators: A New Search toward High Performance Visible

Light Photoinitiating Systems, Macromolecular Chemistry and Physics. 217 (2016) 2145–2153. https://doi.org/10.1002/macp.201600260.
[232] J. Li, X. Zhang, S. Ali, M.Y. Akram, J. Nie, X. Zhu, The effect of polyethylene glycoldiacrylate complexation on type II photoinitiator and promotion for visible light initiation system, Journal of Photochemistry and Photobiology A: Chemistry. 384 (2019) 112037. https://doi.org/10.1016/j.jphotochem.2019.112037.
[233] J. Li, S. Li, Y. Li, R. Li, J. Nie, X. Zhu, In situ monitoring of photopolymerization by photoinitiator with luminescence characteristics, Journal of Photochemistry and Photobiology A: Chemistry. 389 (2020) 112225. https://doi.org/10.1016/j.jphotochem.2019.112225.
[234] J. Li, Y. Hao, M. Zhong, L. Tang, J. Nie, X. Zhu, Synthesis of furan derivative as LED light photoinitiator: One-pot, low usage, photobleaching for light color 3D printing, Dyes and Pigments. 165 (2019) 467–473. https://doi.org/10.1016/j.dyepig.2019.03.011.
[235] Y. Xu, G. Noirbent, D. Brunel, Z. Ding, D. Gigmes, B. Graff, P. Xiao, F. Dumur, J. Lalevée, Novel ketone derivative-based photoinitiating systems for free radical polymerization under mild conditions and 3D printing, Polym. Chem. 11 (2020) 5767–5777. https://doi.org/10.1039/D0PY00990C.
[236] J.P. Fouassier, X. Allonas, D. Burget, Photopolymerization reactions under visible lights: principle, mechanisms and examples of applications, Progress in Organic Coatings. 47 (2003) 16–36. https://doi.org/10.1016/S0300-9440(03)00011-0.
[237] M.A. Lago, A.R.-B. de Quirós, R. Sendón, J. Bustos, M.T. Nieto, P. Paseiro, Photoinitiators: a food safety review, Food Additives & Contaminants: Part A. 32 (2015) 779–798. https://doi.org/10.1080/19440049.2015.1014866.
[238] J. Lalevée, X. Allonas, J.P. Fouassier, H. Tachi, A. Izumitani, M. Shirai, M. Tsunooka, Investigation of the photochemical properties of an important class of photobase generators: the O-acyloximes, Journal of Photochemistry and Photobiology A: Chemistry. 151 (2002) 27–37. https://doi.org/10.1016/S1010-6030(02)00174-0.
[239] R. Mallavia, R. Sastre, F. Amat-Guerri, Photofragmentation and photoisomerization of O-acyl-$\alpha$-oxooximes: Quantum yields and mechanism, Journal of Photochemistry and Photobiology A: Chemistry. 138 (2001) 193–201. https://doi.org/10.1016/S1010-6030(00)00393-2.
[240] A. Werner, A. Piguet, 660. Beckmann'sche Umlagerung durch Benzolsulfonsäurechlorid bei Gegenwart von Alkali oder Pyridin, Berichte Der Deutschen Chemischen Gesellschaft. 37 (1904) 4295–4315. https://doi.org/10.1002/cber.19040370407.
[241] G.A. Delzenne, U. Laridon, H. Peeters, Photopolymerization initiated by O-acyloximes, European Polymer Journal. 6 (1970) 933–943. https://doi.org/10.1016/0014-3057(70)90028-5.
[242] C.J. Groenenboom, H.J. Hageman, P. Oosterhoff, T. Overeem, J. Verbeek, Photoinitiators and photoinitiation Part 11. The photodecomposition of some O-acyl 2-oximinoketones, Journal of Photochemistry and Photobiology A: Chemistry. 107 (1997) 261–269. https://doi.org/10.1016/S1010-6030(96)04617-5.
[243] Y. Miyake, H. Takahashi, N. Akai, K. Shibuya, A. Kawai, Structure and Reactivity of Radicals Produced by Photocleavage of Oxime Ester Compounds Studied by Time-resolved Electron Paramagnetic Resonance Spectroscopy, Chem. Lett. 43 (2014) 1275–1277. https://doi.org/10.1246/cl.140296.
[244] AllonasXavier, LalevéeJacques, FouassierJean-Pierre, TachiHideki, ShiraiMasamitsu, TsunookaMasahiro, Triplet State of O-Acyloximes Studied by Time-Resolved

Absorption Spectroscopy, Chemistry Letters. (2004). https://doi.org/10.1246/cl.2000.1090.
[245] M. Yoshida, H. Sakuragi, T. Nishimura, S. Ishikawa, K. Tokumaru, Nature of the excited triplet states in the photolysis of o-acyloximes, Chem. Lett. 4 (1975) 1125–1130. https://doi.org/10.1246/cl.1975.1125.
[246] J.T. Offenloch, E. Blasco, S. Bastian, C. Barner-Kowollik, H. Mutlu, Self-reporting visible light-induced polymer chain collapse, Polym. Chem. 10 (2019) 4513–4518. https://doi.org/10.1039/C9PY00834A.
[247] H. Kura, J. Tanabe, H. Oka, K. Kunimoto, A. Matsumoto, M. Ohwa, New oxime ester photoinitiators for color filter resists, Radtech Report. 18 (2004) 30–35.
[248] G. Panusa, Y. Pu, J. Wang, C. Moser, D. Psaltis, Fabrication of Sub-Micron Polymer Waveguides through Two-Photon Polymerization in Polydimethylsiloxane, Polymers. 12 (2020). https://doi.org/10.3390/polym12112485.
[249] S. Steenhusen, F. Burmeister, M. Groß, G. Domann, R. Houbertz, S. Nolte, Heterogeneous microoptical structures with sub-micrometer precision, Thin Solid Films. 668 (2018) 74–80. https://doi.org/10.1016/j.tsf.2018.09.013.
[250] T.-Y. Huang, W.-T. Cheng, The Effect of Photo-initiator on the Contrast Curve of Negative-work Photo-resist, Journal of Photopolymer Science and Technology. 24 (2011) 643–646. https://doi.org/10.2494/photopolymer.24.643.
[251] T. Karatsu, M. Narusawa, S. Yagai, A. Kitamura, H. Suzuki, H. Okamura, Effect of Alkyl Group on the Photocrosslinking of Alkyl Methacrylate Based Copolymers, Journal of Photopolymer Science and Technology. 26 (2013) 259–270. https://doi.org/10.2494/photopolymer.26.259.
[252] H. Sugita, K. Tanaka, K. Shirato, R. Yamamoto, K. Tateshima, Styryl silsesquioxane photoresist, Journal of Applied Polymer Science. 132 (2015). https://doi.org/10.1002/app.41459.
[253] M. Ohwa, H. Kura, H. Oka, H. Yamato, Development of Photoinitiators in Electronic Applications, Journal of Photopolymer Science and Technology. 15 (2002) 51–57. https://doi.org/10.2494/photopolymer.15.51.
[254] K. Dietliker, R. Hüsler, J.-L. Birbaum, S. Ilg, S. Villeneuve, K. Studer, T. Jung, J. Benkhoff, H. Kura, A. Matsumoto, H. Oka, Advancements in photoinitiators—Opening up new applications for radiation curing, Progress in Organic Coatings. 58 (2007) 146–157. https://doi.org/10.1016/j.porgcoat.2006.08.021.
[255] Y. Muramatsu, M. Kaji, A. Unno, O. Hirai, Terminal Group Analyses of Photopolymerized Products Using a MALDI-TOFMS for the Study on the Oxime Ester type Photoinitiators, Journal of Photopolymer Science and Technology. 23 (2010) 447–450. https://doi.org/10.2494/photopolymer.23.447.
[256] J. Xu, G. Ma, K. Wang, J. Gu, S. Jiang, J. Nie, Synthesis and photopolymerization kinetics of oxime ester photoinitiators, Journal of Applied Polymer Science. 123 (2012) 725–731. https://doi.org/10.1002/app.34551.
[257] T. Scherzer, U. Decker, Kinetic investigations on the UV-induced photopolymerization of a diacrylate by time-resolved FTIR spectroscopy: the influence of photoinitiator concentration, light intensity and temperature, Radiation Physics and Chemistry. 55 (1999) 615–619. https://doi.org/10.1016/S0969-806X(99)00257-1.
[258] D.E. Fast, A. Lauer, J.P. Menzel, A.-M. Kelterer, G. Gescheidt, C. Barner-Kowollik, Wavelength-Dependent Photochemistry of Oxime Ester Photoinitiators, Macromolecules. 50 (2017) 1815–1823. https://doi.org/10.1021/acs.macromol.7b00089.

[259] D. Voll, T. Junkers, C. Barner-Kowollik, A qualitative and quantitative post-mortem analysis: Studying free-radical initiation processes via soft ionization mass spectrometry, Journal of Polymer Science Part A: Polymer Chemistry. 50 (2012) 2739–2757. https://doi.org/10.1002/pola.26076.
[260] U. Kolczak, G. Rist, K. Dietliker, J. Wirz, Reaction Mechanism of Monoacyl- and Bisacylphosphine Oxide Photoinitiators Studied by 31P-, 13C-, and 1H-CIDNP and ESR, J. Am. Chem. Soc. 118 (1996) 6477–6489. https://doi.org/10.1021/ja9534213.
[261] G.A. Worth, L.S. Cederbaum, BEYOND BORN-OPPENHEIMER: Molecular Dynamics Through a Conical Intersection, Annu. Rev. Phys. Chem. 55 (2004) 127–158. https://doi.org/10.1146/annurev.physchem.55.091602.094335.
[262] R. Zhou, H. Pan, D. Wan, J.-P. Malval, M. Jin, Bicarbazole-based oxime esters as novel efficient photoinitiators for photopolymerization under UV-Vis LEDs, Progress in Organic Coatings. 157 (2021) 106306. https://doi.org/10.1016/j.porgcoat.2021.106306.
[263] R. Zhou, M. Jin, J.-P. Malval, H. Pan, D. Wan, Bicarbazole-based oxalates as photoinitiating systems for photopolymerization under UV–Vis LEDs, Journal of Polymer Science. 58 (2020) 1079–1091. https://doi.org/10.1002/pol.20199298.
[264] K. Sameshima, H. Kura, Y. Matsuoka, H. Sotome, H. Miyasaka, Improvement of the photopolymerization and bottom-curing performance of benzocarbazole oxime ester photoinitiators with red-shifted absorption, Jpn. J. Appl. Phys. 61 (2022) 035504. https://doi.org/10.35848/1347-4065/ac55e4.
[265] X. Ma, R. Gu, L. Yu, W. Han, J. Li, X. Li, T. Wang, Conjugated phenothiazine oxime esters as free radical photoinitiators, Polym. Chem. 8 (2017) 6134–6142. https://doi.org/10.1039/C7PY00797C.
[266] A. Mahmood, S.U.-D. Khan, U.A. Rana, M.H. Tahir, Red shifting of absorption maxima of phenothiazine based dyes by incorporating electron-deficient thiadiazole derivatives as π-spacer, Arabian Journal of Chemistry. 12 (2019) 1447–1453. https://doi.org/10.1016/j.arabjc.2014.11.007.
[267] M. Rahal, M. Abdallah, T.-T. Bui, F. Goubard, B. Graff, F. Dumur, J. Toufaily, T. Hamieh, J. Lalevée, Design of new phenothiazine derivatives as visible light photoinitiators, Polym. Chem. 11 (2020) 3349–3359. https://doi.org/10.1039/D0PY00497A.
[268] S. Dadashi-Silab, X. Pan, K. Matyjaszewski, Phenyl Benzo[b]phenothiazine as a Visible Light Photoredox Catalyst for Metal-Free Atom Transfer Radical Polymerization, Chemistry – A European Journal. 23 (2017) 5972–5977. https://doi.org/10.1002/chem.201605574.
[269] X. Ma, D. Cao, H. Fu, J. You, R. Gu, B. Fan, J. Nie, T. Wang, Multicomponent photoinitiating systems containing arylamino oxime ester for visible light photopolymerization, Progress in Organic Coatings. 135 (2019) 517–524. https://doi.org/10.1016/j.porgcoat.2019.06.027.
[270] M. Makino, K. Uenishi, T. Tsuchimura, Synthesis and Properties of Highly Sensitive Ether Ring Fused O-Acyloxime Esters as Photoradical Initiator, Journal of Photopolymer Science and Technology. 31 (2018) 37–44. https://doi.org/10.2494/photopolymer.31.37.
[271] T. Tsuchimura, M. Makino, New compound, photopolymerizable composition, photopolymerizable composition for color filter, color filter, methods for producing same, solid-state imaging device and lithographic printing original plate, JP 2009-227624A, n.d.

[272] C.P. Schultz, H.H. Eysel, H.H. Mantsch, M. Jackson, Carbon Dioxide in Tissues, Cells, and Biological Fluids Detected by FTIR Spectroscopy, J. Phys. Chem. 100 (1996) 6845–6848. https://doi.org/10.1021/jp953254t.
[273] J. Kumar, S.F. D'Souza, Preparation of PVA membrane for immobilization of GOD for glucose biosensor, Talanta. 75 (2008) 183–188. https://doi.org/10.1016/j.talanta.2007.10.048.
[274] D.J. Henry, M.L. Coote, R. Gómez-Balderas, L. Radom, Comparison of the Kinetics and Thermodynamics for Methyl Radical Addition to CC, CO, and CS Double Bonds, J. Am. Chem. Soc. 126 (2004) 1732–1740. https://doi.org/10.1021/ja039139a.
[275] S.P. Pitre, N.A. Weires, L.E. Overman, Forging C(sp3)–C(sp3) Bonds with Carbon-Centered Radicals in the Synthesis of Complex Molecules, J. Am. Chem. Soc. 141 (2019) 2800–2813. https://doi.org/10.1021/jacs.8b11790.
[276] J.M. Dust, D.R. Arnold, Substituent effects on benzyl radical ESR hyperfine coupling constants. The .sigma..alpha..cntdot. scale based upon spin delocalization, J. Am. Chem. Soc. 105 (1983) 1221–1227. https://doi.org/10.1021/ja00343a024.
[277] R. Zhou, X. Sun, R. Mhanna, J.-P. Malval, M. Jin, H. Pan, D. Wan, F. Morlet-Savary, H. Chaumeil, C. Joyeux, Wavelength-Dependent, Large-Amplitude Photoinitiating Reactivity within a Carbazole-Coumarin Fused Oxime Esters Series, ACS Appl. Polym. Mater. 2 (2020) 2077–2085. https://doi.org/10.1021/acsapm.0c00276.
[278] P. Hu, W. Qiu, S. Naumov, T. Scherzer, Z. Hu, Q. Chen, W. Knolle, Z. Li, Conjugated Bifunctional Carbazole-Based Oxime Esters: Efficient and Versatile Photoinitiators for 3D Printing under One- and Two-Photon Excitation, ChemPhotoChem. 4 (2020) 224–232. https://doi.org/10.1002/cptc.201900246.
[279] H. Lu, Z. Li, Synthesis and Structure-Activity Relationship of N-Substituted Carbazole Oxime Ester Photoinitiators, Journal of Photopolymer Science and Technology. 34 (2021) 307–313. https://doi.org/10.2494/photopolymer.34.307.
[280] F. Hammoud, N. Giacoletto, M. Nechab, B. Graff, A. Hijazi, F. Dumur, J. Lalevée, 5,12-Dialkyl-5,12-dihydroindolo[3,2-a]carbazole-Based Oxime-Esters for LED Photoinitiating Systems and Application on 3D Printing, Macromolecular Materials and Engineering. n/a (2022) 2200082. https://doi.org/10.1002/mame.202200082.
[281] N.A. Kazin, N.S. Demina, R.A. Irgashev, E.F. Zhilina, G.L. Rusinov, Modifications of 5,12-dihydroindolo[3,2-a]carbazole scaffold via its regioselective C2,9-formylation and C2,9-acetylation, Tetrahedron. 75 (2019) 4686–4696. https://doi.org/10.1016/j.tet.2019.07.015.